LISST INSTRUMENTS AS A TOOL IN PHYTOPLANKTON ECOLOGY

A Thesis

by

LAUREN DRAKE RAILEY

Submitted to the Office of Graduate Studies of
Texas A&M University
in partial fulfillment of the requirements for the degree of

MASTER OF SCIENCE

Approved by:

Chair of Committee,	Daniel C. O. Thornton
Committee Members,	Thomas Bianchi
	Sarah Brooks
Head of Department,	Piers Chapman

December 2012

Major Subject: Oceanography

Copyright 2012 Lauren Drake Railey

ABSTRACT

Laser *in situ* scattering and transmissometry (LISST) instruments are used to measure the particle size distributions (PSDs) and volume concentration of individual and groups of phytoplankton in water. The objective of this research was to test the LISST's ability in detecting monospecific blooms *in-situ* and the ability to detect aggregation after diatoms were subjected to different temperatures and bacteria concentrations. The PSDs of ten harmful algal bloom (HAB) species were measured with the LISST characterizing the peak location, peak height, peak width, and peak range resulting in a scattering signature for each species. Each species had specific characteristics that would allow for their detection with the LISST, though microscope observations would be needed for complete accuracy. The LISST was able to detect HABs placed in natural seawater collected off the Texas coast. Blooms of four HAB species before they reached full" bloom concentrations were detected making the LISST a possible low cost, effective tool in the early detection and monitoring of HABs. The diatom, *Odontella aurita*, was used to test how well the LISST could monitor aggregation, an important process in the termination of many phytoplankton blooms. Increasing temperature causes an increase in transparent exopolymer particle (TEP) production in diatoms, which is a critical sticky particle that increases the probability of aggregation. An increase in temperature can also cause an increase in bacteria concentration that can positively effect TEP production and thus aggregation. *O. aurita* was grown at 20 °C and 28 °C and showed a significant increase in TEP abundance with

temperature ($p = 0.002$), though no relationship between TEP production and bacteria concentration existed. Coomassie stained particles (CSP) are proteinaceous gel-like particles, which are currently understudied. CSP was consistently produced though it did not appear to be dependent upon any single factor. The increase in ocean temperatures has implications for an increase in phytoplankton blooms making the monitoring and understanding of these blooms even more important as they can affect the carbon cycle and potentially the microbial loop.

DEDICATION

To my parents, Suzanne and Rodney, and my sister Erika, your support and love continually guided me and made this all possible.

To Mike, your unwavering faith, love, and encouragement supported me through it all.

ACKNOWLEDGEMENTS

First I would like to acknowledge the National Science Foundation (NSF) grant "Effect of temperature on extracellular polymeric substances (EPS) production by diatoms" (OCE 0726369) to DCOT, Texas Sea Grant, and S-STEM as it made conducting this research project possible. Second I would like to thank my committee Sarah Brooks, Thomas Bianchi, and Dan Thornton for all the guidance and wisdom they gave me to conduct and complete my research. I would like to extend thanks to Dr. Lisa Campbell for supplying strains of *Karenia* to be used in this project. I would also like to thank Chen Jie for the advice, help, and for being a wonderful confidante along the way.

TABLE OF CONTENTS

Page

LIST OF FIGURES

LIST OF TABLES

CHAPTER I

INTRODUCTION

The LISST-100X-C instrument

The laser *in situ* scattering and transmissometry (LISST) instruments is a particle analyzer that was originally designed to measure sediment size, distributions, and volume concentrations in water (Agrawal and Pottsmith 2000; Gartner 2001). These instruments use laser diffraction to determine the particle size distribution (PSD) and particle volume concentration in 32 size bins placed on a logarithmic scale in the range of 2.5 to 500 µm. The collimated laser beam (670 nm) shines across a 5 cm path through the water to be analyzed. Suspended particles in the water diffract the light, and the scattered light hits the detector composed of 32 concentric rings. The scattered light is largely dependent upon a particle's size and shape. The size of the suspended particles is determined based on an interpolation of which of the 32 rings the light hits (Agrawal and Pottsmith 2000). The radius of each ring increases logarithmically to correspond with the logarithmic spacing of particles. A particle detected by a ring is assumed to be a spherical object and an equivalent spherical diameter (ESD) is approximated for the particle (see Fig. 1).

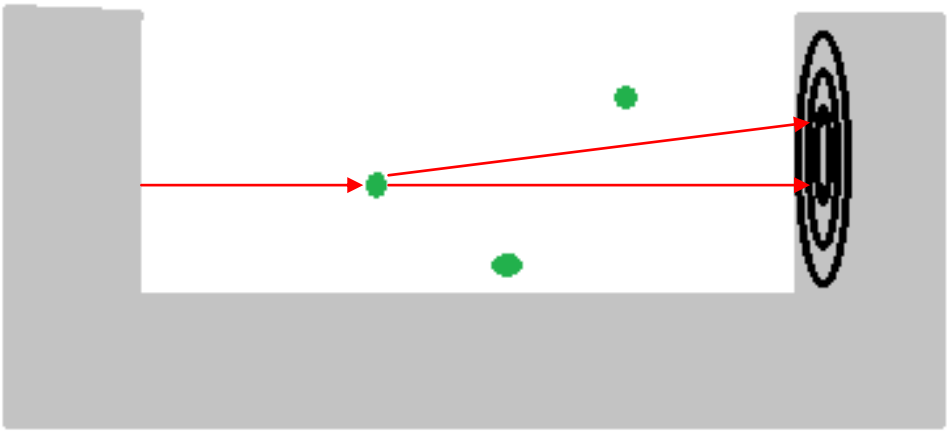

Fig. 1. Simplified image of the LISST sample chamber for laboratory work. The laser passes through the water sample scattering off particles (represented by green circles) that are suspended and strikes the detector rings (black rings). Red arrows represent laser scatter.

The LISST is able to determine total volume by calculating the volume calculated from each of the 32 detector rings to produce a PSD where the height of the peak represents the volume detected at each size bin. As the LISST does not measure particle shapes and assumes that everything is spherical in nature, phytoplankton having different length and width measurements, their orientation to the laser could produce more than one peak on a PSD. The resulting peak location and relative height on the PSD can be used as a tool to identify individual phytoplankton species in the water column assuming different species have different 'scattering signatures' resulting in a distinct PSD that doesn't change with time (Rzadkowolski & Thornton 2012) (Fig. 2).

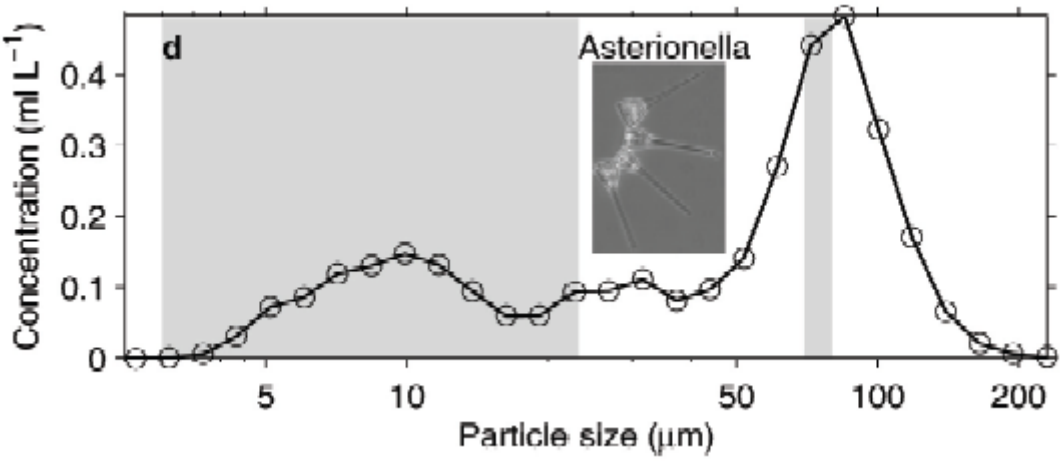

Fig. 2. Scattering signature of *Asterionella* taken from Rienecker et al. (2008). Since phytoplankton are not all spherical objects, peaks will be produced at different ESD based on the particles orientation to the laser. The number of peaks, position of peaks, and relative height of peaks can potentially be used to identify different species. The grey bars indicate the range of cell dimensions measured with a microscope.

Phytoplankton ecology

There are several major taxonomic groups of phytoplankton; diatoms and dinoflagellates are two main types of phytoplankton that make a significant contribution to global primary production, and are chosen for this research due to their ability to form massive harmful blooms, as well as being able to aggregate. For there to be living organisms inorganic carbon must be chemically reduced to an organic state as organic carbon is the foundation of all life. Primary producers synthesize simple organic compounds from the inorganic forms of carbon, and as diatoms and dinoflagellates are autotrophs they use light energy to fix the carbon. Phytoplankton use light that penetrates the water column to produce organic carbon in the euphotic areas of the world's oceans. Blooms of phytoplankton, particularly in the fall and spring, produce

vast amounts of carbon that through cell death the phytoplankton are able to transport the organic carbon to benthic environments via sinking particles (Billet et al. 1983). The sinking of phytoplankton to the depths is dependent upon biological processes such as the size of the cells, cell stickiness, growth characteristics (i.e. single cell or chain), and physical variables like turbulence, currents, and advection (Riebesell and Wolf-Gladrow 1992). These components can causes aggregation of phytoplankton into particles referred to as marine snow (particles greater than 0.5 mm in length; Alldredge and Silver 1988). Diatom aggregation into marine snow and the subsequent sinking alone produces a rapid flux of particulate organic matter to the benthos at rates that can exceed 100 m day^{-1} (Billet et al. 1983, Smetacek 1985). Benthic environments do not support phytoplankton growth and rely on this continuous, seasonally-variable deposition of particulate organic carbon (POC). Approximately 16 of the 45 Pg C per year (i.e. 36%) of total net marine primary production is transported from the euphotic zone to the deep sea (Falkowski 1998).

Unlike terrestrial plants, phytoplankton communities are able to change dramatically in abundance and composition within days or even hours. Different phytoplankton groups and species respond differently to nutrient, temperature, and light conditions. Understanding the phytoplankton environment and how global increases in temperature may affect their biological processes is important considering they photosynthesize more than 99% of the food used by all other marine organisms (Segar 2007), and their continuous sinking to the deep sea affects various biogeochemical cycles (i.e. organic carbon cycle, silica cycle). However, through sinking, phytoplankton

are sequestering carbon from the surface waters and transporting the carbon to the deep sea contributing to the global biological carbon pump which could be forcing global climate change (Broecker 1982, Omta et al. 2006). The significance of understanding the effects of temperature on these organisms is becoming apparent.

Warming oceans effect on phytoplankton

Phytoplankton are found throughout the world's oceans, however the temperature, light, and nutrient concentrations available to phytoplankton is unique depending upon location and can widely vary (Marinov et al. 2010). Every species of phytoplankton thus occupies a region that best suits their temperature (as well as light and nutrient) requirements. Due to changes in climate and the overall increase in temperature, phytoplankton that thrive in the mid-latitudes and tropics where the ocean is thermally stratified, will have increased stratification due to the increase in sea surface temperature thus reducing vertical mixing and limiting the amount of nutrients in the surface waters (Behrenfeld et al. 2006). Under those conditions phytoplankton growth and biomass should decrease. At higher latitudes where phytoplankton growth is generally limited by light, the increased stratification that will occur due to high temperatures will favor the phytoplankton through their retention closer to the surface where there is light (Doney 2006). The increase in sea surface temperature may start favoring the more motile phytoplankton. The more motile phytoplankton would also be favored in mid-latitude and tropical regions where the water could have nutrient limitation. The phytoplankton's ability to move would enable it to find the available nutrients.

This raises concern as to how temperature affects the physiology of phytoplankton and each species ability to adapt to the change. Acclimation of phytoplankton is species dependent and Geider et al. (1997) and Behrenfeld et al. (2008, 2009) showed that acclimation responses can be interpreted from the chl *a*:carbon ratio, which could represent the adjustment in intracellular carbon allocation via the exudation of exopolymers (Geider et al. 1997; Thornton 2002). Carbon allocation in phytoplankton will change with an increase in temperature and Claquin et al. (2008) found that 3 diatom species exuded more exopolymers with an increase in temperature. The role of increased sea temperature and its effects on ecosystems on a local scale and the production of extracellular carbon needs further investigation.

Harmful algal blooms

Algal blooms are referred to as "harmful" when the blooms cause a range of deleterious physiological and environmental effects (Smayda 1997). Harmful algal blooms (HABs) are natural phenomena that affect virtually every coastal nation in the world (Hallegraff 1993). This widespread occurrence of HABs could be caused by physical processes such as currents and storms, or by anthropogenic sources such as transference from ship ballast water, increased aquaculture operations in coastal waters, and stimulation of the blooms due to increased eutrophication (Anderson 1989; Hallegraff 1993; Burkholder 1998; Gilbert et al. 2005; Gilbert and Burkholder 2006). Only 2% of all phytoplankton taxa produce toxins causing HABs and dinoflagellates make up three quarters of these toxin producing algae (Smayda 1997). Phytoplankton that cause HABs can be motile or non-motile, and are present in different sizes.

Algal blooms are considered harmful due to their ability to produce toxins some of which can cause paralytic shellfish poisoning (PSP), neurotoxic shellfish poisoning (NSP), amnesic shellfish poisoning (ASP), and ciguatera fish poisoning (CFP). These blooms can also cause fish mortality, fatalities to marine mammals and benthic organisms, and illness in humans. With global warming causing elevated water temperatures, the seasonal succession and biogeographic boundaries of the HABs will change (Dale et al. 2006), leading to an increase in the occurrence and magnitude of HABs at any given area. The early detection and mitigation of these harmful microorganisms will allow for healthy and safe coastal waters.

Diatom aggregation

Diatoms are a major group of marine phytoplankton that produce an estimated 40-45% of the net oceanic production (Mann 1999). Marine snow, or particles greater than 0.5 mm in length (Alldredge and Silver 1998), can be formed by detritus, living organisms, and inorganic matter (Thornton and Thake 1998). Diatoms are a common component of these aggregates. Marine snow and the diatoms that compose it interact with the surrounding environment, and other microbes such as heterotrophic bacteria. Heterotrophic bacteria are able to either break down marine snow through high hydrolytic enzymatic activities thereby reducing the vertical flux of the organic matter (Smith et al. 1992; Grossart and Ploug 2001), or they may enhance aggregation and stabilize existing aggregates through exopolymer production (Decho 1990; Heissenberger and Herndl 1994).

A possible pathway for exopolymer production is the carbon fixed by diatoms via

photosynthesis forms glucan, a carbohydrate (Bellinger et al. 2005; Abdullahi et al. 2006), which is exuded as exopolymers during normal growth. The exopolymers produced by diatoms can form three different substances depending on their solubility, molecular weight and structure: cell coatings, water soluble exopolymers, and transparent exopolymeric particles (TEP) (Thornton 2002).

TEP is a matrix of sticky, gel-like particles, and is defined as an independent polysaccharide (i.e. detached from a cell) that is stained by Alcian blue and can be retained on a 0.4 μm filter (Alldredge et al. 1993). These particles are formed abiotically from dissolved and colloidal organic matter via spontaneous assembly (Chin et al. 1998), shear coagulation (Passow 2000), or bubble adsorption (Mopper et al. 1995; Zhou et al. 1998; Mari 1999). TEP exists as discrete particles rather than as cell surface coatings (Alldredge et al. 1993). Due to the sticky nature of TEP, it is important to the formation of diatom aggregations in marine ecosystems (Passow et al. 1994; Engel 2000), although the presence of TEP does not ensure aggregate formation (Thornton 2002). The coagulation of particles depends on the probability of particles colliding together, and on the probability of the two particles sticking together once they collide (i.e. the stickiness of the particles) (Jackson 1990). TEP, as a sticky substance, is thought to play a large role in the aggregation process. Diatoms produce small TEP particles, or precursors to TEP during early growth, the large TEP particles are formed by aggregation, and have the potential to envelop most of the phytoplankton in the bloom (Passow and Alldredge 1995).

Marine phytoplankton remove dissolved inorganic carbon from the euphotic zone

via photosynthesis and then redirect it to the deep ocean through sedimentation (Engel and Passow 2001) powering the biological carbon pump. These vertical fluxes are believed to influence global climate by leading to a net burial of carbon in the ocean floor, which could potentially reduce the amount of carbon dioxide in the atmosphere (Kiørboe 2001). The vertical sinking of these large marine snow aggregates is therefore important on the global scale. TEP may affect the flux of organic carbon from the euphotic layer to the bottom of the ocean, due to its role in the coagulation process (Jackson 1990; Logan et al. 1995). As aggregates age, TEP persists, suggesting that TEP may be resistant to microbial decay, which can explain how the aggregates are held together long enough to reach the deep areas of the ocean (Alldredge et al. 1998).

The polysaccharide TEP is not the only particulate organic matter that may play a role in diatom aggregation. Coomassie stained particles (CSP) are protein particles that are defined by being stained with Coomassie Brilliant Blue (CBB) dye. Most work has focused more on the role of TEP and bacteria in diatom aggregation while little is known about the role CSP may play. Bhasker et al. (2005) showed that CSP are more abundant than TEP in water collected from the Pacific Ocean off of Scripps Pier (California), however it is unknown whether there is overlap between the two particles as they could serve as smaller subunits of the same particle (Engel 2009). Prieto et al. (2002) questioned the relative stickiness of CSP as results showed TEP was of more importance in diatom aggregation. TEP is well studied, but the effects of CSP are largely unknown. CSP could play a role in the aggregation of diatoms, and regardless of that CSP still

could serve as a potentially important pool of nitrogen in the nitrogen cycle and could be produced and consumed by bacteria.

Heterotrophic bacteria colonize plankton generally once they become more senescent and form marine snow or aggregates (Smith et al. 1995). Once attached to the aggregates, bacteria cause particulate organic carbon (POC) solubilization to dissolved organic carbon (DOC) (Smith et al. 1992; Grossart and Ploug 2001). The role of bacteria in decomposing POC derived from phytopolankton is well studied, but their role in the decomposition of DOC derived from phytoplankton and how this effects the production of TEP, CSP, and aggregation is not understood.

Study objectives

The LISST-100X though originally designed for sediments, has become a tool to identify and quantify biological organisms (Serra et al. 2001; Karp-Boss et al. 2007; Rienecker et al. 2008; Rzadkowolski and Thornton 2012). The LISST can be a potential tool for monoculture bloom identification (Karp-Boss et al. 2007; Rienecker et al. 2008), as well as detecting aggregates in the water column (Rzadkowolski & Thornton 2012). To look more into the LISST's potential; two experiments were designed to test its ability in both areas.

To determine the ability of the LISST to identify and quantify individual species, harmful algae taxa were studied. The LISSTs ability to detect and distinguish between HAB species at realistic bloom concentrations, and against populations of natural particles found in coastal waters needs to be determined.

My main hypotheses for this experiment were:

1. Different HAB species have significantly different scattering signatures as measured by the LISST-100X particle analyzer.

   Approach: The LISST-100X estimates the equivalent spherical diameter of particles and places them in logarithmically spaced bins (Gartner 2001; Agrawal et al. 2008). The LISST produces a PSD based on the shape of the cells and the scattering caused by different orientation of the cells relative to the laser, which will give sufficient information to identify the HAB species.

2. The volume concentration measured by the LISST is proportional to the concentration of dinoflagellates in the water sample.

   Approach: The LISST takes the volume concentration of a sample and separates it into 32 size bins assuming all the particles are spherical. Using careful dilutions, the LISST will be tested to determine whether it can accurately calculate cell abundance.

3. HAB species can be detected at bloom concentrations or less against the background particle field in natural seawater.

   Approach: In a "full-bloom" situation, the bloom is largely monospecific and there is a high concentration of the dinoflagellate causing the bloom. Rienecker et al. (2008) showed the LISST was able to detect a diatom bloom *in-situ*. I will use the LISST to determine whether bloom and sub-bloom concentrations of dinoflagellates can be detected in natural waters by identifying their

scattering signatures from the resulting PSD measured with the LISST-100X.

The ability to identify and quantify aggregates in the water column and in laboratory experiments using the LISST-100X needs to be further studied, especially with the current increase in global temperatures possibly effecting aggregation rates in the ocean. To study this, an experiment was designed to determine how temperature affects the abundance of sticky particles, (TEP and CSP) in cultures of the diatom *Odontella aurita*, as well as how the abundance of bacteria affects the production of TEP and CSP and aggregation. The LISST was used to measure the aggregation.

My main hypotheses for this experiment were:

4. TEP concentration, CSP concentration, and aggregation increases with increasing temperature.

   Approach: Metabolic processes, such as photosynthesis, are affected by temperature (Davison 1991). TEP production per chlorophyll *a* unit varies as a function of temperature in diatom species; it has been shown that TEP increases with temperature until it reaches a maximum where it then decreases (Claquin et al. 2008). If TEP production increases, the increased stickiness in the cultures should enhance the ability of diatoms to stick together upon collision, and thus form larger aggregates.

5. TEP concentration and aggregation increases with increasing bacterial abundance.

Approach: As bacteria are able to increase the amount of TEP production in diatoms (Gärdes et al. 2011), the increase in bacterial community should lead to an increase in TEP and thus aggregation.

CHAPTER II

LASER SCATTERING SIGNATURES OF HARMFUL ALGAL BLOOM SPECIES

Methods

Harmful algae selection and arrival. Several harmful algae were selected and obtained from the Provasoli-Guillard National Center for Marine Algae and Microbiota (NCMA), and some species obtained from Dr. Lisa Campbell (Texas A&M University, College Station, TX) (see Table 1). Species were selected based on their known occurrence as HABs in the Gulf of Mexico. This work was carried out as part of a Texas Sea Grant project to develop the LISST as a tool to identify and quantify HABs in the Gulf of Mexico.

When cultures arrived from Provasoli-Guillard, 1 ml was taken from the *Prorocentrum minimum* (2780), *Karenia brevis* (2228), *Karlodinium veneficum* (2936), and *Aureoumbra lagunensis* (1502) 15 ml tubes and inoculated into triplicate flasks of 40 ml of 0.2 µm filtered autoclaved artificial seawater (Harrison et al. 1980; Berges et al. 2001). L1 nutrients were added aseptically and *P. minimum* (2780) and *A. lagunensis* (1502) were incubated at 20 ºC (14 h light: 10 h dark) while *K. brevis* (2228) and *K. veneficum* (2936) were incubated at 28 ºC (14 h light: 10 h dark) to maintain actively growing cultures. No other algae species was grown continuously. On the day the harmful algae species arrived, 8 ml were taken from every species culture tubes and diluted with 72 ml of 0.2 µm-filtered artificial seawater. The sample was put in the LISST chamber to establish archival data in case the species began to look different after

acclimating to the growth conditions in our experiment compared to conditions at NCMA.

Table 1. Harmful algae species obtained from Provasoli-Guillard NCMA and from Dr. Lisa Campbell. Shown are species approximate size, nutrient medium grown in, where the species was collected, and where it occurs in the Gulf of Mexico. Name monikers were given based on genus, species, and strain. L1 is a nutrient supplement recipe added to artificial seawater (Andersen 2005). Size, nutrient medium, and collection site are data obtained from NCMA. Dashes represent not recorded data.

Harmful algae species	Size (l x w)	Nutrient medium	Collection Site	Bloom location in Gulf of Mexico
AM3105 *Alexandium monilatum*	-	L1-Si	Gulfport, MS	TX-FL
AL1502 *Aureoumbra lagunensis*	5 µm - 5µm	L1 + 150 µm NH_4Cl	Laguna Madre, TX	TX coast (Laguna Madre)
CL1770 *Ceratuim longipes*	160 µm x 215µm	L1 - Si	West Boothbay Harbor, ME	TX coast
K. BREVIS (2228) *Karenia brevis*	26 µm x 24 µm	L1 - Si	Sarasota Bay, FL	TX and FL coast
KBcampbell *Karenia brevis*	-	-	Port Aransas, TX	TX coast
KMcampbell *Karenia mikimotoi*	-	-	Port Aransas, TX	TX coast
KV2936 *Karlodinium veneficum*	14 µm x 13 µm	L1 - Si (11 psu)	Inland Bays, DE	TX and FL
PP1830 *Pfiesteria piscicida*	11 µm x 11 µm	Seawater (12 psu) Rhodomonas sp. as food	Chesapeake Bay, MD	TX-FL
PM2780 *Prorocentrum minimum*	15 µm x 15 µm	L1-Si	Tampa, FL	TX and FL
PN1309 *Pseudo-nitzchia* sp.	-	L1	Baffin Bay, Canada	Northern

LISST operation. The LISST 100X Type C (Sequoia Instruments) uses laser scattering to analyze particle size in a laboratory or *in-situ*. Through light diffracting off particles at small forward angles in the water column, the LISST estimates the equivalent spherical diameter (ESD) and the total volume concentration of the particles in the water, and the light that is transmitted through the particle accounts for an inconsequential portion of the measured scatter (Agrawal & Pottsmith, 2000). The light hitting each of the 32 logarithmically concentric detector rings is used to estimate the volume concentration in each of the 32 size bins. The rings are able to measure particles in the range of 2.5 to 500 µm in diameter. This subsequent volume concentration is processed against a background scattering file of 0.2 µm filtered artificial seawater used as a blank in the Sequoia Scientific LISST software for work with algae. The LISST was operated through a PC running LISST SOP software (Sequoia Scientific). For laboratory work, the instrument was fitted with a chamber for liquid samples to be held in. Samples were approximately 80 ml in volume, which was sufficient to cover the laser beam path, and a piece of aluminum foil was placed over the top of the chamber to prevent overhead light and particles in the air from effecting the measurement.

Cell counting and sizing. One ml from each dinoflagellates culture was placed in a centrifuge tube and preserved with a drop of Lugol's iodine (Parsons et al. 1984) for use in cell counts. Cell counts were determined using a cell hemocytometer (Hauser Scientific Fuchs-Rosenthal) where 400 cells per culture were counted and a calculation subsequently made to determine the amount of cells per ml (Guillard and Sieracki 2005).

Since preservation can effect cell dimensions (Menden-Deuer et al. 2001), the major and minor axis of 100 living cells were measured using a Carl-Zeiss Axioplan2 microscope.

LISST measurements. The PSD of each of the harmful algae species was measured at a rate of 1 Hz for 100s resulting in 100 measurements per sample as described by Rzadkowolski and Thornton (2012). The sampling time had to be restricted due to particles sinking out of the water column (Rzadkowolski & Thornton 2012). To obtain a scattering signature that could be used to identify the different species, 8 ml of each species was mixed with 72 ml of 0.2 µm filtered artificial seawater and put in the sampling chamber. The data presented by the LISST recounts the volume concentration ($\mu l\ l^{-1}$) of the particles in each of the 32 size bins based on the particles ESD. The size bins are represented by the median particle diameter for each ring with 2.72 µm being the smallest and 460 µm being the largest. The size bins contain a range of particle diameters and the size bins range increase with increasing particle size as the upper particle diameter range in each size bin is 1.18 x the smallest diameter in that size bin (LISST-100X User's Manual, Sequoia Scientific). In the subsequent experiments, the size bins will be named according to the median particle size that occurs in that size bin.

Once *K. brevis* (2228) grew into a dense culture, monoculture samples were mixed at different concentrations with 0.2 µm filtered artificial seawater to provide dilutions of 100, 90, 70, 50, 30, 20, 10, 5, and 1% (v/v) which was measured by the LISST and then compared with cell counts via hemocytometer and cell sizing using a Carl-Zeiss Axioplan 2 microscope. This dilutions series were conducted to determine

whether there was a positive correlation between the counted concentration of the dinoflagellate and the volume concentration measured by the LISST.

Collected seawater background. In February 2011 surf zone seawater was collected from Crystal Beach, TX (29.45ºN, 94.63ºW), and in April 2011 surf zone seawater was collected from Galveston, TX (29.28ºN, 94.83ºW). To test whether the LISST would be able to detect harmful algal blooms against a backscatter of natural seawater particles, *K. brevis* (2228), *P. minimum* (2780), *A. lagunensis* (1502), and *K. veneficum* (2936) were put in the LISST chamber in combination with seawater at different bloom concentrations. Water was collected at different months in the year to allow for different organisms to be present in the sample. For this experiment "bloom" concentrations for each of these 4 dinoflagellates came from literature: *K. brevis* bloom, 5.35×10^3 cells ml^{-1} (Vargo et al., 2002); *K. veneficum* bloom, 2.00×10^5 cells ml^{-1} (Hall et al., 2008); *A. lagunensis* bloom, 1.4×10^6 cells ml^{-1} (Buskey et al., 2001), and *P. minimum* bloom, $> 10^5$ cells ml^{-1} (Tango et al., 2005).

Each dinoflagellate was measured with the LISST after being diluted with the collected natural seawater to obtain bloom concentrations of 100, 50, and 10% of a "full bloom" concentration. In addition to these measurements another LISST measurement was taken with only the collected seawater in the chamber to determine baseline measurements. The seawater collected from Crystal Beach had time for the particles in the water to settle out because the LISST measurements were done 2 days after collection to allow for large particles such as sand to settle out but allow for biological organisms to remain in the water. The seawater collected at Galveston was used to run

this experiment twice. On the day the water was collected the 3 different bloom concentrations of each dinoflagellate species was run through the LISST. Due to this being surf zone water, the water was extremely cloudy and turbid. A base line of the seawater was also measured. Two days after the Galveston water was collected, the experiment was run again once the sediments in the sample had settled out.

Karenia brevis growth curve. A flask of 750 ml of autoclaved 0.2 μm filtered artificial seawater with L1 nutrients and K. BREVIS (2228) was grown in a 22 °C incubator (14 h light: 10 h dark). The growth of K. BREVIS (2228) was monitored by measuring culture absorbance at 664 nm with a UV-Mini Shimadzu spectrophotometer. LISST measurements were taken during cell growth and during the stationary phase to determine whether there is a change in PSD at different stages of growth. Data was analyzed using SigmaPlot 11.0. Two-way analysis of variance (ANOVA) was used to determine whether there was a significant difference in the PSDs produced by the LISST at different times of growth. ANOVA was conducted on data that met the assumptions of normality and equality of variance.

Results

Scattering signatures of HAB species. The volume concentration in the last size bin (median particle size of 460 μm) was highly variable; because of this the volume concentration data from this size bin was not included in the subsequent analysis. The volume concentration calculated from each size bin was normalized to the total volume concentration in the 31 size bins in order to directly compare the harmful algae species (Rzadkowolski and Thornton 2012). The PSD of each HAB species produced a different

scattering signature, though some are very similar. A peak in the PSD was defined as 3 or more sequential size bins that contained a volume concentration greater than the mean volume concentration. As the scattering signatures reported are the fraction of total volume concentration from data in the first 31 size bins, the mean volume concentration in all graphs is a constant 0.032. Fig. 3a, Fig. 3b, and Fig. 3c represent the PSDs produced by the LISST for each of the 10 HAB species. A summary of the PSD differences can be found in Table 2.

In Fig. 3a each of the *Karenia* cultures were compared to determine whether the LISST could detect differences in the PSD of the same genus, and even the same species though they were different genetic strains. *K. brevis* (2228) had a sharp peak at 23.4 μm while the Texas strains *K. brevis* (Campbell) and *K. mikimotoi* (Campbell) had a sharp peak at 27.6 μm though *K. mikimotoi* (Campbell) had a larger relative peak height (i.e. volume concentration).

The larger of the HAB species measured *C. longipes* (1770), *A. monilatum* (3105), and *P. piscicida* (1830) were compared to determine the LISSTs ability to detect differences in the larger particles (Fig. 3b). While *A. monilatum* (3105) had one sharp peak at 45.3 μm, *P. piscicida* (1830) produced the largest range of peaks covering 17 size bins. *C. longipes* (1770) produced a peak in the last size bin used in this analysis (390 μm). Though *C. longipes* (1770) is not that large of a phytoplankton (refer to Table 1) the peak could be due to the formation of aggregates. Lastly, the PSD of *A. lagunensis* (1502), *P. minimum* (2780), *K. veneficum* (2936), and *Pseudo-nitzchia* sp. (1309) were compared (Fig. 3c). *A. lagunensis* (1502) and *Pseudo-nitzchia* sp. (1309)

produced similar scattering signatures with the difference coming in the location of their second peak, 27.6 μm and 19.8 μm respectively *K. veneficum* (2936) and *P. minimum* (2780) have a peak at 10.2 and 12.1 m respectively, with their main difference being in the relative peak height with *K. veneficum* (2936) being 2.8 and *P. minimum* (2780) being at 5.2 (Table 2).

Dilution series of dinoflagellates. Dilution series of the dinoflagellate *K. brevis* (2228) was done in monoculture to show the relationship between dinoflagellate biomass based on cell counts and integrated volume concentration via the LISST (Fig. 4). For *K. brevis* (2228) the laser was significantly attenuated at a concentration of 4.85×10^5 cells ml^{-1}. In this monoculture situation, the dilutions have shown that the total LISST volume and cell concentration have a proportional, linear relationship (*K. brevis* (2228) $r^2=0.94$).

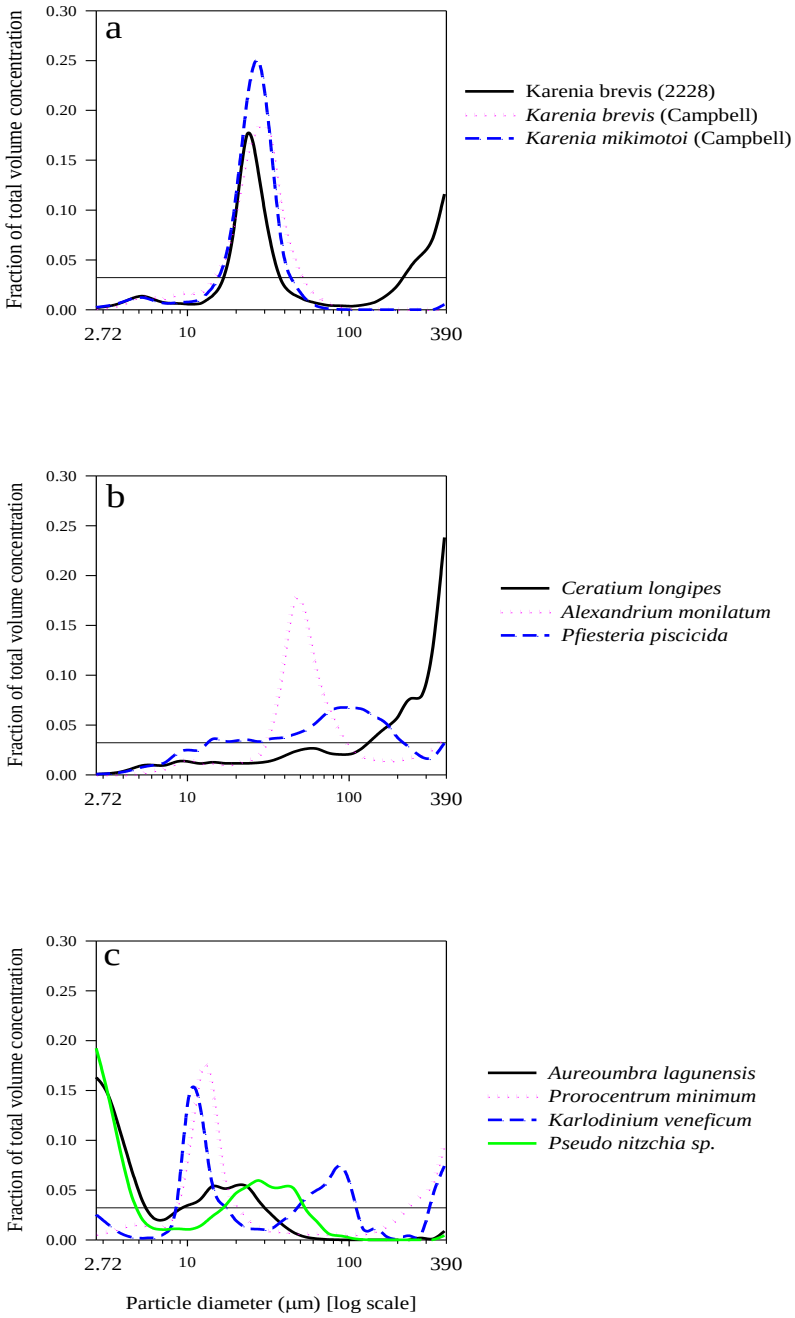

Fig. 3. Particle size distributions (PSDs) of ten harmful algal bloom (HAB) species in 31 size bins normalized to the total volume concentration of particles. The horizontal line represents the mean volume concentration. The smooth curves were drawn through the average (n=100) fraction of volume concentration in each size bin. (a),*K. brevis* (2228), *K. brevis* (Campbell), and *K. mikimotoi* (Campbell) (b), *C. longipes* (1770), *A. monilatum* (3105), and *P. piscicida* (1830) (c), *A. lagunensis* (1502), *P. minimum* (2780), *K. veneficum* (2936), and *Pseudo-nitzchia* sp. (1309).

Table 2. Scattering signature characteristics of 10 HAB species measured with the LISST. The table shows the number of peaks, the median size bin of the peak at which the particles are located (μm), relative peak height, the range of the peak referred to by the number of size bins it spans, and the width of the peak (μm). The analysis of the PSD did not include the largest size bin (460 μm).

	Peaks	Size bin (median, μm)	Relative peak height	Range of peak (# of size bins)	Width (μm)
Alexandrium monilatum (3105)	1	45.3	5.4	7	55.4
Aureoumbra lagunensis (1502)	1	2.72	5.1	5	2.55
	2	19.8	1.7	7	17.4
Ceratium longipes (1770)	1	390	7.4	7	246
Karenia brevis (2228)	1	23.4	5.5	5	15.7
	2	390	3.2	4	153
Karenia brevis (Campbell)	1	27.6	5.6	7	28.5
Karenia mikimotoi (Campbell)	1	27.6	7.7	6	21.6
Karlodinium veneficum (2936)	1	10.2	2.8	5	8.15
	2	87.9	1.3	5	50.5
Pfiesteria piscicida (1830)	1	87.9	2.1	17	186.8
Prorocentrum minimum (2780)	1	12.1	5.2	6	11.15
	2	390	3	4	153
Pseudo-nitzchia sp. (1309)	1	2.72	6	4	1.74
	2	27.6	1.8	7	28.5

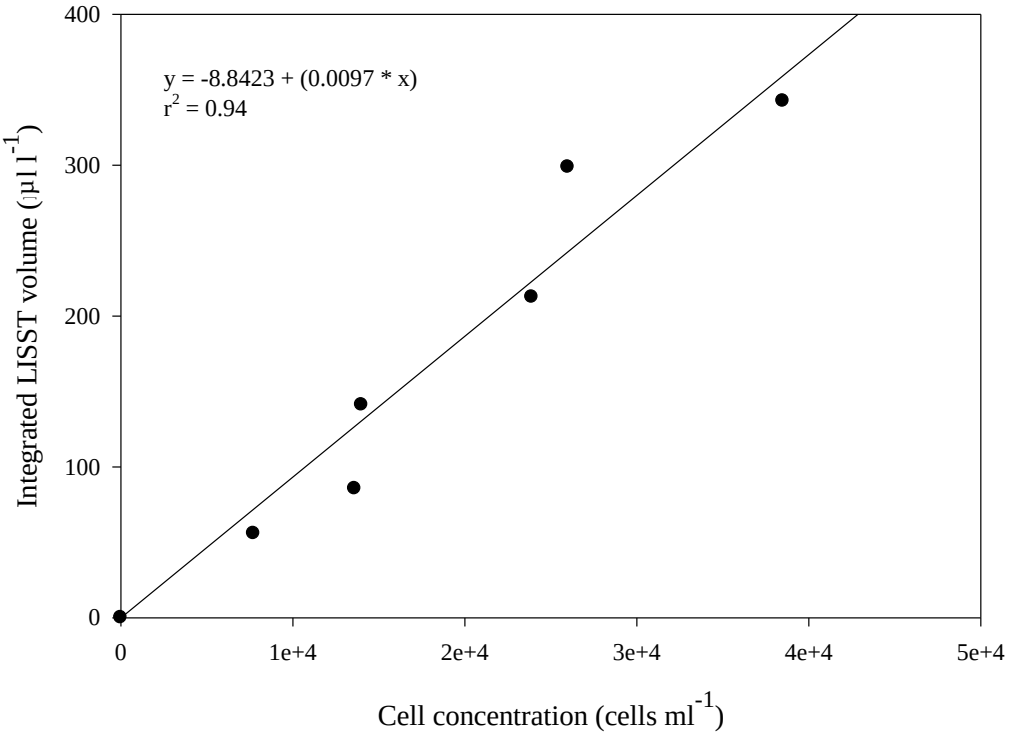

Fig. 4. Dilution series of the dinoflagellate *K. brevis* (2228) compared to integrated LISST PSD volumes. This represents the relationship between cell concentration and integrated LISST volume (n=100).

LISST detection of harmful algae against background of collected natural seawater: Crystal Beach. At 10% of an *A. lagunensis* (1502) bloom (1.4 x 10^4 cells ml^{-1}, Buskey et al. 2001), the LISST detected a peak at 2.72 µm (Fig. 5a) corresponding with *A. lagunensis* (1502) scattering signature. With cell concentrations higher than 10% of a bloom, the laser in the LISST attenuated. *P. minimum* (2780) could not be detected at 10% concentration, but at 50% and 100% (5.00 x 10^4 cells ml^{-1} and >10^5 cells ml^{-1} respectively, Tango et al. 2005) there was a peak at 2.72 and 12.1 µm similar to its scattering signature (Fig. 5b). The *K. veneficum* (2936) peak was similar to that of *P. minimum* (2780) with the same peaks at 50% concentration and an additional broad peak at 144 µm (Fig. 5c). The only real way to distinguish between *P. minimum* (2780) and *K. veneficum* (2936) is that *P. minimum* (2780) had a larger volume concentration. *K. brevis* (2228) could not be detected at 10% bloom concentration (535 cells ml^{-1}, Vargo et al. 2002), but at 50 and 100% the 23.4 µm peak corresponded with *K. brevis* (2228)and there was an additional peak at 87.9 µm at 50% concentration (Fig. 5d). With Crystal Beach surf zone water, at some concentrations the dinoflagellates were detected with the LISST.

Turbid Galveston seawater. A. lagunensis (1502) was not detected at any bloom concentration due to background particles and laser attenuation (Fig. 6a). *P. minimum* (2780) could not be detected at 10% or at full bloom concentration due to background particles and laser attenuation respectively. At 50% bloom concentration, a peak was produced at 2.72 and 12.1 µm again indicating that the LISST was able to detect *P. minimum* (2780) in the water sample (Fig. 6b). *K. veneficum* (2936) could not be

detected at 10% but at 50% peaks were produced at 12.1 and 144 µm with an additional peak at 2.72 µm at 100% bloom concentration (Fig. 6c). Again, this PSD was very similar to *P. minimum* (2780) but at 50% concentration *P. minimum* (2780) again had the higher volume concentration. *K. brevis* (2228) could not be distinguished against background particles at 10 or 50% bloom concentration. However, at 100% there was a slight peak at 23.4 µm (Fig. 6d) indicating that *K. brevis* (2228) was present.

Settled Galveston seawater. At 10% *A. lagunensis* (1502) produced a single peak at 45.3 µm. At 50% concentration, a peak is formed at 2.72 and 45.3 making *A. lagunensis* (1502) more distinguishable in the water sample (Fig. 7a). Laser attenuation occurred at the "full" bloom concentration. At 10% *P. minimum* (2780) could not be detected, but at 50 and 100% the *P. minimum* (2780) scattering signature could be seen with a peak at 2.72 and 12.1 µm (Fig. 7b). *K. veneficum* (2936) had the same PSD for each concentration as *P. minimum* (2780), but again *P. minimum* (2780) had the larger volume concentration with 23 µl l^{-1} compared to 13 µl l^{-1} (Fig. 7c). *K. brevis* (2228) was not distinguishable based on the scattering signature produced for it at any bloom concentration (Fig. 7d).

Karenia brevis growth curve. K. brevis (2228) was used to determine whether the LISST would be able to monitor the dinoflagellate at different phases of growth. The growth curve showed that growth occurred for 28 days before hitting the stationary phase for 6 days followed by cell death (Fig. 8). On day 13 of growth, *K. brevis* (2228) was at a concentration of 7.92×10^4 cells $ml^{-1}$and a measurement was taken with the LISST producing a scattering signature typical of *K. brevis* (2228) with a peak at 23.4

μm (Fig.9). On Day 22 of growth, the culture had reached a concentration of 1.03 x 10^5 cells $ml^{-1}$and another LISST measurement was taken. No data was gathered due to laser attenuation. On Day 34 when *K. brevis* (2228) had decreased in concentration (5.84 x 10^4 cells ml^{-1}) another LISST measurement was taken. The data gathered from the LISST was normalized so the difference in biomass would not affect the scattering signatures produced. During cell death, the scattering signature produced by the LISST was different from data produced during the growth phase. Day 34 produced 2 peaks with the volume of particles in the 23.4 μm size bin decreasing and shifting towards the larger 87.9 μm size bin (Fig. 9). Although visually different, a two-way ANOVA with day and LISST size bins as a source of variation showed that there was no statistically significant difference.

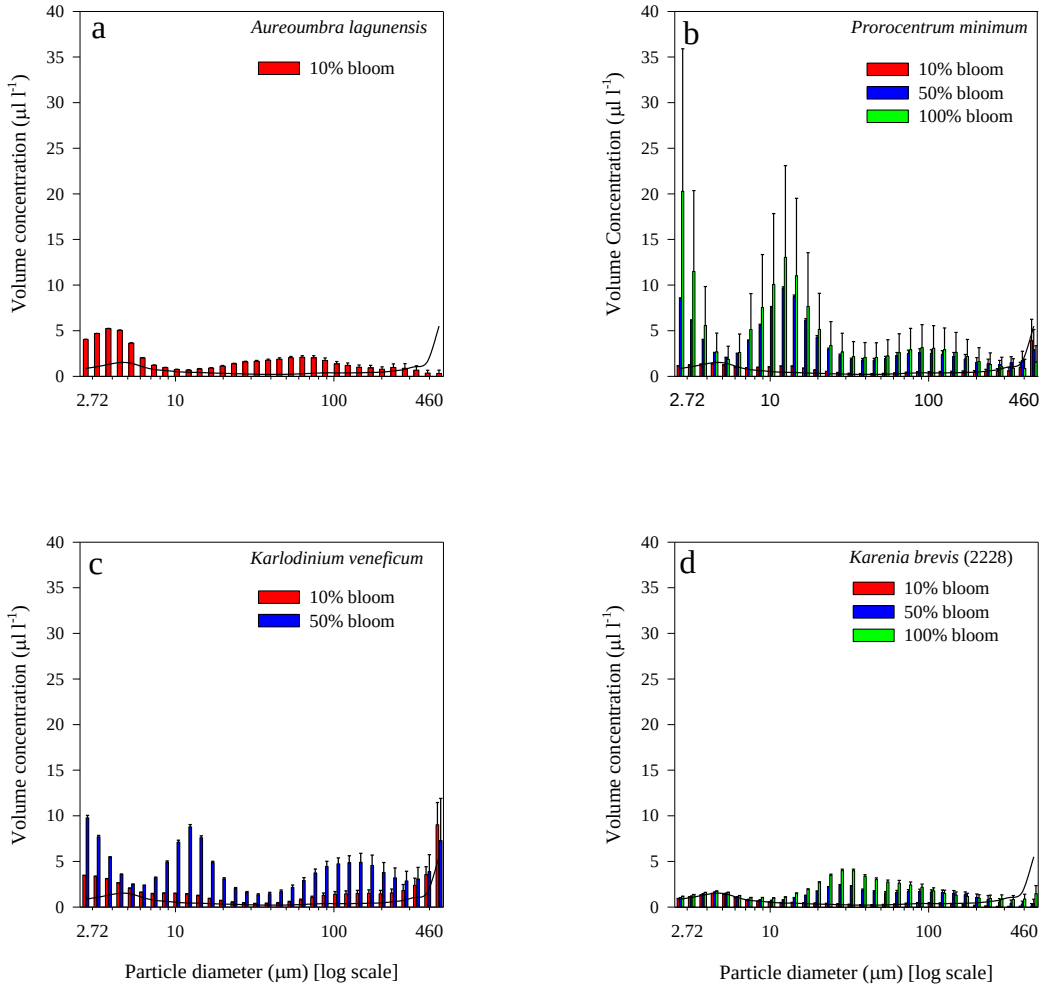

Fig. 5 The PSD of dinoflagellates against a background of collected surf zone seawater from Crystal Beach, TX in February 2011. Measurements were taken 2 days after collection. The spline curve represents the PSD of the collected water with no other additions. Red bars indicate 10% of a bloom concentration, blue bars 50% bloom concentration, and green bars 100% of a bloom concentration. Bars represent mean (n = 100) + SD. (a), *A. lagunensis* (1502) (b),*P.minimum* (2780) (c), *K. veneficum* (2936) (d), *K. brevis* (2228).

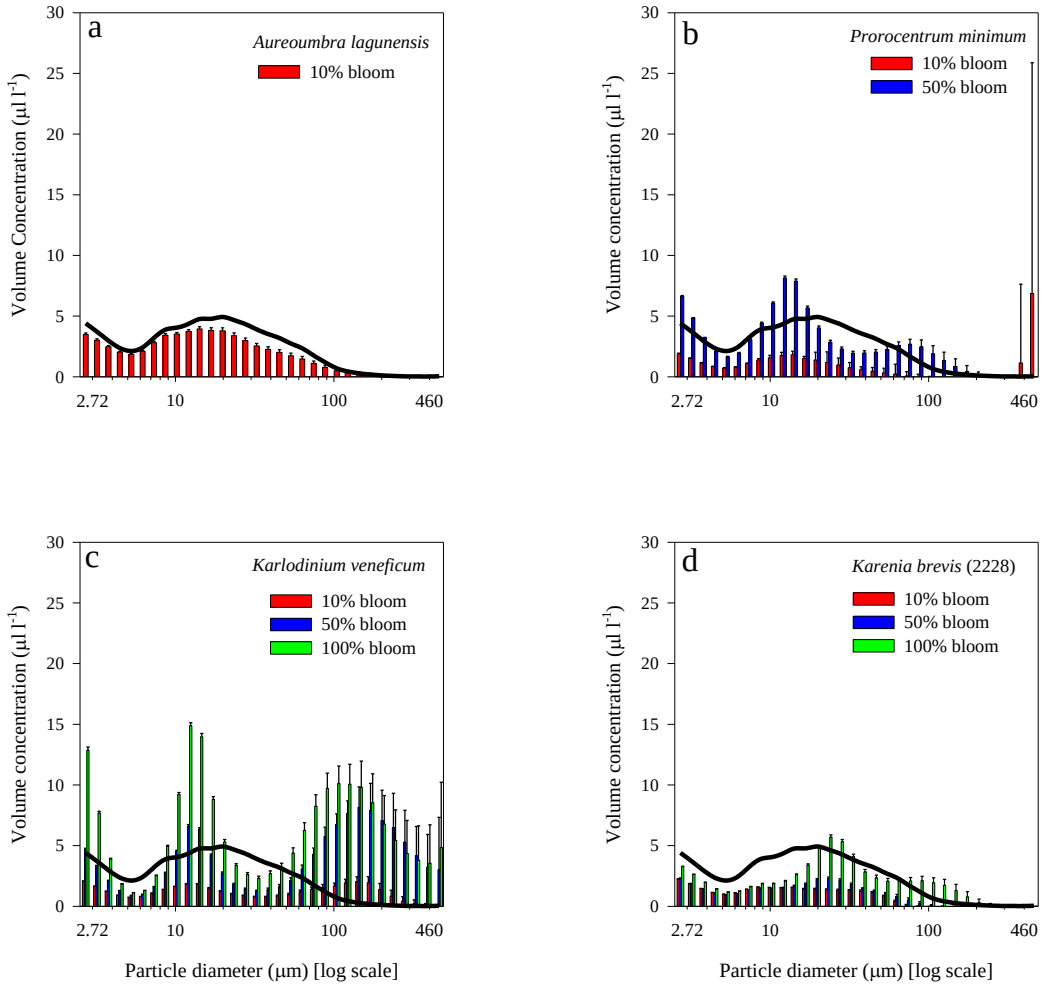

Fig. 6 The PSD of dinoflagellates against a background of collected surf zone seawater from Galveston, TX in April 2011. Measurements with the LISST were made the same day the water was collected. The spline curve represents the PSD of the collected water with no other additions. Red bars indicate 10% of a bloom concentration, blue bars 50% bloom concentration, and green bars a 100% of a bloom concentration. Bars represent mean (n = 100) + SD. (a), *A. lagunensis* (1502) (b),*P.minimum* (2780) (c), *K. veneficum* (2936) (d), *K. brevis* (2228).

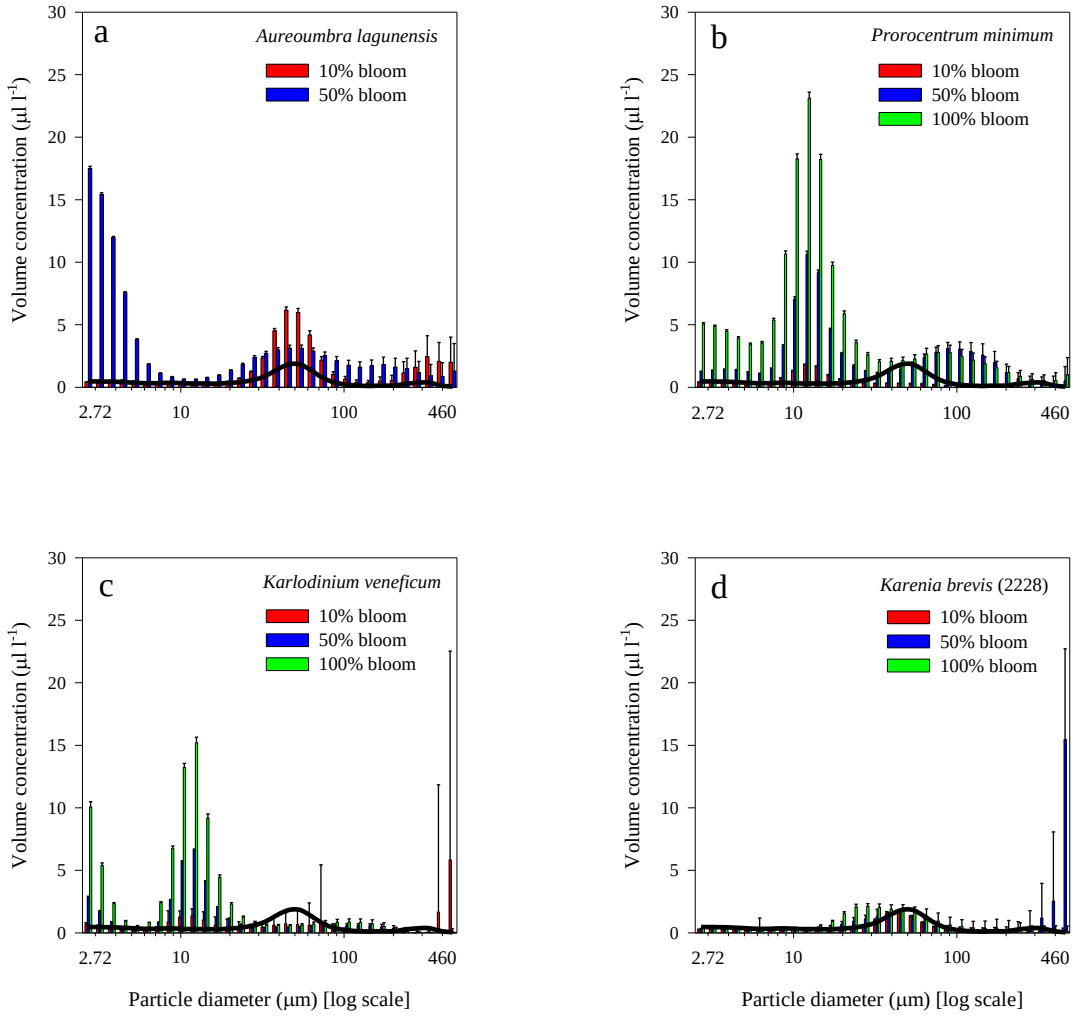

Fig. 7 The PSD of dinoflagellates against a background of collected surf zone seawater from Galveston, TX in April 2011. The measurements were taken 2 days after the collection of the water so larger sediment particles could settle out. The spline curve represents the PSD of the collected water with no other additions. Red bars indicate 10% of a bloom concentration, blue bars 50% bloom concentration, and green bars a 100% of a bloom concentration. Bars represent mean (n = 100) + SD. (a), *A. lagunensis* (1502) (b),*P.minimum* (2780) (c), *K. veneficum* (2936) (d), *K. brevis* (2228).

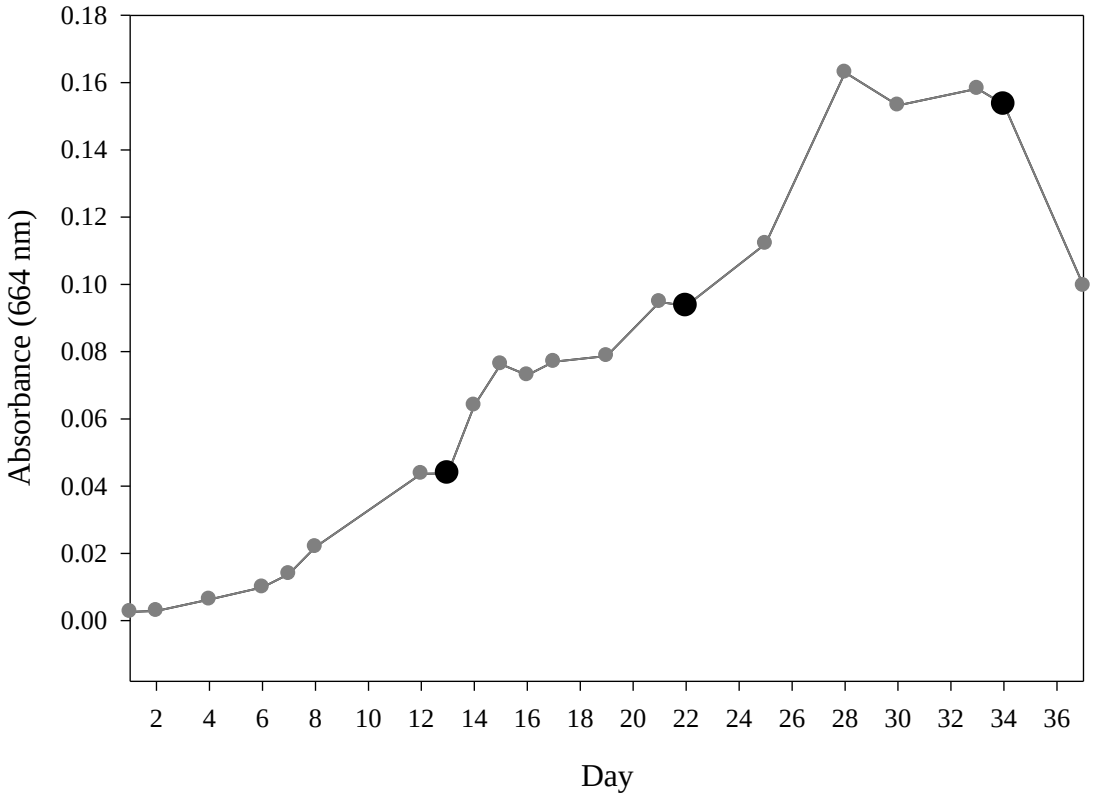

Fig. 8 Growth curve of *K. brevis* (2228) determined using a Shimadzu UV-Mini spectrophotometer at an absorbance of 664 nm. Black filled dots indicate days at which samples were taken and run through the LISST-100X (Type C).

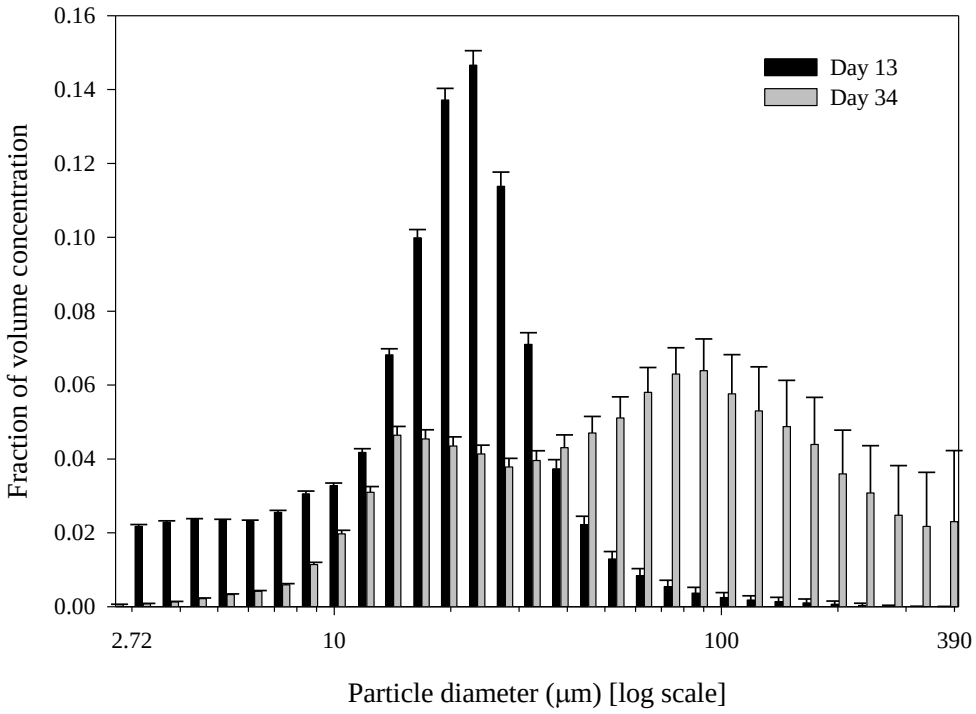

Fig. 9 Particle size distribution (PSD) of day 13 and day 34 of *K. brevis* (2228)growth experiment showing the difference in scattering signatures between growth phase and stationary phase. Bars represent mean (n=100) + SD.

Discussion

The LISST is able to measure particles from a range of 2.5 to 500 μm, though due to measurement noise affecting the inversion calculations made; only 10-12 distinct peaks are able to be resolved over this size range (Sequoia Scientific, Bellvue, WA). Harmful algae, especially the dinoflagellates, tend to have a similar shape and though they may have different cellular dimensions under the microscope, their similar size can cause them to become indistinguishable in PSDs produced by the LISST. For this reason, as Table 3 shows, a PSD can give more information to characterize different harmful algae species than just peak location. Through a combination of peak location, number of peaks, peak widths, and range of the peaks, the harmful algae species were able to be distinguished from one another. Rzadkowolski and Thornton (2012) measured six different diatom species with the LISST and determined that the LISST could be used as a tool to monitor the distribution, growth and aggregation of diatoms. Rienecker et al. (2008) measured the PSDs of three dinoflagellates (*Alexandrium*, *Ceratocorys*, and *Pyrocystis*) which were all spherical in nature and produced a single peak in the PSDs. Rienecker et al. (2008) also proved that the harmful algae *Pseudo-nitzchia* produced a PSD in the lab that matched ones taken *in-situ* providing a basis that the LISST could be used to monitor and detect harmful algae. Using these results as a foundation for this experiment, the LISST has shown that it is able to produce PSDs for each of the ten harmful algae species used in this experiment (Fig. 3). During this experiment, samples in the LISST were taken based off visual inspection of the culture flasks to ensure cells were still in the growth phase. As each species grew at a different

rate it was important to normalize the volume of each size bin to the total volume of all size bins to account for the difference in cell concentrations and to compare the PSDs of the harmful algae species. An organism's aspect ratio, the ratio of the cells length to width, will allow us to predict how many peaks will be on the PSD produced by the LISST. Organisms that contained a high aspect ratio (length:width > 2) such as *Pseudo-nitzchia* produced multiple peaks while low aspect ratios produced one. Harmful algae that produced one peak due to a low aspect ratio (< 2), and the LISST not being able to detect the difference in cell dimensions corresponds with the findings of Traykovski et al. (1999) who concluded that for there to be two peaks on a PSD of a mixture of two natural sediment, the diameter of the two sediments would have to differ by at least a factor of 2.

Against a background of seawater collected at different locations, different time of year, and different turbidity, harmful algae at times could be detected if they produced peaks distinct from that of the background particles and their abundance was relatively high (but not sufficient to attenuate the laser) compared with the volume concentration of the background particles. Our data indicated that the volume concentration produced by the LISST corresponds to the cell biomass put in the chamber (Fig. 4). This indicates the LISST can be used not only to determine the presence of a HAB species, but can be used to measure the abundance of the HAB species in water. However, the relationship between the LISST volume concentration and a species biomass differs with different species. Rzadkowolski and Thornton (2012) found that there was a linear relationship between cell concentration and volume concentration measured with the LISST in

cultures of the diatom *Chaetoceros mulleri*. The slope and intercept for each linear relationship is different, based upon the shape of the species. Against different backgrounds, the PSD of the HAB species did not always have the same peak location. For example, Fig. 6d and Fig. 7d show the scattering signature of *K. brevis* (2228) against collected water from Galveston, with one sample being run the day the water was collected and the other two days later. On the day the water was collected *K. brevis* (2228) produced a scattering signature similar to the PSD recorded (Fig. 3a) with the peak location at 23.4 µm. Two days later when measurements were taken again the peak shifted to 27.6 µm. Agrawal and Pottsmith (2000) noted that particles of the same diameter class could occupy several size bins due to the mathematical models used by the LISST limiting the resolution of the particle size class detection leading to leakage of particles into the size bins closest to the particles actual diameter. This could apply for single particles, but leakage would not occur for an entire population of particles, leading to the conclusion that leakage does not explain the shift in size bins. These results give further confirmation to what previous researchers has noted that peak location provided by the PSDs produced by the LISST is insufficient to determine the presence of HAB species on its own (Andrews et al. 2010). The *K. brevis* (2228) strain must have had a change in the culture or in the medium to produce such a distinct shift. The cells could have acclimated to new culture conditions due to their lack of being in their natural environment, or growth of other organisms in the seawater could have occurred causing this change in the PSD. LISST instruments are not able to distinguish between phytoplankton and other particles in the seawater, nor is it able to determine the

physiology of the cells in the water. Aggregation, or increase cell size due to environmental change could all be possible reasons for the shift in the PSD. To account for the limitations of the LISST, it should be combined with other technologies, such as chlorophyll fluorometers and species confirmation should be done by microscopic observation (Serra et al. 2001).

When different concentrations of bloom densities were placed in the LISST with natural seawater, laser attenuation occurred at high cell biomasses. Once a bloom reaches a concentration high enough to cause laser attenuation, the bloom would already be established and any warning given to the public would be too late. The LISST has shown it can be a tool in the early detection of HAB formation. HABs generally form thin layers which are dramatic patches where large numbers of photosynthetic organisms are found generally several centimeters thick and extending for kilometers horizontally (Dekshenieks et al. 2001, Moline et al. 2010, Durham and Stocker 2012). These thin layers can be beneath the surface causing satellite monitoring of HABs to be ineffective, offering little warning time to alert fisheries (McManus et al. 2008). Since the LISST can be placed on a mobile platform it would be able to monitor bloom formation beneath the surface.

Unfortunately for this experiment, only surf zone seawater could be easily accessed. Harmful algal blooms do not generate in the surf zone off coasts, and therefore that water was not ideal for testing the LISST's abilities in detecting HABs. Water should be collected slightly offshore where blooms occur, and where crashing waves are not causing increased turbidity. Although the surf zone water collected caused problems

with laser attenuation in the LISST, it did show that even against a background particle field on extremely turbid water, the LISST was able to detect HABs at some bloom concentrations. With this knowledge, it is a natural assumption that in clearer water offshore where blooms form, the LISST will be able to detect HABs at early concentrations of a full bloom to allow for their early detection.

To determine whether the LISST would be able to detect HAB formation and continue to monitor the bloom through different growth phases, *K. brevis* (2228) was continuously monitored. As Fig. 9 shows, on day 13, *K. brevis* (2228) produced its signature PSD. As time went on day 34 of *K. brevis* (2228) growth, the PSD produced is nothing like a *K. brevis* (2228) scattering signature. Dinoflagellates such as *K. brevis* (2228) can have complicated life cycles, though bloom formation for *Karenia brevis* generally occurs during their vegetative cell state (Van Dolah et al. 2008). The vegetative cell of *K. brevis* (2228) produces the peak shown in Fig. 9 on day 13. The PSD produced on day 34 could be due to cell death and more particles being in the sample due to the release of the organelles from inside the cell. The organelles could have caused aggregation of the cells due to their stickiness. These data show that the LISST can be used to monitor the initial growth of the HAB species into the bloom, but cannot be used for continued monitoring through cell death. To further refine what stages the LISST would be able to detect, this experiment should be run again with more frequent LISST measurements taken to determine exactly when the PSD produced changes. Microscopic observations should also be made at times to determine the state of the cells in the culture to understand what is happening to the culture.

As much as an advantage the LISST is in detecting HABs, with it being low cost, easy to use, and no moving parts, there are some limitations as to what the LISST is able to measure. Honjo et al. (1984) showed that stringy scatters are present in marine environments and therefore the LISST with its spherical approximation is not a suitable instrument for *in-situ* detection. In natural environments there may be particles smaller (e.g. bacteria) or larger (e.g. zooplankton) than the size range measured by the LISST, which in turn could affect the laser scattering (Rzadkowolski and Thornton 2012). The LISST is limited to monitoring blooms because a diverse community of phytoplankton would cause overlying scattering signatures, but as HABs are generally monospecific in nature, this would not be an issue. LISST instruments are not able to detect individual particles unlike flow cytometry imaging instruments; however those instruments are more complex to run and are more expensive than the LISST. The LISST has been proven to map the distribution of dinoflagellates such as *Ceratium* in Monterey Bay (Rienecker et al. 2008), *Alexandium taylori* in the Meditteranean Sea off the coast of Spain (Anglès et al. 2008), and *Lingulodinium polyedrum* in California coastal waters (Ahn and Grant 2007). Although the LISST has limitations, the LISST can be used as a low cost tool to detect the early formation of HABs *in-situ*. For complete accuracy, samples should be taken and looked at underneath a microscope when blooms are suspected to be forming for species verification.

CHAPTER III

EFFEECTS OF TEMPERATURE AND BACTERIA ON THE PRECUROSRS FOR DIATOM AGGREGATION

Methods: Temperature effects on *Odontella aurita*

Experimental design. To test the effect of temperature, bacterial abundance, TEP concentration, and CSP concentration on diatom aggregation the diatom *Odontella aurita* was chosen to act as a model as it is a cosmopolitan species. The diatom *O. aurita* was purchased from Provasoli-Guillard NCMA strain number 1776. One ml of *O. aurita* was placed in each of the 6 flasks of 40 ml autoclaved 0.2 µm filtered Harrison's artificial seawater (Harrison et al. 1980; Berges et al. 2001) with L1 nutrients and incubated at 20 ºC (14 h light: 10 h dark). Three of the flasks contained bacteria and the other three had 400 µl of penicillin (400 µg ml^{-1}) and streptomycin (200 µg ml^{-1}) added. After 24 hours, 400 µl of neomycin (200 µg ml^{-1}) and ampicillin (200 µg ml^{-1}) were added to the same 3 flasks to produce an axenic culture. After 2 weeks of growth each bottle was subcultured and 1 ml of each flask was aseptically placed in a new flask of 40 ml autoclaved 0.2 µm Harrison's artificial seawater with L1 nutrients and placed back into the 20 ºC incubator (14 h light: 10 h dark) for an additional 2 weeks. Bacteria counts (see method below) were used to determine which cultures were axenic.

After the 2 weeks, twelve glass bottles were filled with 500 ml of autoclaved 0.2 µm filtered Harrison's artificial seawater and L1 nutrients were added to each bottle. Bottles 1, 2, 3, and 4 (referred to as Control group) had 1 ml of *O. aurita* added that

contained bacteria to be used as a control. Bottles 5, 6, 7, and 8 (referred to as Antibiotic group) also had 1 ml of *O. aurita* added that contained bacteria, and 5 ml of penicillin (400 µg ml^{-1}), streptomycin (200 µg ml^{-1}), neomycin (200 µg ml^{-1}), and ampicillin (200 µg ml^{-1}) were added to the bottles to determine the effects that antibiotics have on *O. aurita* aggregation. Bottles 9, 10, 11, and 12 (referred to as Axenic group) had 1 ml of an *O. aurita* culture added in that was considered axenic. The bottles were placed in a fish tank with a temperature controlled water bath (VWR recirculating pump model 1196D) with two 40 watt Deluxe bulbs placed on two side of the tank supplying 160 µmol photons m^2 s^{-1} to illuminate cultures (14h light: 10 h dark). The bottles were set up like this for three different experiments run at different times. One experiment was run at 20 ºC where cell counts were taken every 24 hours while chlorophyll *a*, carbohydrates via the phenol-sulfuric acid method, LISST measurements, and TEP staining and analysis samples were done on Days 7 and 11 with bacteria counts via DAPI were done on Day 11. The experiment was run again at 20 ºC and once more at 28 ºC. Cell counts and cell density measurements via absorbance (Shimadzu UV-Mini spectrophotometer at 750 nm) were taken every 24 hours while chlorophyll *a*, carbohydrates via the phenol-sulfuric acid method, LISST measurements, and TEP staining and analysis were done on Days 6, 9, and 13, and CSP staining and analysis was done on Days 6 and 13. Bacteria counts using DAPI were done on Day 13.

Cell counting and cell densities. Cell counts (see method under LISST characterization of harmful algae) of each culture were taken every day of the experiment. Cell densities were determined by taking 1 ml of each culture and placing it

in a cuvette and measuring the absorbance with a (Shimadzu UV-Mini spectrophotometer) at a wavelength of 750 nm and were measured every day.

Phenol-sulfuric acid carbohydrate analysis. From each culture on Days 6, 9, and 13, a 1.2 ml aliquot was used to determine the total carbohydrate concentration. Total carbohydrate concentration was determined based on the phenol-sulfuric acid method as described by DuBois et al. (1956) . A calibration curve was constructed by the addition of 1 g of D-glucose in 1000 ml UHP water creating dilutions of 100, 50, 40, 30, 20, 10, 5, and 0 µg D-glucose ml^{-1}. Using the Dubois et al. (1956) method, the standards, as well as the samples, were analyzed spectrophtometrically using a Shimadzu UV-Mini spectrophotometer following the combination of 0.8 ml of sample to be analyzed, 0.4 ml phenol (5% w/v), and the quick addition of 2 ml concentrated sulfuric acid in a glass boiling tube. The boiling tubes were agitated and then left to sit for thirty minutes. The calculation of total carbohydrates for each culture was calculated based on their absorbance at 485 nm from the standard represented in µg D-glucose equivalents per milliliter.

Chlorophyll a analysis. At 20 ºC and 28 ºC on Days 6, 9, and 13 a 1 ml aliquot per culture was filtered down onto a 25 mm GF/C filter and placed into a centrifuge tube and frozen in the dark at -20 ºC until analysis. A calibration curve was made based off TD-700 Laboratory Fluorometer Application Note (www.turnerdesigns.com).When analyzed, 4 ml of cold (4 ºC) 90% acetone was combined with the macerated filters in 15 ml centrifuge tubes. The tubes were covered with foil to prevent light penetration and were placed in the refrigerator to extract for 24 hours. The tubes were centrifuged at

1000 rcf for 5 minutes to obtain the supernatant and the absorbance of the extract was measured with a Turner Designs 700 fluorometer. To correct for blanks, blanks of 90% acetone were measured with the fluorometer and the concentration recorded was referred to as R_b. One drop of HCl was added to the acetone blank and left to sit for 5 minutes before measurement with the fluorometer. The concentration was recorded as R_a. To obtain the before:after ratio of a pure chlorophyll *a* solution (r):

$$r = R_b/R_a$$

Samples were then measured with the fluorometer and the concentrations recorded were referred to as R_d. A drop of HCl was added to each sample and measurements were taken after the sample sat for 5 minutes, and the concentration shown was recorded as R_c. To determine the amount of chlorophyll *a*, the following equation was used:

$$\text{Chlorophll } a, \mu g/l = (r/r\text{-}1)(R_d\text{-}R_c)$$

To obtain the concentration of chlorophyll *a* in the entire sample:

Total chl *a* = (chlorophyll *a* µg/l)*(extraction volume of acetone ml)/(volume of sample filtered ml)

TEP Staining. TEP was stained and size measured according to the methods in Alldredge et al. (1993) and Passow et al. (1994). On Day 6, 1.25 ml of Harrison's artificial seawater (Harrison et al. 1980; Berges et al. 2001) and 0.75 ml of a culture were filtered together using a glass column under low pressure (150 mm Hg) onto a 0.4 µm polycarbonate filter on top of a GF/C glass fiber filter. Then this was followed by 1 ml of Alcian Blue to stain the TEP particles, and lastly two separate rinses of 0.5 ml of 0.2µm-filtered UHP water were used to remove any excess dye. The 0.4 µm

polycarbonate filter was taken off the apparatus and mounted in fluorescent stable microscopy oil atop a GE Osmotics CytoClear® frosted slide and placed in a microscope slide box and stored in the freezer (-20 ºC) until analysis. On Days 9 and 13, TEP slides were made following the same technique as described above however 1.75 ml of Harrison's artificial seawater will be used in combination with 0.25 ml of a culture. A total of 2 ml was always filtered to ensure even distribution of sample on filter (Hobbie et al. 1977).

CSP Staining. CSP staining followed the procedure of Long and Azam (1996). On Day 6 and 13 CSP slides were made. A Coomassie Brilliant Blue (CBB) dye working solution was prepared by diluting the CBB stock dye 25 times with 0.2 µm filtered artificial seawater. The filtration apparatus was set up using a GF/C glass fiber filter placed under a 0.4 µm Nucleopore filter which collected the organic particles. A specified volume of 2 ml was filtered on both days to ensure an even distribution of the sample. On Day 6, 1.25 ml of Harrison's artificial seawater and 0.75 ml of a culture was filtered together using a glass column under low pressure (150 mm Hg) onto the 0.4 µm polycarbonate filter. Then this was followed by 1 ml of CBB to stain the CSP particles, and lastly two separate rinses of 1 ml 0.2µm-filtered UHP water to remove the excess dye. The 0.4 µm polycarbonate filter was taken off the apparatus and mounted in fluorescent stable microscopy oil atop a GE Osmotics CytoClear® frosted slide and placed in a microscope slide box and stored in the freezer (-20 ºC) until analysis. On Day 13 the same procedure was used with the exception of only 0.25 ml of each culture was

used and combined with 1.75 ml of Harrison's artificial seawater due to the density of cell biomass.

Roller experiment. To determine the practicality of LISST instruments as tools in detecting changes in particle size distributions due to diatom aggregation, rollers were set up in incubators to induce aggregation in the different *Odontella aurita* cultures. This allowed for aggregation to be related to TEP concentration, CSP concentration, and bacteria abundance. In the first experiment at 20 ºC, on Days 7 and 11, 80 ml of each culture was transferred under sterile conditions into a 100 ml amber glass bottle. Each was sampled with the LISST before being placed on one of two roller tables, rolling at approximately 12 rpm, in the 20 ºC incubator. After a culture had been on one roller table for 2 hours it was transferred to the other table to ensure every bottle was being rolled evenly. After 4 hours on the roller tables each culture was carefully poured into the LISST chamber and another measurement was taken. A histogram was produced for each sample day of the differences in PSDs from before aggregation was induced to after aggregation had occurred.

In the second and third experiment at 20 and 28 ºC respectively, the same method as above was used, however, each culture was diluted with 0.2 µm filtered artificial seawater that had an overall temperature of 20 or 28 ºC based on the experiment. The cultures were diluted to a specific concentration to obtain a constant cell concentration to ensure that cell concentration did not affect aggregation. At 20 ºC each culture was diluted to 3.70×10^4 cells ml^{-1}, while at 28 ºC the Control group and Axenic group were diluted to a concentration of 3.70×10^4 cells ml^{-1} and the Antibiotic group was diluted to

a concentration of 2.29 x 10^4 cells ml^{-1} due to their slower growth rate. Cultures were placed on the roller tables and LISST measurements were taken on Days 6, 9, and 13 and a histogram was produced for each day showing the difference in PSDs from before aggregation occurred to after.

TEP - microscopic analysis. To determine the amount of TEP particles in the culture, the CytoClear® TEP slides were placed atop a Carl-Zeiss Axioplan2 microscope and observed underneath 100x brightfield. Pictures were taken d their perimeters were manually outlined using Axiovision (Carl-Zeiss), in order to determine TEP surface area for each culture. As this technique is not time efficient, TEP particles from the first 20 ºC experiment were analyzed like this and the Control group for Days 6, 9, and 13 in the second 20 ºC experiment were done this way. All other TEP particles were analyzed via image analysis and a graph comparing the two techniques was produced.

TEP and CSP – image analysis. To provide more quantitative measurements of TEP and CSP present in the cultures, average particle size, total area, and particle numbers were computed using image analysis. The National Institue of Health's (NIH) WCIF Image J open source image analysis suite (http://www.uhnresearch.ca/facilities/wcif/download.ntml) was used to analyze TEP and CSP particles produced by *O. aurita*. Using the CytoClear® slides made containing the filters of TEP and CSP particles, each slide was mounted on a Carl-Zeiss Axioplan2 microscope and observed underneath 100x brightfield. Each slide had 10 adjacent pictures taken moving from top to bottom on each slide (Fig. 10a). Each image had to have the cells removed from the picture by coloring over them as this analysis was only

looking at the organic particles not the diatoms (Fig. 10b). ImageJ requires a binary image in order to automatically analyze the particles. To do this, a threshold range was chosen that included all the pixels that composed of the particles being looked at, in this case TEP and CSP. Since TEP and CSP have to be stained to be seen, the color information of these particles was used to enhance the contrast between the particles and the background. This led to the composite RGB picture to be split into individual red, blue, and green channels. The red channel provided the best contrast and accentuated the stained particles, so it was used to set the threshold range (Fig. 10c) The original photo with no modifications and the red channel are compared visually to confirm that that threshold set includes as many as the stained particles as possible without background noise being included in the analysis. Once this threshold was set, a binary image was produced (Fig. 10d). Image J has an "Analyze particle" algorithm which was used to draw an outline around each particle, recording particle areas as small as 10 μm^2 with no upper limit to how large the particle can be (Fig. 10e). Particles on the edge of the picture that are not fully shown were not counted nor measured to get a more accurate particle size and average particle area. The particle size information gathered can be gained from the major or minor axis of the particle based of the best fitted ellipse surrounding it.

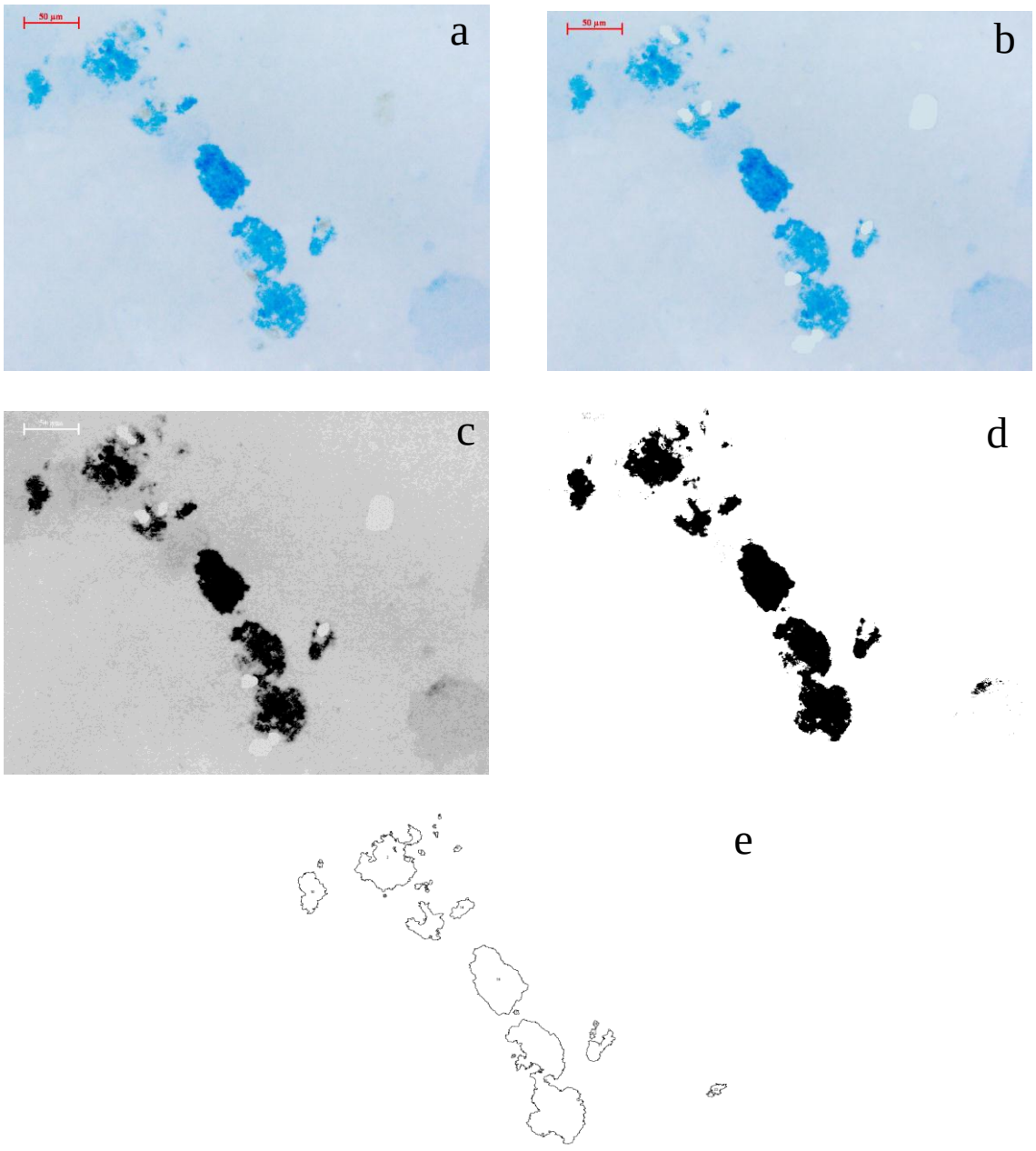

Fig. 10 Series of images produced by ImageJ to determine particle size.. (a) original photo taken with microscope, (b) diatom cells colored out using ImageJ so only particles being analyzed will be seen, (c) red color channel to better distinguish particles, (d) color threshold set to produce the binary image used to size particles, (e) final outline of particles being studied.

Bacteria abundance. Before the beginning of the temperature experiments and on the last day of the temperature experiments bacteria counts were used to determine the bacteria abundance in each culture. Microcentrifuge tubes were autoclaved under sterile conditions, 1 ml of each culture was placed in a centrifuge tube and stained with 50 µl of DAPI (4'6-diamidino-2-phenylindole di hydrochloride) and placed in the refrigerator (4 ºC) for one hour (Proctor et al., 1991). After 1 hour under sterile conditions, 0.5 ml of the sample and 1.5 ml of 0.2 µm filtered autoclaved UHP water were filtered together onto a 0.2 µm black membrane filter and rinsed twice with UHP water. The membranes were then transferred onto a glass slide and placed in a microscope slide case in the freezer (-20 ºC) until analysis. Bacteria in each culture were analyzed by counting 400 bacteria in the cultures under a fluorescence microscope according to Porter and Feig (1980).

Data analysis. Data gathered was analyzed using SigmaPlot 11.0 (Systat software). Correlation analysis was conducted using the Pearson product moment correlation to determine whether TEP and CSP production in *Odontella aurita* correlated with cell growth. One-way and two-way ANOVA was conducted on data that met the assumptions of normality and equality of variance. When the data did not meet these assumptions, the data was log transformed (log[x + 1]) before analysis or a non-parametric ANOVA was carried out on ranks (Kruskal-Wallis ANOVA). With data that compared fixed factors, pairwise comparisons were made using post-hoc tests. The Holm-Sidak method was used to make pair-wise comparisons of the data when the group sizes were equal and there was no missing data.

Methods: Bacteria effects on *Odontella aurita*

Experimental design. Bacteria and abiotic processes can affect TEP and CSP formation (Passow 2000) therefore looking at how these processes interact will reveal more about TEP and CSP. A flask containing 750 ml of autoclaved 0.2 µm filtered artificial seawater with L1 nutrients and 6 ml of *Odontella aurita* was placed in a 20 ºC incubator (14 h light: 10 h dark) and left to grow for two weeks. At the end of two weeks, under sterile conditions 200 ml of the 750 ml was double filtered through two 2 µm filters to remove diatoms. The filtrate was placed in a separate flask. To enhance bacterial growth in the filtrate, 1 mM glucose and 0.5 mM urea was added. Three days later, triplicate tissue culture flasks of five different treatments were made (see Table 3). To get bacteria filtrate, the bacteria culture was filtered twice with a 0.2 µm filter, and to get the diatom filtrate, the flask of diatoms was filtered twice with a 0.2 µm filter. Each of the 15 tissue culture flasks was placed randomly on a shaker table in the 20 ºC incubator (14 h light: 10 h dark) shaking at a rate of 70 rpm. Each tissue culture was moved on the shaker table every 2 hours when the light in the incubator was on to ensure equal light intensity to each flask. Bacteria counts were made using the technique described above after 2 days of shaking, and diatoms were counted as described above. TEP slides were prepared and analyzed.

TEP staining and analysis. TEP was stained and size measured according to the methods in Alldredge et al. (1993) and Passow et al. (1994). For Treatments 1, 2, and 3 1.25 ml of Harrison's artificial seawater and 0.75 ml of each triplicate flask culture were filtered together using a glass column under low pressure (150 mm Hg) onto a 0.4 µm

polycarbonate filter placed on top of a GF/C glass fiber filter. This was followed by 1 ml of Alcian Blue to stain the TEP particles, and lastly two separate rinses of 0.5 ml of 0.2µm-filtered UHP water were used to remove any excess dye. The 0.4 µm polycarbonate filter was taken off the apparatus and mounted in fluorescent stable microscopy oil atop a GE Osmotics CytoClear® frosted slide and placed in a microscope slide box and stored in the freezer (-20 ºC) until analysis. For Treatments 4 and 5 2 ml of each triplicate flask was filtered onto the 0.4 µm polycarbonate filter since the treatments contained no cells, stained, and stored the same as the previous treatments.

CSP staining and analysis. CSP was stained and size measured following the procedure of Long and Azam (1996). For Treatments 1, 2, and 3 1.25 ml of Harrison's artificial seawater and 0.75 ml of each triplicate flask culture were filtered together using a glass column under low pressure (150 mm Hg) onto a 0.4 µm polycarbonate filter placed on top of a GF/C glass fiber filter. This was followed by 1 ml of CBB to stain the CSP particles, and lastly two separate rinses of 1 ml of 0.2µm-filtered UHP water were used to remove any excess dye. The 0.4 µm polycarbonate filter was taken off the apparatus and mounted in fluorescent stable microscopy oil atop a GE Osmotics CytoClear® frosted slide and placed in a microscope slide box and stored in the freezer (-20 ºC) until analysis. For Treatments 4 and 5 2 ml of each triplicate flask was filtered onto the 0.4 µm polycarbonate filter since the treatments contained no cells, stained, and stored the same as the previous treatments.

Image J image analysis was used to determine the amount of TEP in each treatment, and was used in the same way as described above with a slight difference

between some treatments. For all treatments the "Analyze particles" algorithm was set so only particles 10 μm^2 or larger would be counted as TEP particles.

Table 3. Different culture combinations to determine whether bacteria or abiotic processes effects TEP and CSP production in the diatom *Odontella aurita*. The treatments will be referred to by the bold words.

	Diatom (*O. aurita*)	Bacteria	Bacteria filtrate	Diatom filtrate	HAR + L1 nutrients
Treatment1: **100% bacteria**	40 ml	10 ml	-	-	-
Treatment 2: **50% bacteria**	40 ml	5 ml	5 ml	-	-
Treatment 3: **No bacteria**	40 ml	-	10 ml	-	-
Treatment 4: **Medium control**	-	-	-	-	50 ml
Treatment 5: **Organic control**	-	-	10 ml	40 ml	-

Results

Temperature effect on cell growth. With an increase in growth temperature, the Control and Axenic groups of *O. aurita* had increased cell abundance from a maximum concentration of 1.10 x 10^5 cells ml^{-1} to 1.45 x 10^5 cells ml^{-1} and from 8.00 x 10^4 to 1.10 x 10^5 cell ml^{-1} respectively. Samples were taken on Day 7 and 11 in the first 20 °C based off the growth curve of the diatom made from cell counts (Fig. 11a). The growth curve was used to determine when the diatom would be in the growth phase and when it was in the stationary phase to ensure sampling in both growth stages. In the second 20 °C experiment and in the 28°C experiment samples for chlorophyll *a*, total carbohydrates, TEP, and CSP were taken on days 6, 9, and 13 based on the stage of growth of *O. aurita* (Figs. 12 & 13). Although there was an increase in cell concentration, the amount of chlorophyll *a* in each culture decreased significantly with the increase in temperature as shown by a one-way ANOVA analysis with the chlorophyll data log transformed, $F_{1,71}$ = 32.079, $p < 0.001$, and the Holm-Sidak post-hoc test showed an overall significance level of 0.05. At 20 °C the carbohydrates of each culture (Control, Antibiotics, and Axenic) followed a trend of going from approximately 25 to 80 to 30 µg ml^{-1} D-glucose equivalents with each sample day, while there was an increase in chlorophyll *a* overtime with the Antibiotic cultures having the most chlorophyll out of the three treatments with a concentration of approximately 300 µg l^{-1} (Fig. 12). With the increase in temperature to 28 °C, the Control and Axenic cultures reached a maximum of approximately 30 µg ml^{-1} D-glucose equivalents, while the Antibiotics cultures reached 65 µg ml^{-1} D-glucose equivalents (Fig. 13). The chlorophyll *a* concentration in the Antibiotic group and the

Axenic group were the highest, but only reached a third of the concentration of the Antibiotic cultures in the 20 °C experiment at approximately 90 µg l^{-1} chlorophyll *a* (Fig. 12).

Temperature effects on aggregation. In the first 20 °C temperature experiment, equal volumes of each treatment of *O. aurita* were measured with the LISST to generate a baseline measurement of the diatom before aggregation was initiated for comparison. *O. aurita* was gently rolled at 20 °C and another LISST sample was taken to generate a PSD demonstrating the effects of temperature on diatom aggregation formation. Fig. 14 represents the difference in aggregation from after being rolled to before with volume normalized PSDs for each treatment. The cell concentration placed in the LISST chamber for each sample was not standardized, causing laser attenuation to occur when the cell concentration was too high as represented in Fig. 14b. At 20 °C the Antibiotic cultures were extremely dense causing errors in the LISST. This is one reason why the 20 °C experiment was run again with a standardized cell concentration placed in the LISST chamber. All figures in Fig. 14, except Fig. 14b, show a shift in particle size from the smaller size bins to the larger size bins after rolling suggesting aggregates had formed.

In the next 20 °C experiment and in the 28 °C experiment the cell concentrations placed in the LISST chamber for each sample day (days 6, 9, and 13) were diluted with artificial seawater at the same temperature to reach a concentration of 3.70×10^4 cells ml^{-1}. The antibiotic cultures at 28 °C grew slowly at first and consequently were diluted to a concentration of 2.29×10^4 cells ml^{-1}. The control cultures had fewer large

aggregates form after rolling at 28 °C compared to 20 °C (Fig. 15). This could be due to the bacteria concentration in the cultures or due to the concentration of transparent exopolymeric particles (TEP) and coomassie stained particles (CSP). Contrarily, the Antibiotic cultures had more large aggregates form at 28 °C but there is evidence of large particles in the cultures before rolling was initiated (Fig. 16). *O. aurita* is an extremely sticky diatom, and the addition of antibiotics made it appear "stringy". This could explain the larger particles before rolling; some of the diatoms had already formed chains (Fig. 16f). The Axenic cultures had similar PSDs at both temperatures with a shift in particle diameter from the smaller size bins to the larger ones after rolling (Fig. 17).

Bacteria concentration for each temperature experiment is shown in Table 4. The bacteria counts were done on the last day of the experiment. Sterile technique was used to keep bacteria from entering the cultures, however bacteria was still able to contaminate the cultures. The control treatment has the highest bacteria concentration in each experiment which was expected, however the Axenic group was measurably contaminated, and the concentration of bacteria in the group increased with temperature. Antibiotic treated cultures had a relatively constant bacteria concentration even when the temperature was increased. The bacteria concentration did not significantly correlate with an increase in temperature between the treatments. Bacteria concentration in the cultures is significant however because bacteria are able to affect the total carbohydrate concentration detected and they can use or remineralize the nutrients intended for diatom growth.

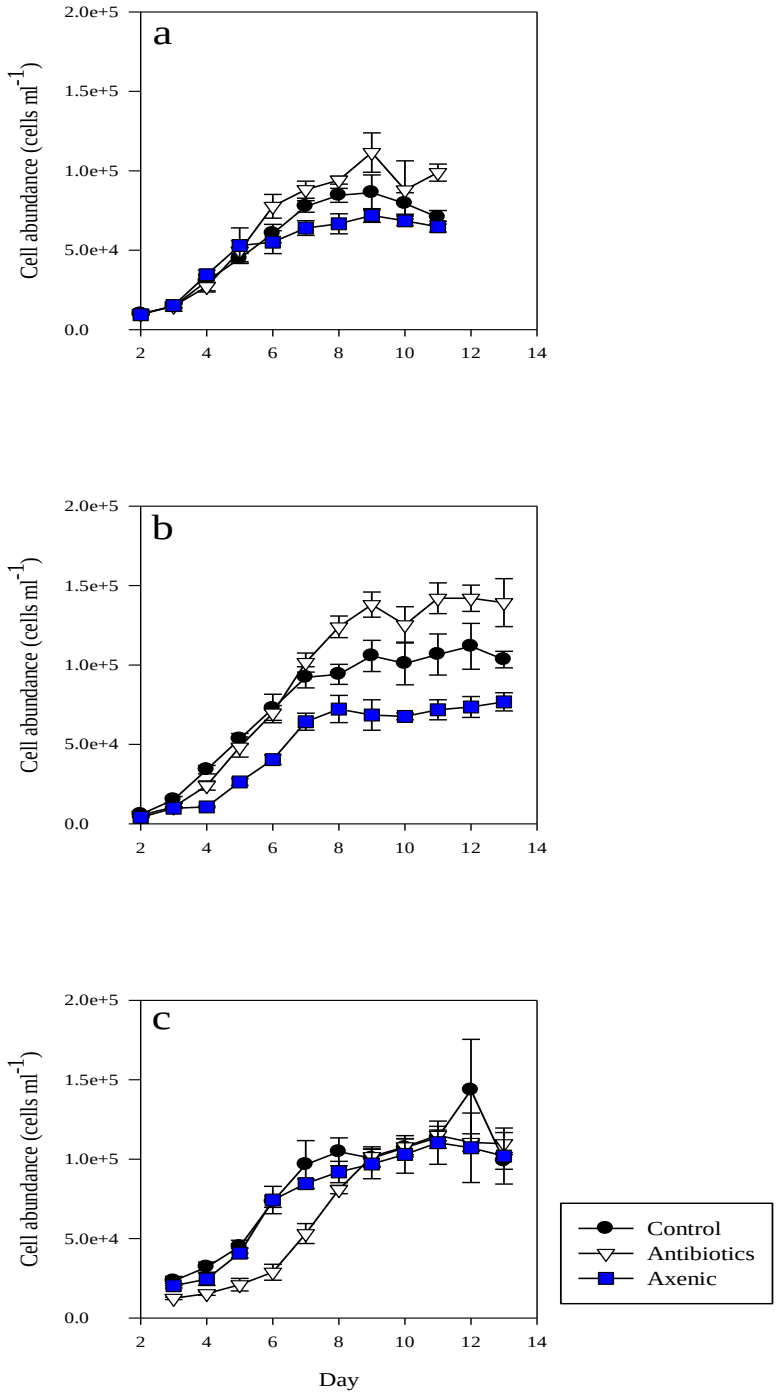

Fig. 11 Growth curve of *Odontella aurita* based off cell abundance. Points indicate mean cell abundance (n = 4) ± SD. Black circles represent the Control cultures, upside down triangles represent Antibiotic cultures, and blue squares represent Axenic cultures. (a) Cell abundances at 20 °C, (b) cell abundances of the second experiment run at 20 °C, and (c) cell abundances at 28 °C.

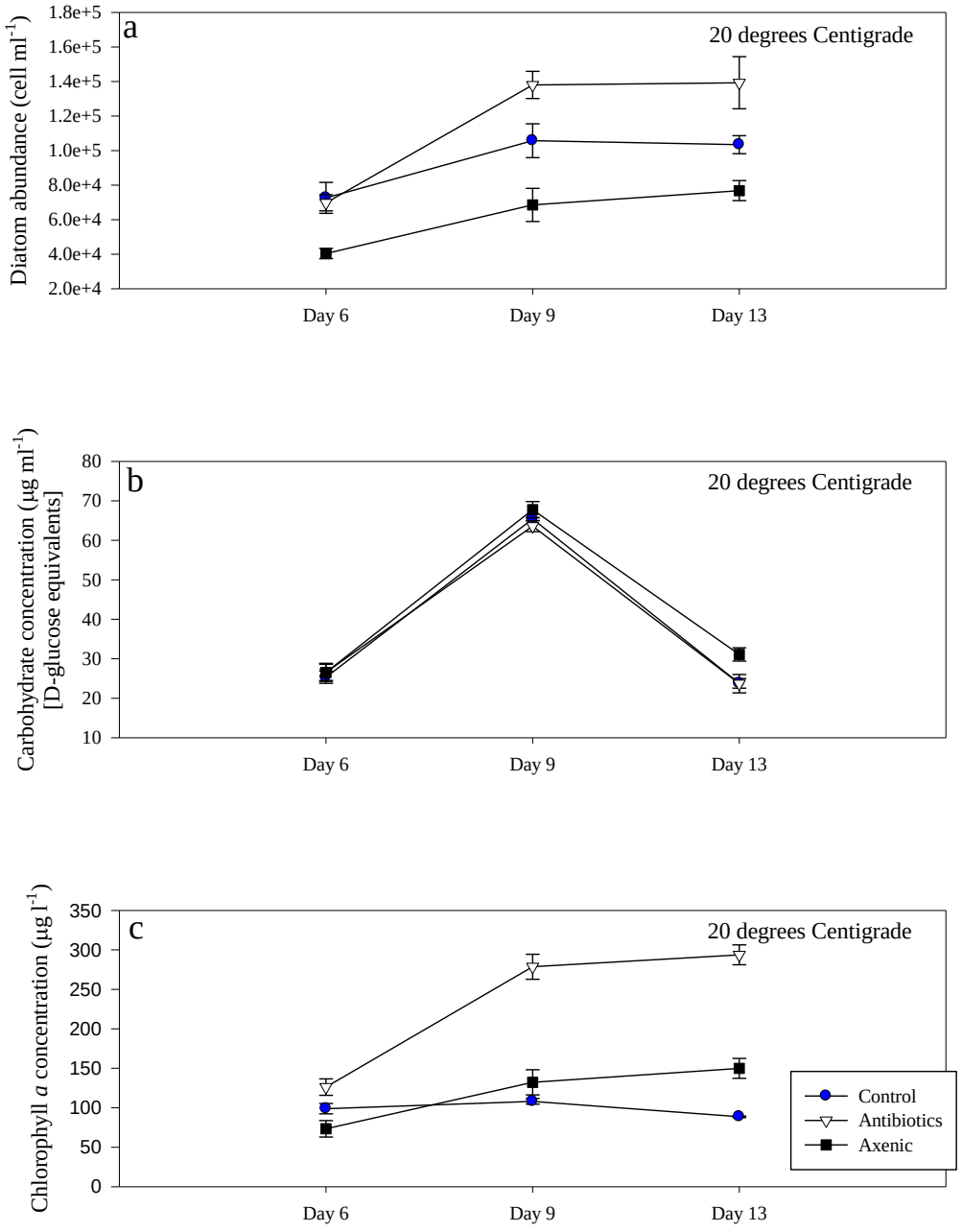

Fig. 12. *Odontella aurita* growth curve at 20 °C. Solid circles represent the Control group, upside down white triangles represent the Antibiotic cultures, and blue squares represent the Axenic cultures. (a), Diatom concentration in the cultures in cells ml^{-1} (mean ± SD; n=4) (b), total carbohydrate concentration (mean ± SD; n=4) (c), chlorophyll *a* concentration (mean ± SD; n=4).

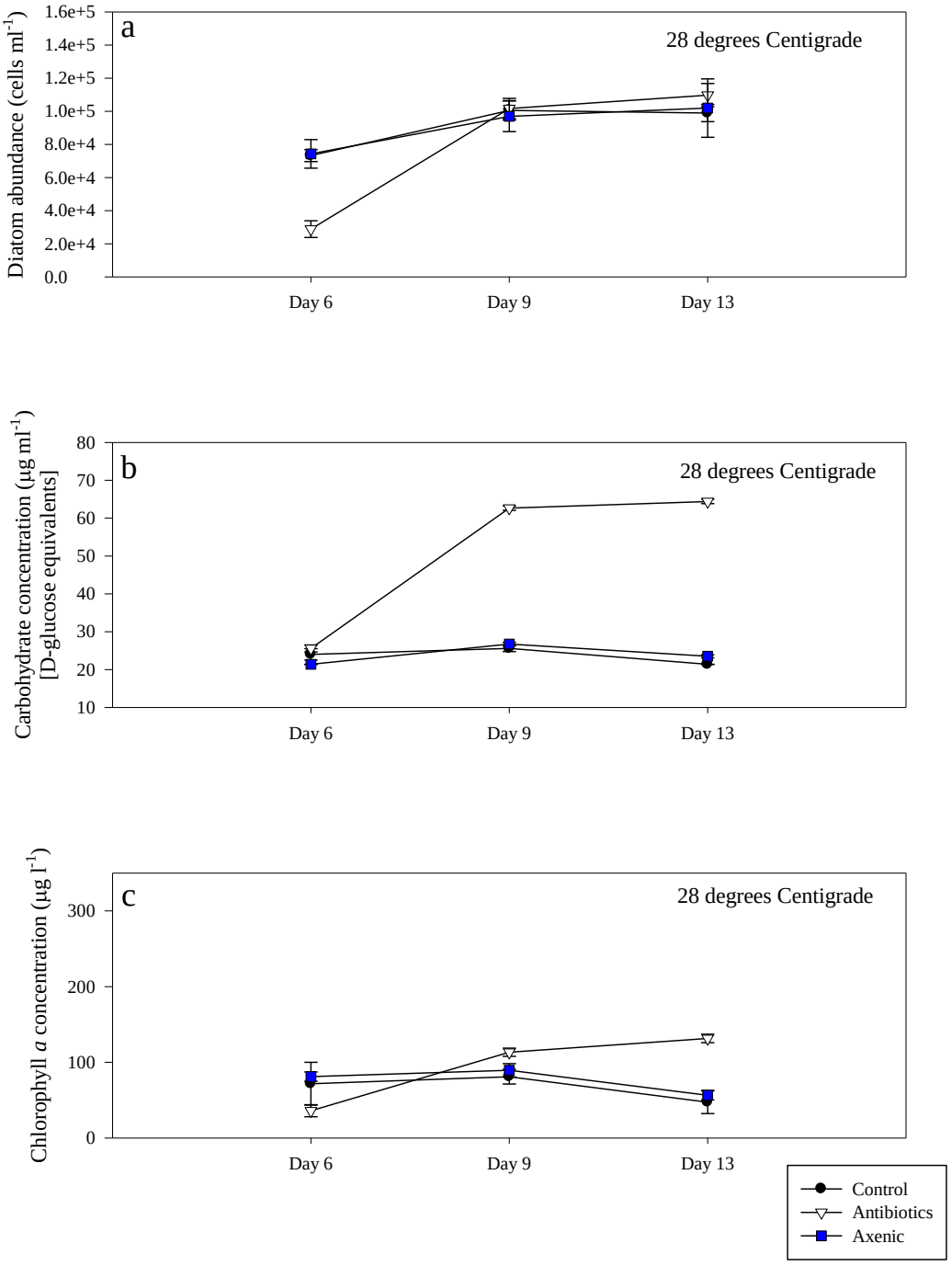

Fig. 13. *Odontella aurita* growth curve at 28 °C. Solid circles represent the Control group, upside down white triangles represent the Antibiotic cultures, and blue squares represent the Axenic cultures. (a), Diatom concentration in the cultures in cells ml^{-1} (mean ± SD; n=4) (b), total carbohydrate concentration (mean ± SD; n=4) (c), chlorophyll *a* concentration (mean ± SD; n=4).

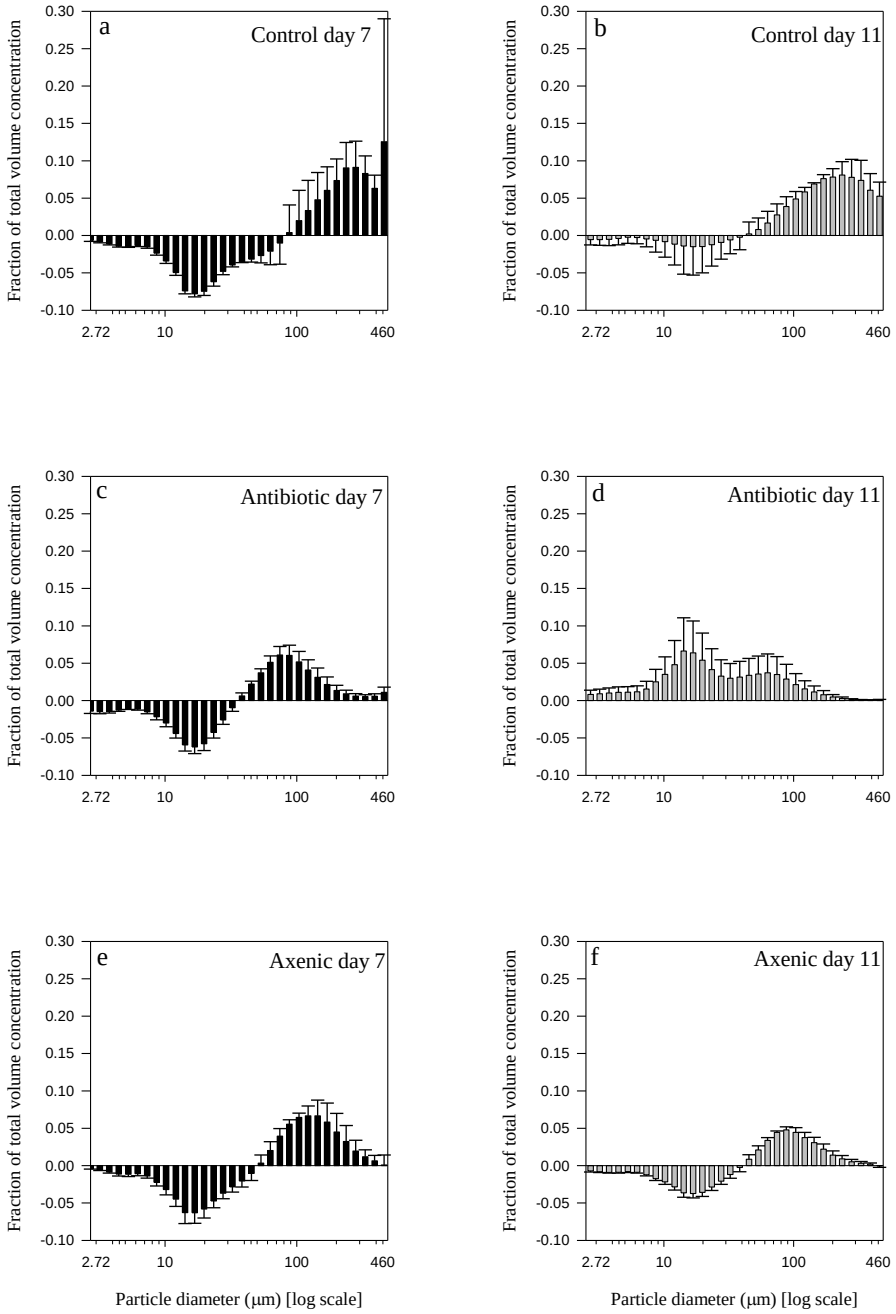

Fig. 14. Difference in particle size distributions (PSDs) of each three treatments of *O. aurita* cultures at 20 °C from being rolled to before aggregation was initiated. PSDs normalized to total volume concentration (mean values ± SD; n = 4).Black bars represent samples on day 7 and grey bars represent samples on day 11. (a) and (b) are the Control cultures. (c) and (d) are the Antibiotic cultures, and (e) and (f) are the Axenic cultures.

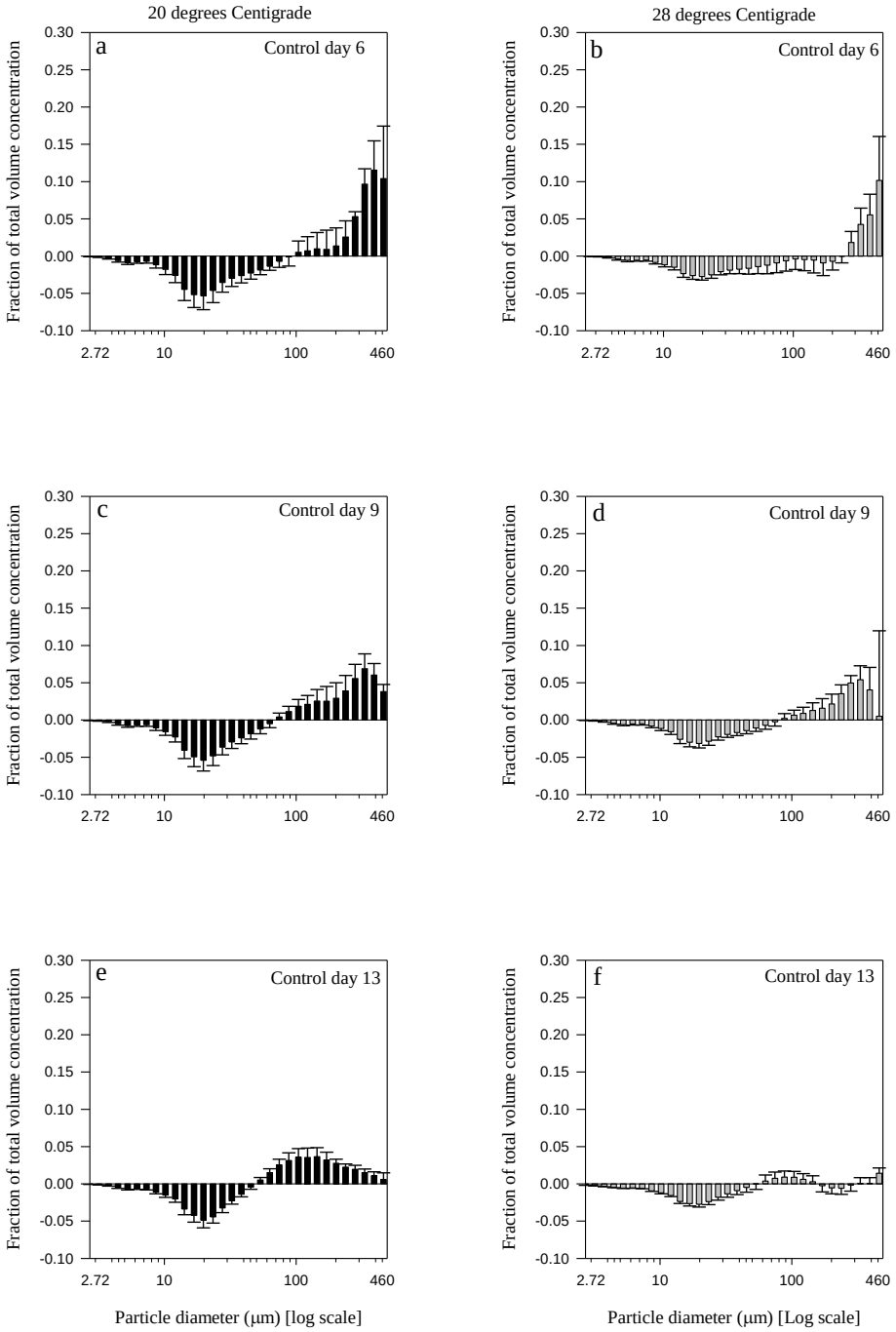

Fig 15. Difference in particle size distributions (PSDs) of the Control cultures of *O. aurita* at 20 and 28 °C from being rolled to before aggregation was initiated. PSDs normalized to total volume concentration (mean values ± SD; n = 4).Black bars represent 20 °C and grey bars represent 28 °C. (a) and (b) are LISST measurements taken on day 6. (c) and (d) are measurements taken on day 9, and (e) and (f) are day 13 measurements.

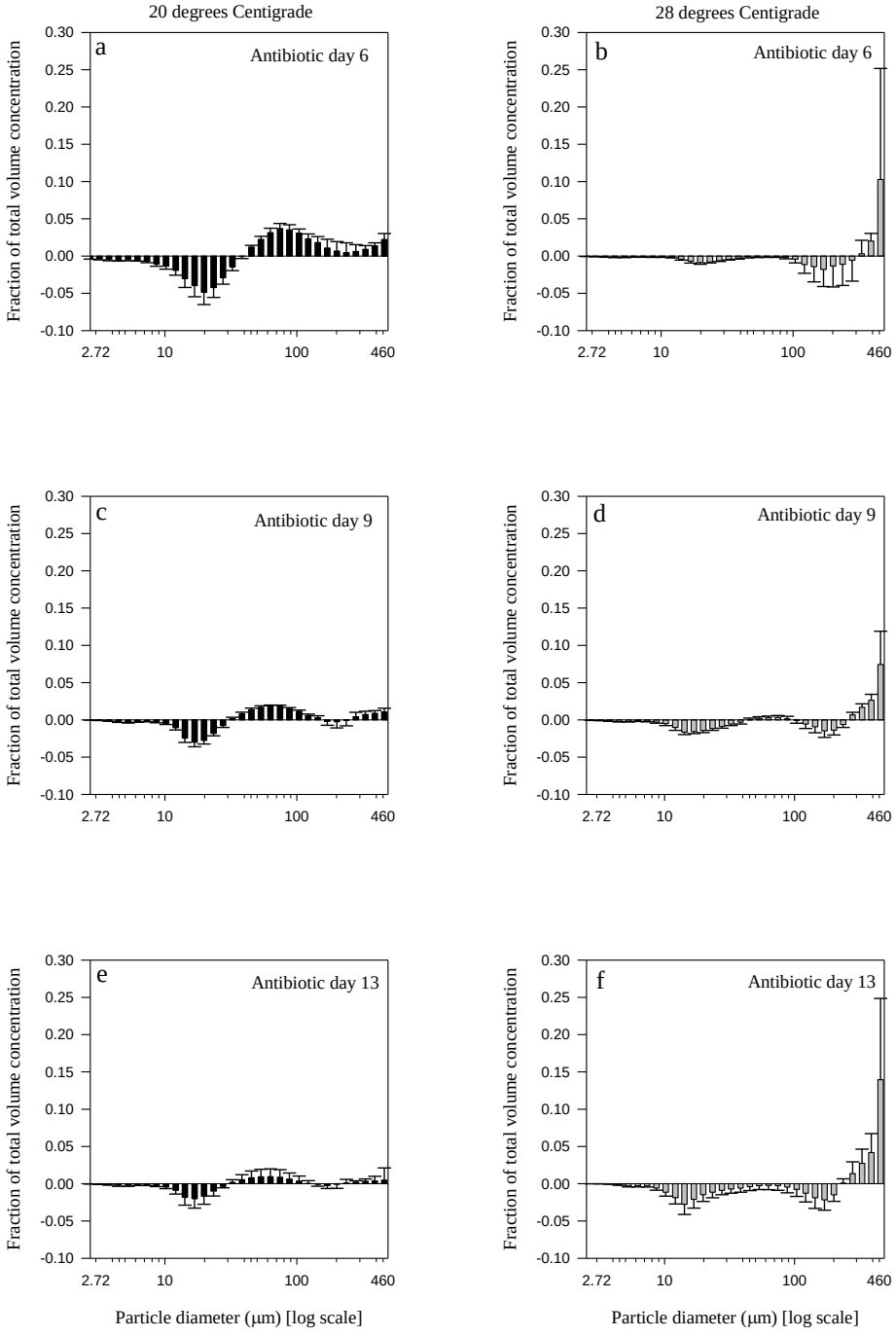

Fig 16. Difference in particle size distributions (PSDs) of the Antibiotic cultures of *O. aurita* at 20 and 28°C from being rolled to before aggregation was initiated. PSDs normalized to total volume concentration (mean values ± SD; n = 4).Black bars represent 20 °C and grey bars represent 28 °C. (a) and (b) are LISST measurements taken on day 6. (c) and (d) are measurements taken on day 9, and (e) and (f) are day 13 measurements.

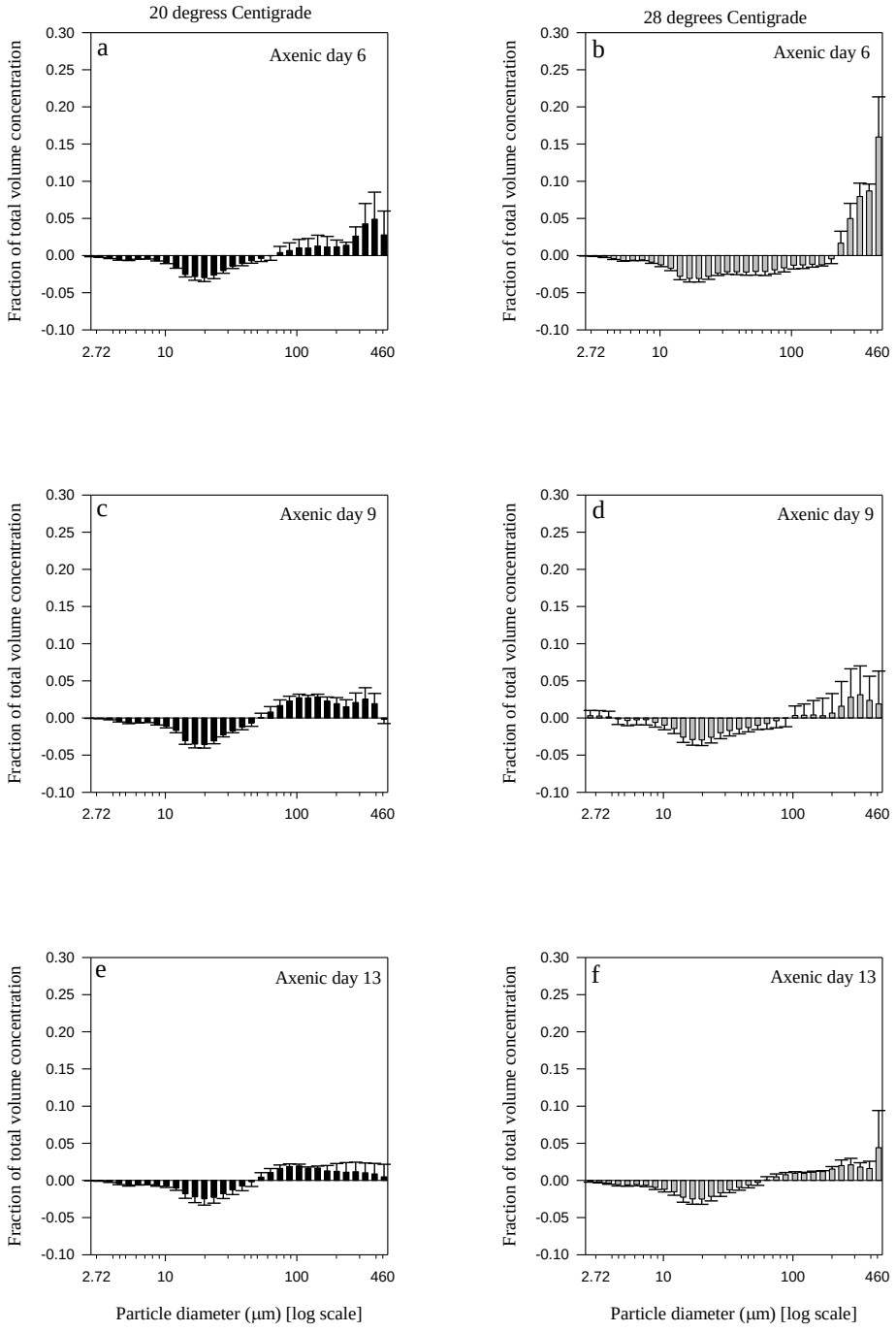

Fig 17. Difference in particle size distributions (PSDs) of the Axenic cultures of *O. aurita* at 20 and 28°C from being rolled to before aggregation was initiated. PSDs normalized to total volume concentration (mean values ± SD; n=4).Black bars represent 20 °C and grey bars represent 28 °C. (a) and (b) are LISST measurements taken on day 6. (c) and (d) are measurements taken on day 9, and (e) and (f) are day 13 measurements.

Table 4. Bacteria cell concentration in three different treatments at different temperatures. Data is referred to as mean concentration ± SD on the last day of each experiment (n=4).

	Bacteria concentration (cells ml^{-1}) ± SD		
Treatment	20 °C (1)	20 °C (2)	28 °C
Control	$7.21 \times 10^4 \pm 3.78 \times 10^4$	$1.07 \times 10^5 \pm 5.65 \times 10^4$	$7.51 \times 10^4 \pm 2.10 \times 10^4$
Antibiotic	$1.93 \times 10^2 \pm 89.5$	$1.52 \times 10^2 \pm 43.3$	$1.86 \times 10^2 \pm 34.1$
Axenic	$1.52 \times 10^4 \pm 2.51 \times 10^4$	$1.66 \times 10^4 \pm 1.45 \times 10^4$	$3.41 \times 10^4 \pm 9.64 \times 10^3$

Transparent exopolymer particles (TEP) were stained with Alcian blue (an acid polysaccharide dye) with the expectation that the TEP particles would be seen as independent particles or with cells embedded within the TEP. Under brightfield microscopy (100x magnification) TEP particles were observed as well as acid polysaccharides that appeared to coat the outside of the cells (Fig 18). The TEP particles and polysaccharides on the cells vary in size, shape, and the staining on each can be different intensities. The average size (longest dimension of the TEP particle) of the TEP particles at 20 °C and 28 °C can be seen in Fig. 19. An increase in temperature caused an overall decrease in average size of the TEP particles. However, the Axenic cultures appeared to have an increase in TEP size with temperature which could be due to an increase in the amount of bacteria in the cultures. Fig. 20 shows that there appears to be no correlation between TEP size and bacteria concentration. The decrease in particle size with temperature could explain why the Control and Antibiotic cultures did not form as many large aggregates as the Axenic cultures did (Figs. 15, 16, and 17). Total TEP area in the cultures did vary with temperature. TEP concentration in the control cultures

initially increased at 28 °C; however after day 6 it steadily decreased (Fig. 21b). The Axenic cultures remained relatively the same with temperature but there was a large increase in TEP area in the Antibiotic cultures jumping from 4,000 μm^2 at 20 °C to 10,000 μm^2 at 28 °C (Fig. 21). Total TEP per ml did not correlate with cell or bacteria concentration at either temperature (Fig. 22 and 23) suggesting a different or a number of factors affect the amount of TEP produced. Generally the amount of TEP per ml decreased over time, with the exception of the Axenic cultures at 28 °C where a large increase occurred (Fig. 22a). A two-way ANOVA with temperature and treatments as factors showed that there was a significant difference between TEP concentration per ml when the data was transformed with the change in temperature $p < 0.01$, as well as a significant difference in TEP concentration between the three different cultures, $p < 0.05$.

TEP particles were measured and counted for the Control group of the second 20 °C experiment using the microscope so a comparison could be made between TEP analysis with the microscope vs. Image J image analysis. The results show that though they have similar numbers of large particles, the average size of the particles is smaller with Image J analysis because it is able to detect the smaller particles in the photos (Fig. 24). Total TEP abundance increases when using Image J because of its ability to detect and accurately measure particles.

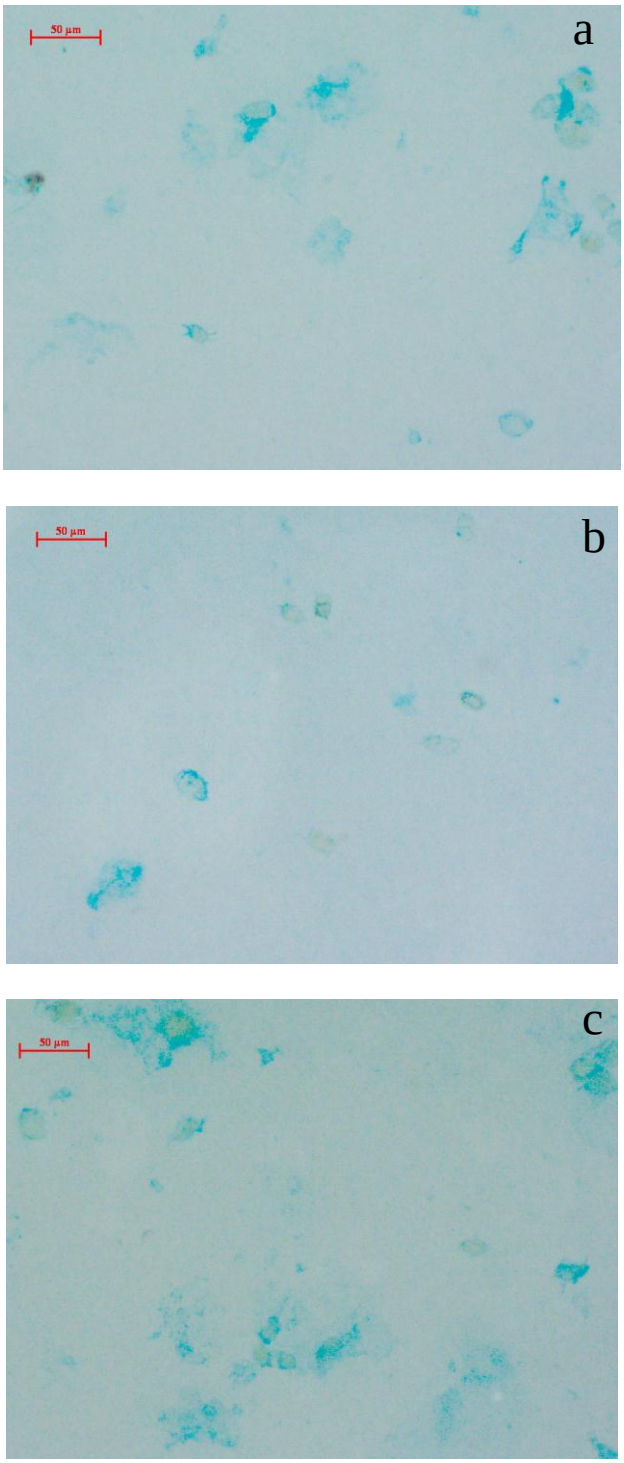

Fig. 18 Pictures of TEP particles in the *Odontella aurita* cultures at 28 °C stained with Alcian blue at 100x magnification. (a) Control culture (b) Antibiotic culture, and (c) Axenic culture. Note the presence of blue staining around the edges of the *O. aurita* cells.

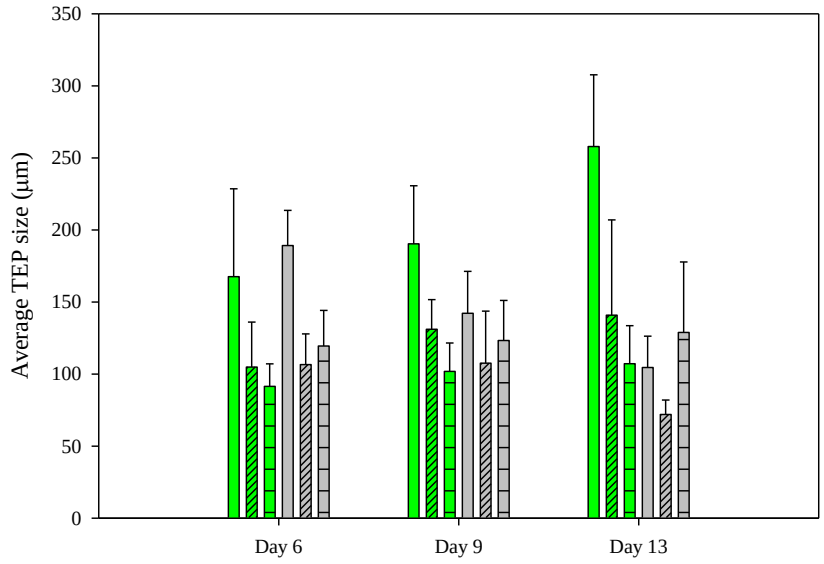

Fig. 19 Average size of TEP particles (µm), (i.e. longest cell dimension) for each culture group at different temperatures. Green bars represent average TEP size at 20 °C while the grey bars represent 28 °C. Solid bars represent the Control cultures, diagonal stripes represent Antibiotic cultures, and horizontal stripes represent Axenic cultures. Bars represent mean + SD (n=4).

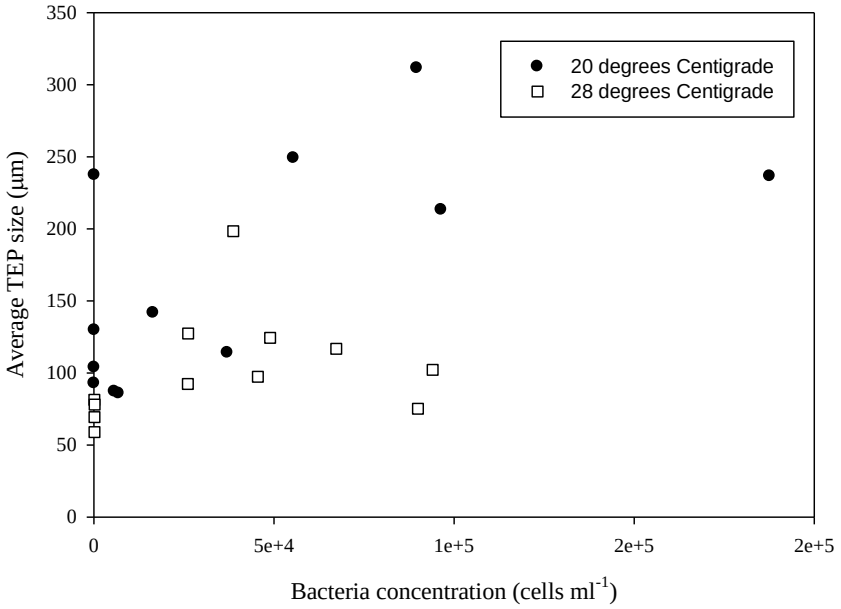

Fig. 20 Average size of TEP particles (µm) (i.e longest cell dimension) for each culture at different temperatures on day 13 of the experiment compared to bacteria concentration (cells ml^{-1}). Black dots represent cultures at 20 °C and white squares represent cultures at 28 °C.

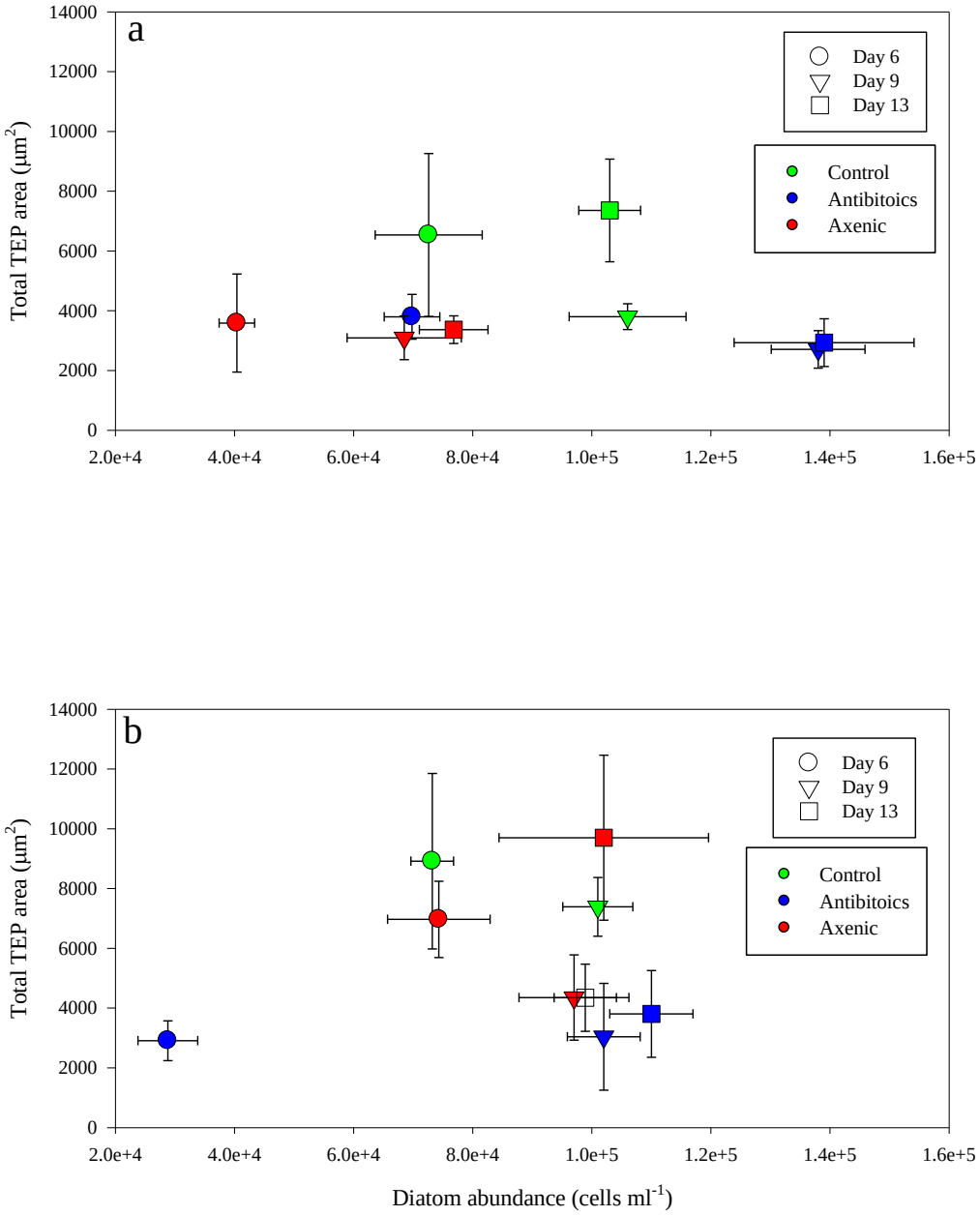

Fig 21 Total TEP area (µm^2) in the different *Odontella aurita* cultures compared to total cell abundance. Circles represent TEP area on day 6, upside down triangles day 9, and squares day 13. Green shapes represent the Control cultures, blue the Antibiotic cultures, and red the Axenic cultures (mean ± SD; n=4). (a) Total TEP area at 20 °C and (b) at 28 °C.

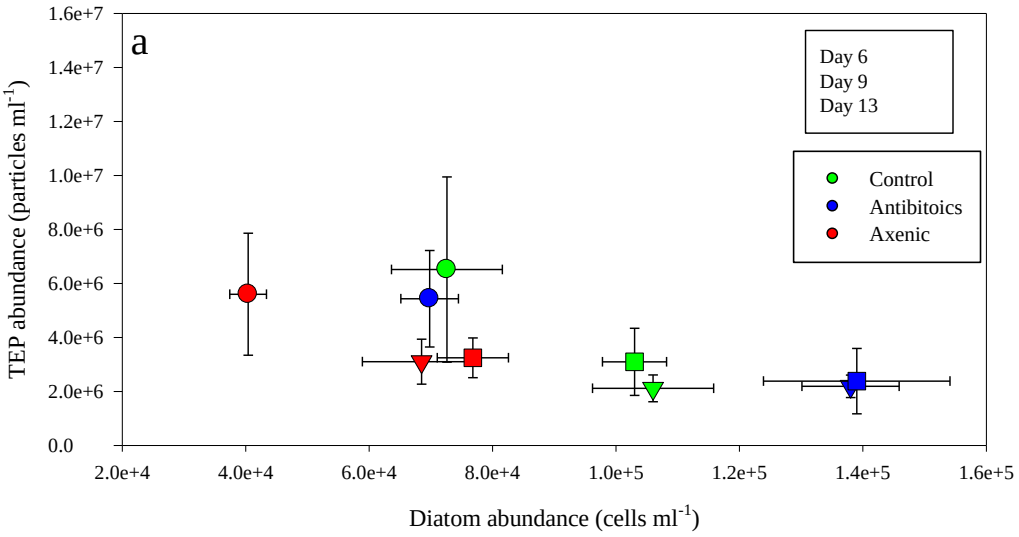

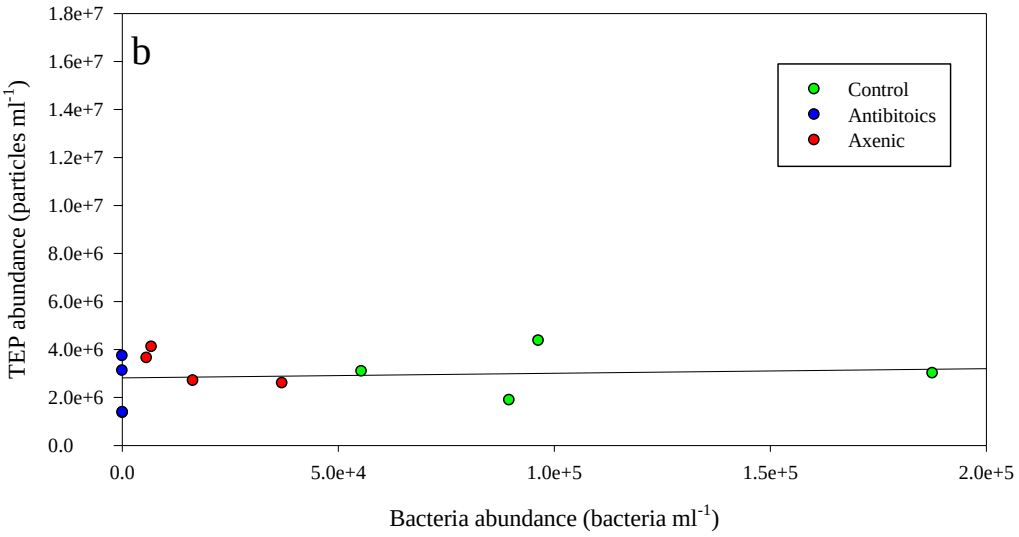

Fig 22 Total TEP abundance in *Odontella aurita* cultures at 20 °C. (a) Total TEP abundance related to cell abundance (mean ± SD; n=4). Circles represent TEP abundance on day 6, upside down triangles day 9, and squares day 13. (b) TEP abundance in each bottle on day 13 in relation to total amount of bacteria in the bottles. Green shapes represent Control culture samples, blue shapes Antibiotic cultures, and red shapes Axenic cultures.

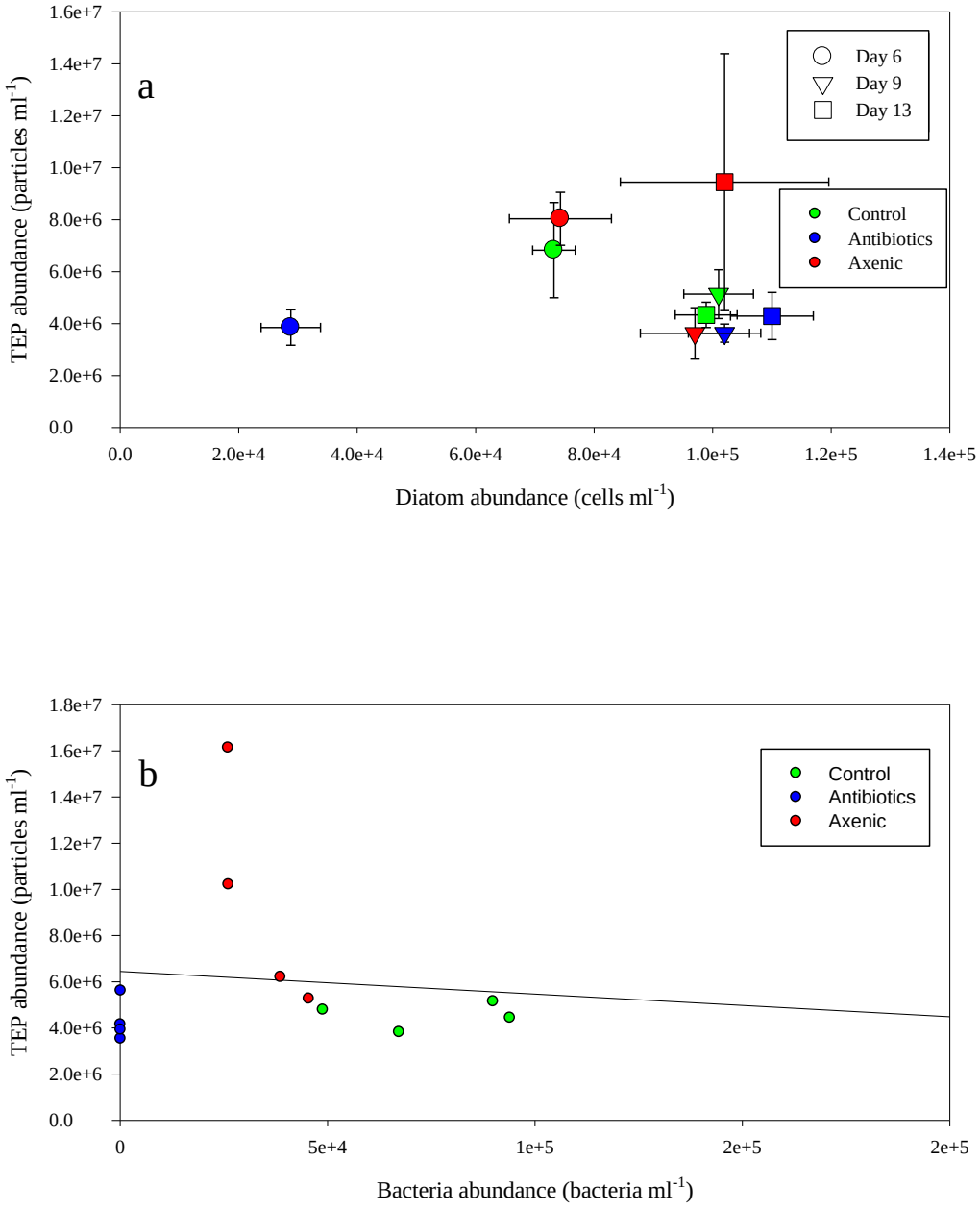

Fig. 23 Total TEP abundance in *Odontella aurita* cultures at 28 °C. (a) Total TEP abundance related to cell abundance (mean ± SD; n=4). Circles represent TEP abundance on day 6, upside down triangles day 9, and squares day 13. (b) TEP abundance in each bottle on day 13 in relation to total amount of bacteria in the bottles. Green shapes represent Control culture samples, blue shapes Antibiotic cultures, and red shapes Axenic cultures.

Coomassie stained particles (CSP) detected under a brightfield microscope at 100x magnification, were identified by being independent of diatom cells (Fig. 25). These organic particles do not appear to effect diatom aggregation. The average size (longest dimension of the CSP particle) of CSP particles in *O. aurita* cultures ranged from 142.07 µm in the Antibiotics cultures at 20 °C, to 1120.29 µm in the Axenic cultures at 28 °C (Table 5). With an increase in temperature, CSP particles appear to get larger. At both temperatures the Antibiotic treatment has the smallest CSP particles recorded. Coinciding with the increase in average size of CSP, with an increase in temperature there was an increase in CSP area (Fig. 26), although with time the total area decreases. No correlation between CSP and bacteria concentration occurred at either temperature (Fig. 27 and 28), but at 20 °C cell concentration and CSP per ml correlated with an r^2 value of 0.81 (Fig. 27a). However, at 28 °C the CSP per ml and cell concentration were not correlated ($r^2 = 0.03$; Fig. 28a). The Axenic cultures had the highest amount of CSP per ml while Antibiotics had the least at both temperatures (Fig. 27 and 28). There were significant positive correlations ($r > 0.80$) between the total amount of carbohydrates and chlorophyll *a* in the cultures at both 20 and 28 ºC, however there were no more significant relationships that continuously occurred with the change in temperature (Table 6).

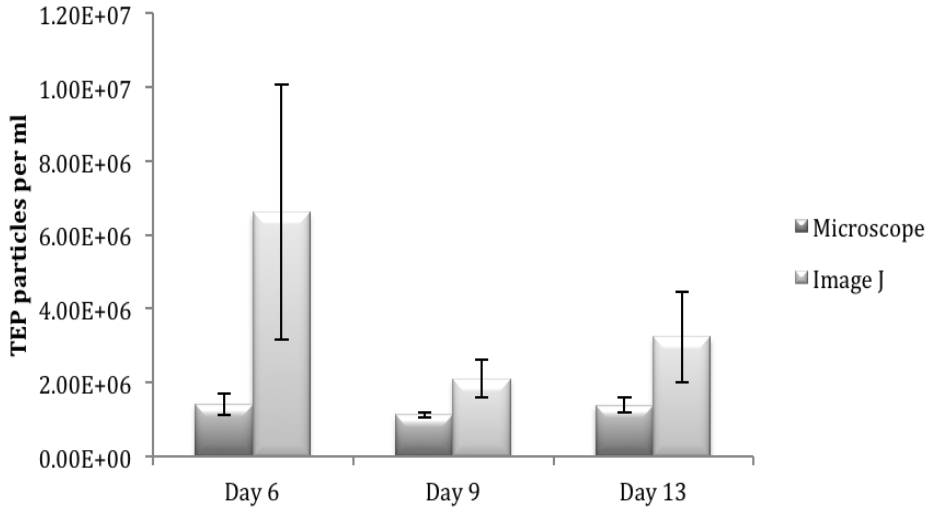

Fig 24. Difference between microscope and ImageJ technique to count particles in a sample. Bars represent the control cultures at 20 °C (mean ± SD; n = 4).

Table 5. Average CSP particle size in *O. aurita* cultures. Three different treatments were used (Control, Antibiotics, and Axenic) to determine how temperature and bacteria affected CSP production. (mean size ± SD; n=4).

Average CSP size (μm)		
	Odontella aurita @ 20 °C	
	Day 6	Day 13
Control	508.30 ± 188.87	613.86 ± 145.59
Antibiotics	142.07 ± 11.43	376.10 ± 226.12
Axenic	248.61 ± 73.62	364.07 ± 136.87
	Odontella aurita @ 28 °C	
Control	607.73 ± 123.95	720.62 ± 480.09
Antibiotics	216.65 ± 180.69	205.76 ± 137.08
Axenic	488.87 ± 50.82	1130.29 ± 921.87

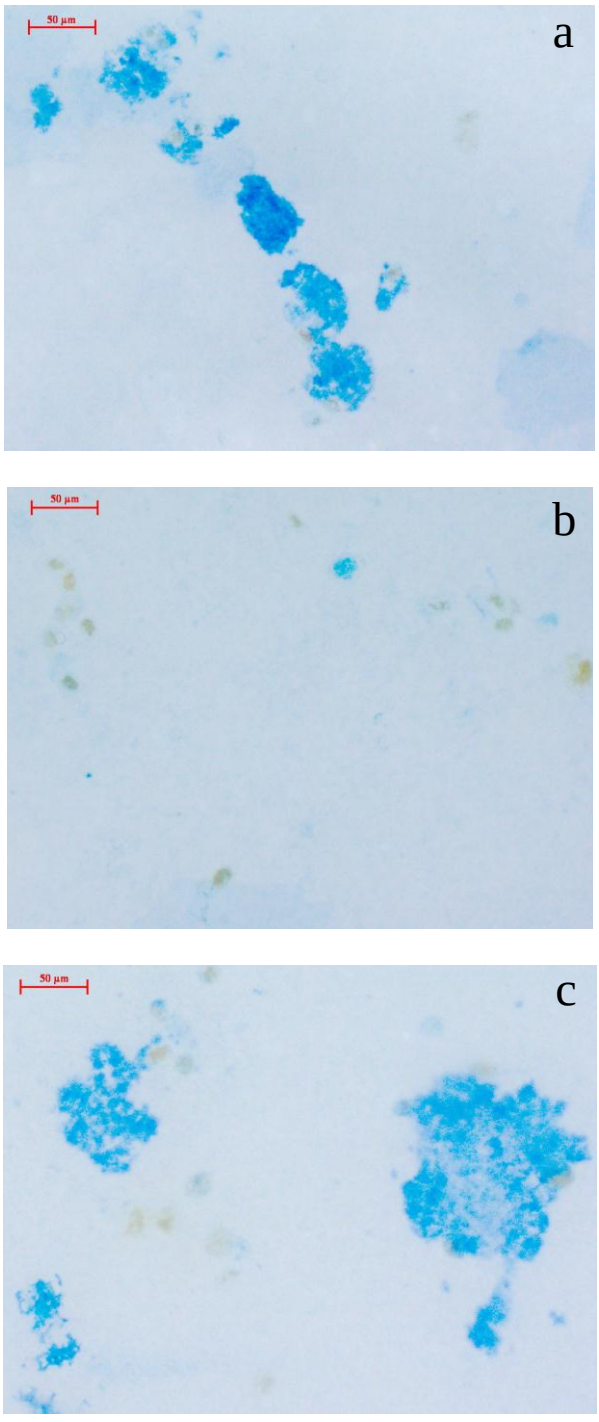

Fig. 25 Pictures of CSP particles in the *Odontella aurita* cultures at 28 °C stained with Coomassie Brilliant Blue (CBB) at 100x magnification. (a) Control culture (b) Antibiotic culture, and (c) Axenic culture.

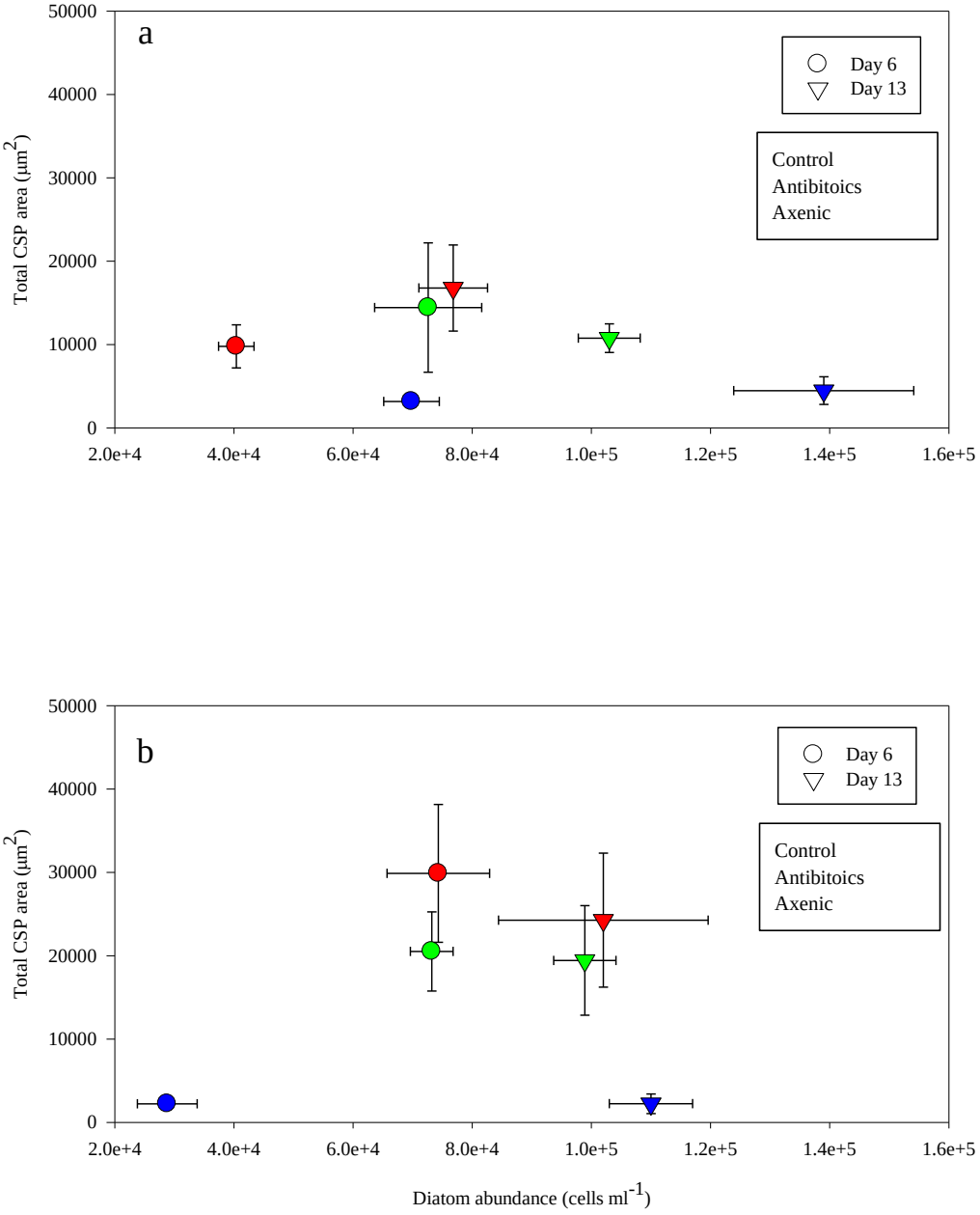

Fig. 26 Total CSP area (µm^2) in the different *Odontella aurita* cultures compared to total cell abundance. Circles represent CSP area on day 6 and upside down triangles day 13. Green shapes represent the Control cultures, blue the Antibiotic cultures, and red the Axenic cultures (mean ± SD; n=4). (a) Total CSP area at 20 °C and (b) at 28 °C.

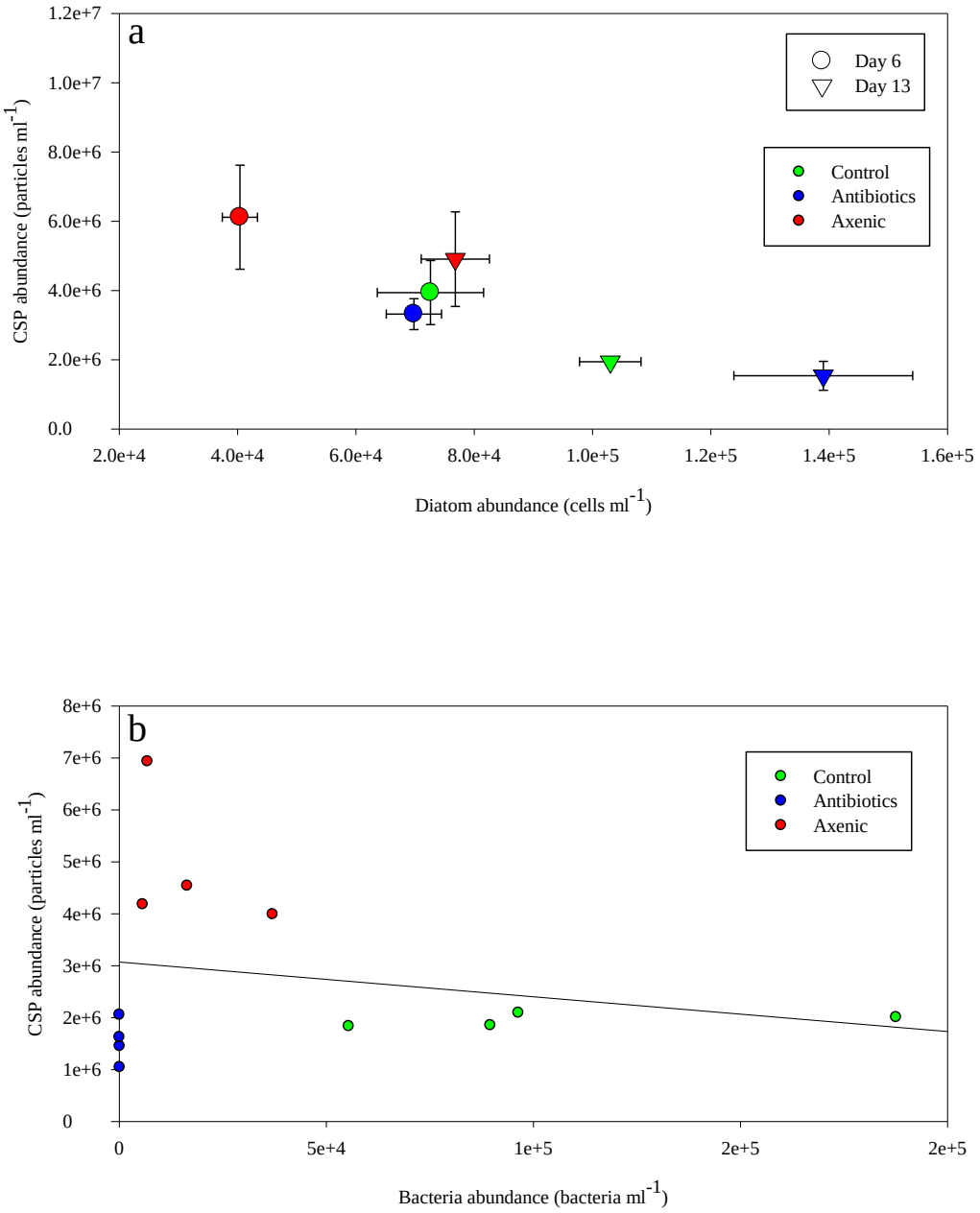

Fig. 27 Total CSP abundance in *Odontella aurita* cultures at 20 °C. (a) Total CSP abundance related to cell abundance (mean ± SD; n=4). Circles represent CSP abundance on day 6 and upside down triangles day 13. (b) CSP abundance in each bottle on day 13 in relation to total amount of bacteria in the bottles. Green shapes represent Control culture samples, blue shapes Antibiotic cultures, and red shapes Axenic cultures.

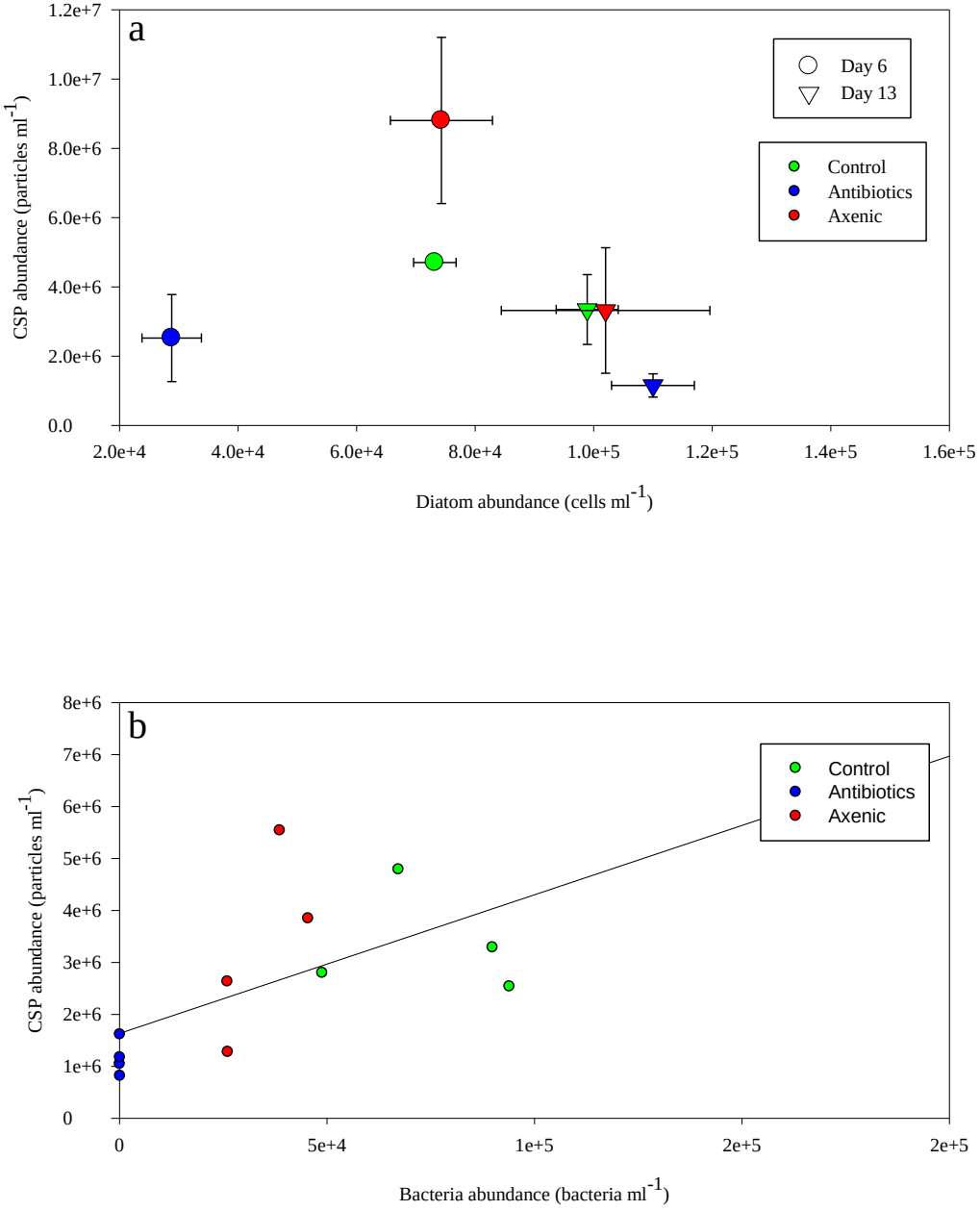

Fig 28 Total CSP abundance in *Odontella aurita* cultures at 28 °C. (a) Total CSP abundance related to cell abundance (mean ± SD; n=4). Circles represent CSP abundance on day 6 and upside down triangles day 13. (b) CSP abundance in each bottle on day 13 in relation to total amount of bacteria in the bottles. Green shapes represent Control culture samples, blue shapes Antibiotic cultures, and red shapes Axenic cultures.

Table 6. Pearson product moment correlation coefficients (r) between data gathered from *Odontella aurita* cultures at 20 and 28 ºC. Data was pooled from Day 13 at both temperatures; at 20 ºC n = 4 and at 28 ºC n = 4. *p < 0.05, **p < 0.01, ***p < 0.001.

***Odontella aurita*@ 20 °C**					
	Chl *a*	Bacteria	TEP	CSP	Cells
Total carbohydrates	0.973***	-0.615*	-0.269	-0.427	0.804**
Chl *a*		-0.695*	-0.291	-0.284	0.698*
Bacteria			0.0725	-0.223	0.182
TEP				0.460	0.468
CSP					0.773**
***Odontella aurita*@ 28 °C**					
	Chl *a*	Bacteria	TEP	CSP	Cells
Total carbohydrates	0.965***	-0.855***	-0.264	-0.705**	0.378
Chl *a*		-0.785**	-0.297	-0.713**	0.483
Bacteria			-0.0926	0.595*	0.218
TEP				-0.0338	0.422
CSP					0.014

Bacteria concentration effects on aggregation. TEP particles from each of the five treatments of *Odontella aurita* (see Table 2) were stained with Alcian blue. When mixed with only bacteria filtrate (No bacteria treatment), *O. aurita* cultures produced the largest average TEP size of approximately 260 µm (Fig. 29). The medium control, which consisted of 50 ml Harrison's artificial seawater and L1 nutrients, had a large average TEP size of approximately 220 µm though this number could be overestimated due to the larger particle size threshold used during image analysis (Fig. 29). Coinciding with the largest average TEP size, the no bacteria treatment also had the highest total TEP area at approximately 5,400 μm^2 (Fig. 30a). The medium control and organic control had the smallest total TEP area suggesting some biological factors affect TEP formation. Bacterial abundance seems to have some effect on the amount of TEP particles in each culture with a linear regression r^2 value of 0.65, though the treatment with the most bacteria does not have the highest amount of TEP particles per milliliter (Fig. 30b). The 100% bacteria treatment had the largest CSP particle size but there was no pattern between particle size and bacteria concentration (Fig. 31). The total CSP area increased with an increase in bacteria concentration (Fig. 32a), but with the medium control and organic control resulting in the least amount of CSP area, it suggests that the diatoms are needed for CSP production. Bacterial abundance seems to have some effect of CSP abundance in each culture with a linear relationship (r^2) of 0.67 (Fig. 32b).

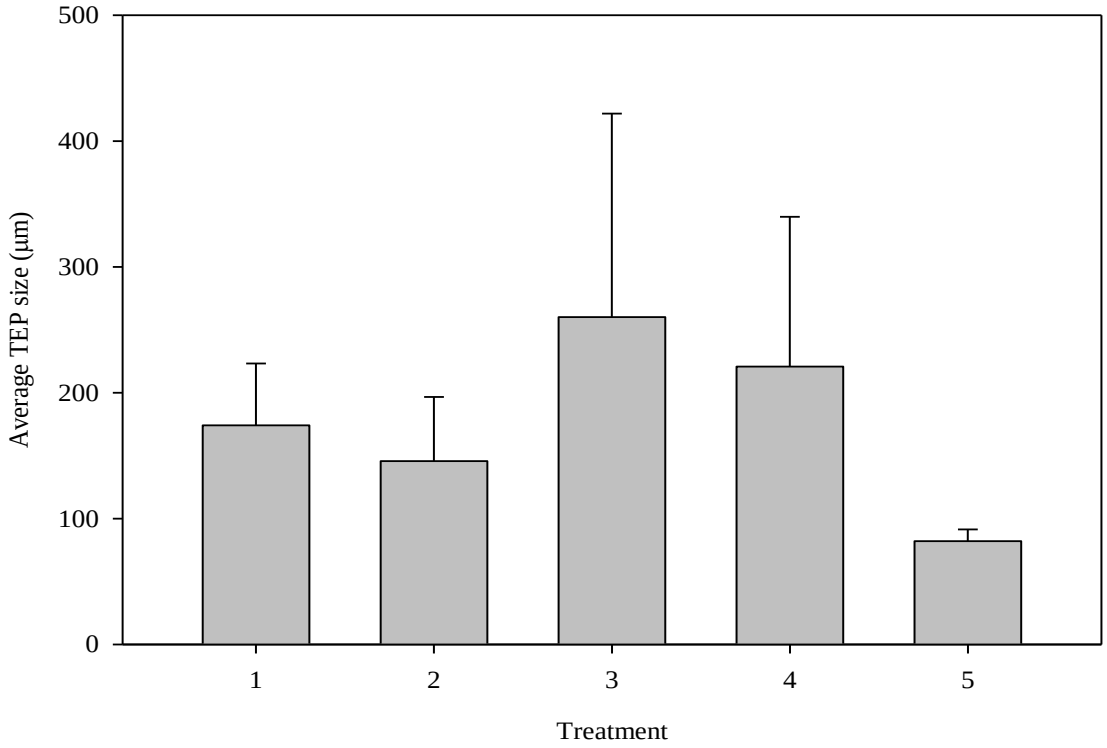

Fig. 29 Average TEP particle size (length of an individual particle in µm) in the five different bacterial treatments to *Odontella aurita* at 20 °C. The five treatments were used to determine how biotic and abiotic processes affected TEP production (mean size + SD; n = 3). Refer back to Table 3 for treatment definitions.

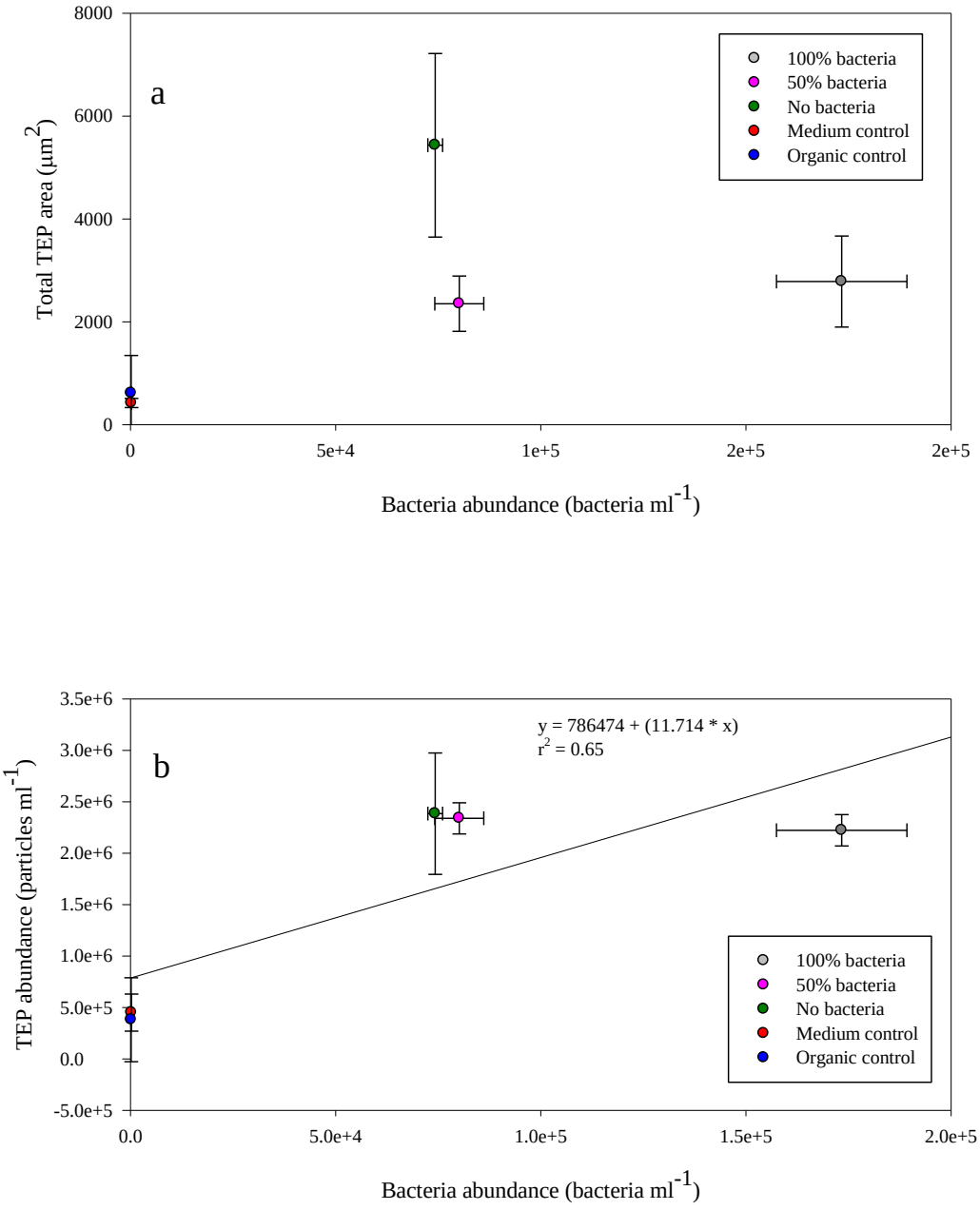

Fig. 30 TEP production as it relates to bacterial abundance under the influence of biotic and abiotic processes (mean ± SD; n = 3). (a) Relationship between total TEP area and bacterial abundance, and (b) relationship between total TEP abundance and bacterial abundance ($r^2 = 0.65$).

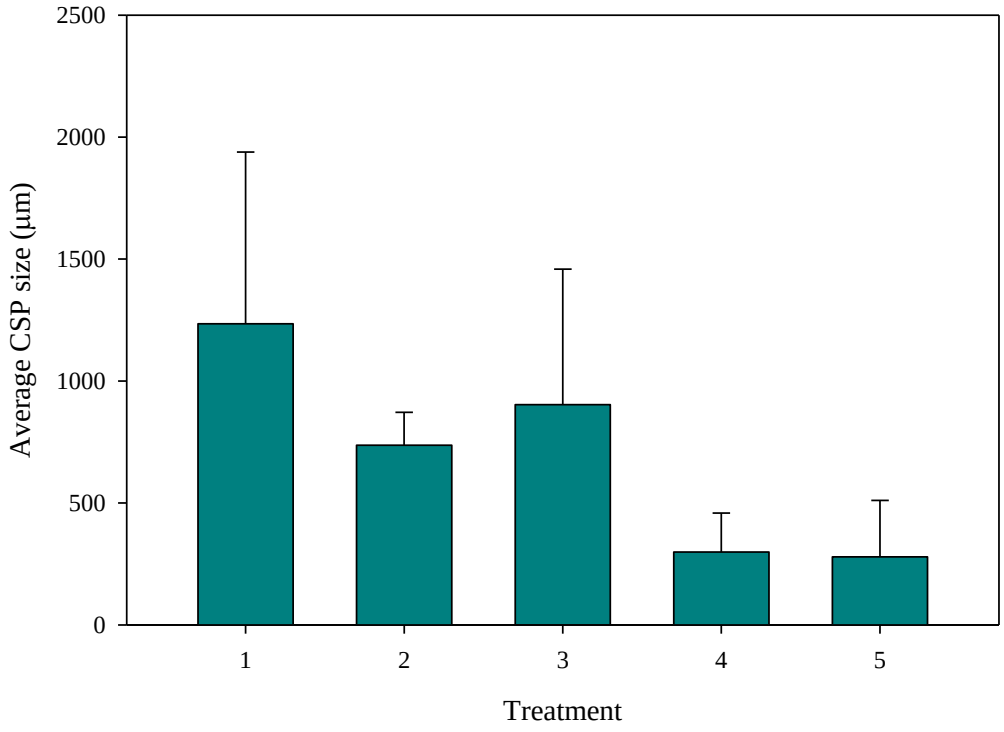

Fig. 31 Average CSP particle size (length of an individual particle in µm) in the five different bacterial treatments to *Odontella aurita* at 20 °C. The five treatments were used to determine how biotic and abiotic processes affected CSP production (mean size + SD; n = 3). Refer back to Table 3 for treatment definitions.

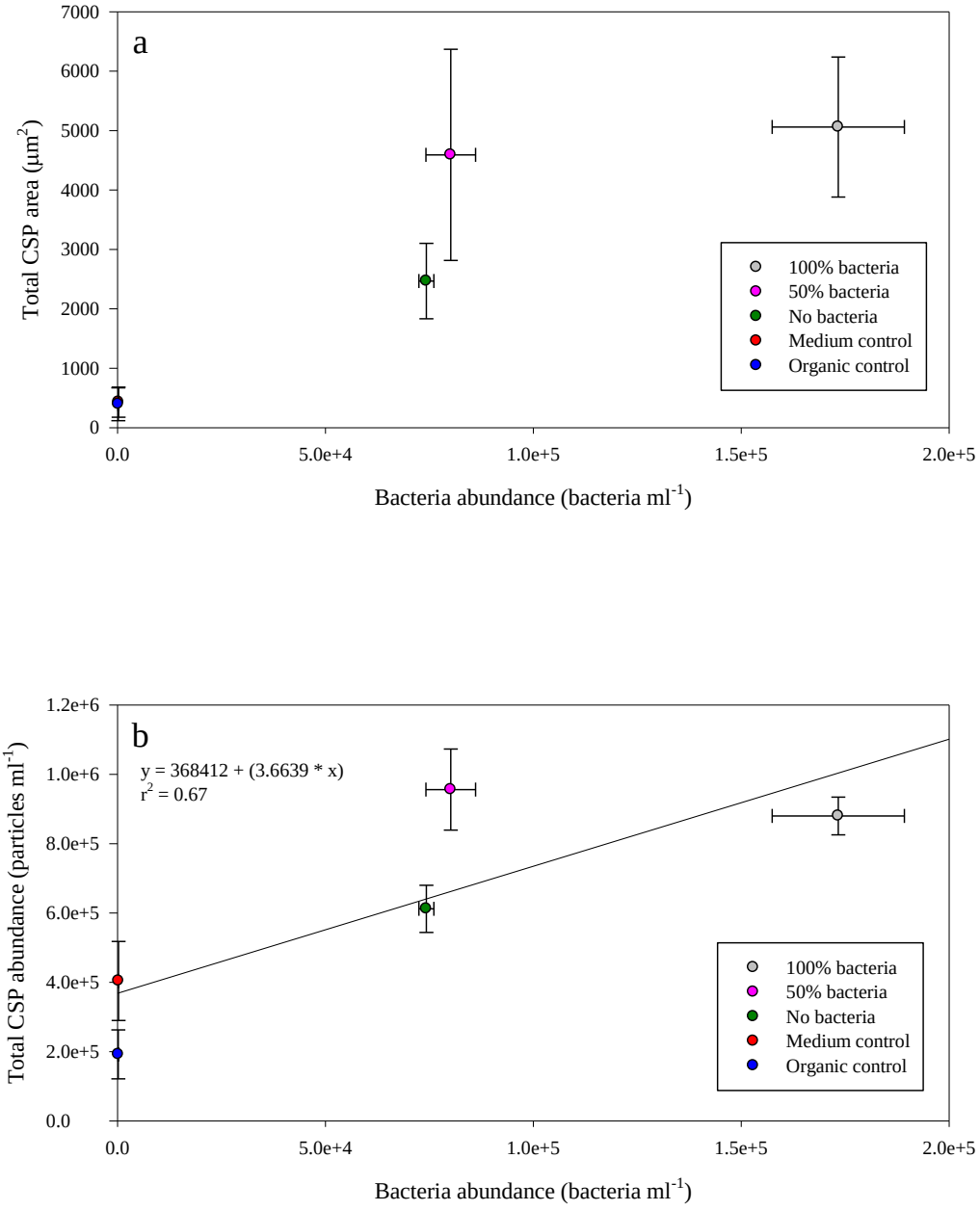

Fig. 32 CSP production as it relates to bacterial abundance under the influence of biotic and abiotic processes (mean ± SD; n = 3). (a) Relationship between total CSP area and bacterial abundance, and (b) relationship between total CSP abundance and bacterial abundance ($r^2 = 0.67$).

Discussion

Temperature effects on TEP and CSP production. The presence of exopolymeric substances (EPS) such as TEP and CSP alters particle stickiness influencing the production of aggregates thereby affecting the microbial community, sedimentation, and nutrient cycling in marine ecosystems (Berman and Viner-Mozzini 2001). Claquin et al. (2008) found that an increased in temperature increased TEP production in 3 diatoms until the diatoms reached a maximum temperature threshold where the amount of TEP produced decreased significantly. This coincides with the TEP results gained from *O. aurita* where a one-way ANOVA was done and concluded that the TEP concentration per ml was significantly different between 20 and 28 °C ($F_{1,71} = 10.307$, $p < 0.01$), with an overall significance level from the Holm-Sidak post-hoc test being 0.05.

Long and Azam (1996) showed that the seawater from the Pacific Ocean off Scripps Pier (California) contained more CSP than TEP and the CSP had larger total surface area. Our results indicate that in the laboratory, TEP was produced at a higher concentration than CSP, though CSP had the larger total surface area. Particle abundance may differ in this study compared to that of Long and Azam (1996) because the TEP and CSP in that experiment were produced by dinoflagellates instead of diatoms.

The presence of TEP is essential for diatom aggregation formation (Passow et al. 1994; Dam and Drapeau 1995; Jackson 1995; Logan et al. 1995). Placing the diatoms on the rollers showed that aggregation did occur (Figs. 14, 15, and 16). The increase in temperature from 20 to 28 °C caused a general increase in fraction of total volume in the

largest size bins on the PSD produced by the LISST. Rzadkowolski and Thornton (2012) reported the same results with the diatom *Skeletonema costatum* where with a 10 ºC increase in temperature, 82% of the volume concentration was located in size bins greater than 80 µm. This corresponds with the increase in TEP production with temperature leading to larger aggregates. The LISST can be used to show aggregation occurrence in diatoms though specific size of some aggregates could not accurately be determined due to aggregate breakage. Error did occur in the Control cultures rolling (Fig. 14) due to the presence of large aggregates (> 1 cm) that disassembled when being poured into the LISST chamber.

CSP increased with temperature, but as time continued the amount of CSP in the cultures decreased. This suggests that the diatom growth stage may influence the release of dissolved organic matter and consequently CSP formation. Wetz and Wheeler (2007) discovered a higher release of dissolved organic carbon (DOC) during the exponential and transitional growth phases of diatoms compared to DOC discharge during the transitional phase.

Coomassie brilliant blue (CBB) stains protein, resulting in the CSP observed containing protein, though the fraction of the particles mass which consist of protein cannot be determined (Long and Azam 1996). As the particles were filtered to view under the microscope, the particles were probably flattened so the calculations of the surface area of the particles are likely to be underestimated by at least a factor of 2, while the average size (length of the particle) could be overestimated.

The warming trend of ocean temperature makes it critical to understand how an increase in temperature effects EPS formation because of its influence on aggregation, grazing and virus attack, processes involved in phytoplankton bloom fate, sedimentation, and nutrient cycling (Claquin et al. 2008). For example, increased temperature caused TEP production by *O. aurita* to increase. Higher levels of TEP could lead to lower grazing rates on phytoplankton by zooplankton as the TEP could replace phytoplankton as a zooplankton food source (Passow and Alldredge 1999). However, this does not mean that there will be an increase in the growth rate of phytoplankton, as producing more TEP means the phytoplankton has to release a lot more EPS. The increased TEP production could also lead to more large aggregate formation leading to a decrease in predation by zooplankton due to the phytoplankton's increased size. This production and movement of TEP with the increased temperature could alter the traditional foodweb of zooplankton predation on phytoplankton (Passow and Alldredge 1999).

In conclusion, an increase in temperature causes an increase in TEP production, and an increase in surface area and size of CSP. This increase in TEP caused larger aggregates to form due to the increase in sticky particles, and the increased probability of the diatoms colliding with the TEP. There was not an exponential increase in TEP with the 8 °C increase in temperature, which could be due to 28 °C being too high of a temperature for *O. aurita* to acclimate to and the TEP production could have been declining from this maximum production temperature (Claquin et al. 2008). The stickiness of CSP could not be determined, nor could the role CSP played in diatom aggregation. CSP is obviously being produced by diatoms. CSP is made from protein

and thus contain nitrogen. This infers that the diatoms are losing nitrogen as they produce CSP, and nitrogen could then potentially become a limiting nutrient which could in turn inhibit cell growth. The CSP produced by the diatoms could be produced solely for the benefit of bacteria formation. Increased bacteria concentrations could benefit the diatom as bacteria could enhance TEP formation in diatoms (Passow 2001).

Bacterial abundance in cultures. Passow et al. (2000) found that TEP formation was positively affected by bacteria abundance as the bacteria enhanced TEP production by the diatoms. In the temperature experiments, there was no correlation between bacteria abundance and TEP or CSP abundance (Figs. 21b, 22b, 26b, and 27b). The amount of TEP produced in the bacteria experiment treatments where diatoms were present was significantly higher than in the treatments that contained no diatoms. Bacterial exopolymeric substances (EPS) contain high molecular weight colloids that are capable of producing TEP (Bhaskar et al. 2005). The treatment with no bacteria had the most TEP area and the largest TEP particle size suggesting that a combination of diatoms and EPS produced by bacteria produces the greatest TEP area and size. Bhaskar et al. (2005) showed that aggregates of diatoms were produced under exclusively abiotic conditions. TEP does not appear to be a carbon substrate that is used by bacteria, but it has been shown to have a weak, inverse correlation with total bacterial abundance (Bhaskar and Bhosle 2006). My experiment showed that TEP abundance had a weak linear regression with bacterial abundance with an r^2 value of 0.65 (Fig. 29b). Gärdes et al. (2011) found that specific bacterial strains had to be attached to the diatom *Thalassiosira weissflogii* for TEP production and aggregation formation to occur. The

composition of the bacterial community in the *O. aurita* cultures was unknown and whether it was a specific bacteria taxa causing TEP production in the cultures is also unknown. Further work should be done to characterize whether a specific bacterium or a consortium of bacteria causes increased TEP production. One method that could be used to determine this would be fluorescent *in-situ* hybridization where the ribosomal-RNA of bacteria is stained to identify the taxonomic affiliation of individual bacterial cells (Llobet-Brossa et al. 1998, Ishii et al. 2004).

It is unknown whether bacteria have to be present for TEP and aggregation formation in diatoms. The Axenic cultures in the temperature experiments became contaminated with time and therefore they cannot give conclusive evidence. The bacteria experiment showed that organics in the bacteria filtrate seem to play a large role in TEP area and size, though all the cultures containing bacteria had similar TEP abundance (Fig. 29b) suggesting than an increase in bacteria concentration does not result in more total TEP particles. More work needs to be done to determine if it is a specific taxa of bacteria that cause TEP production and diatom aggregation, or if only certain diatom species require bacteria since it has been shown that bacteria may degrade and break down TEP (Passow and Alldredge 1995).

Proteinaceous matter is critical to the energy flow of the surface ocean due to it being a source of dissolved organic matter and particulate organic matter (Kuznetsova et al. 2005). Kuznetsova et al. (2005) found that 20-40% of the CSP was colonized by bacteria suggesting that the particles could be potentially providing a pool of nitrogen for bacterial production. Our data suggests that there is more CSP when bacteria are present

in cultures suggesting that there is a relationship between the two. As CSP is a source of nitrogen and carbon, it could support bacteria growth.

This experiment has shown that there is a complex relationship between bacteria, diatoms, TEP, CSP, and aggregation. Diatoms are required for diatom aggregation to occur. It seems that the exponential growth of the diatom plays a role in the amount of TEP and CSP production. The healthier the diatom, the more TEP and CSP produced. TEP is a sticky particle and thus increases the probability of aggregation, and is therefore a critical particle in the aggregation process. Diatoms also produce CSP. CSP was not shown to directly affect diatom aggregation. CSP is exuded from diatoms and is made up of proteins and is therefore rich in nitrogen. Bacteria associated with the diatoms, or in the surrounding environment can use this nitrogen as a source of energy. Gärdes et al. (2011) have shown that bacteria are required for TEP production in diatoms. As TEP is needed for aggregation, diatoms could be producing CSP as a source of energy for bacteria, which they need for TEP formation (Fig. 33). This is an extremely complicated relationship that needs to be further studied, as there are probably even more variables involved. This is just one suggestion as to the interactions between these variables.

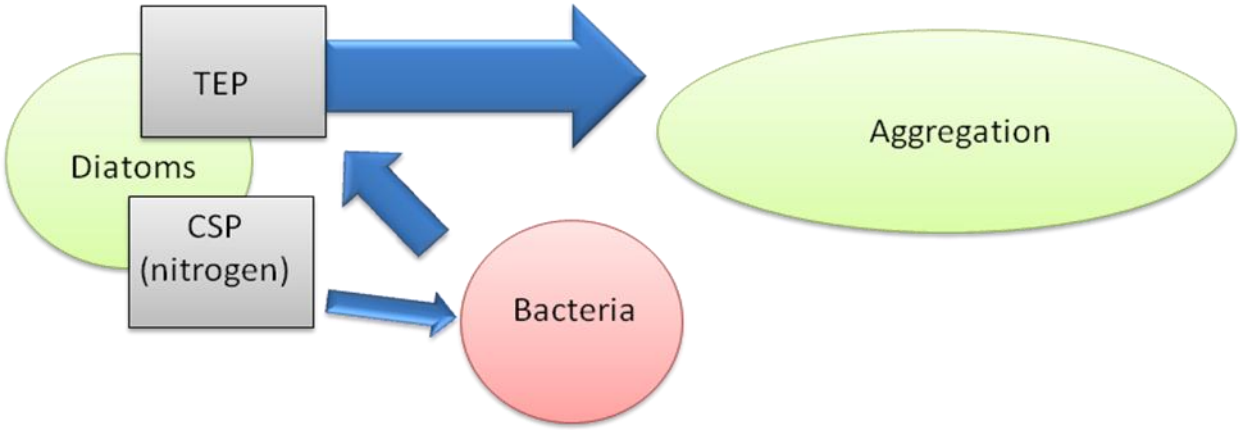

Fig. 33 Flow diagram of how diatom production of TEP and CSP results in aggregation. Diatoms are needed for aggregation to occur, and the healthier the diatom cell, then the more TEP production will result, and aggregation can occur. Diatoms produce TEP as a sticky particle which increases the probability of aggregation. CSP is also produced by diatoms and has shown no direct role in diatom aggregation. CSP is made up of nitrogen and can thus be used as a source of energy for bacteria. Bacteria have been shown to increase TEP production in diatoms which increases the chance of aggregation. All these aspects interact with each other to lead to aggregation.

Image analysis errors. The size threshold set for the Image J software was 10 μm^2 in an attempt to reduce the signal to noise ratio in the measurements, where the noise is the inclusion of particles that are not TEP or CSP (i.e. excess dye on filter) and will increase the TEP/CSP area slightly and will have a huge effect on the total count. The 10 μm^2 was calculated based off a minimum curve which showed that it would include the most TEP/CSP particles without having too much noise. However, there will always be some noise when smaller TEP/CSP particles are included in the analysis causing the area and total count to be slightly overestimated. The color threshold used was based on eyesight, where everything that was judged to be a particle was included as the threshold was set. The original photo was used to compare with the grey scale image to determine what color blue was considered a particle and what blue was background noise.

When studying the pictures to do the analysis, diatoms have carbohydrate coatings surrounding the cell that stain blue but are not actually TEP or CSP particles. In this case they were colored out so only TEP particles were counted. However, at times there can be large blue gel like particles of exopolymers that are attached to the cell as they are sticky. In this case I included these particles as TEP or CSP, which could again cause an overestimation of total count, size, and area. There is no distinct way to determine whether those particles are TEP/CSP or not so it was a judgment call.

In some of the pictures, particles will be on the edge of the picture so the whole particle is not shown. In this case particles on the edge of the photo that could not be fully seen were not included in this analysis. This gives a more accurate average size of

the particles, but underestimates the total area and abundance of the particles. The particles on the edge could be included in analysis; however it is probable to overestimate total number of particles if the pictures are taken in a sequential order as a large particle could be on more than one photo. There is not one specific way to use the Image J analysis software, but depending on what you are studying, parameters can be set up for accurate measurements.

Diatom and carbon cycling. In the marine carbon cycle, TEP is extremely important as it will either sediment or be grazed (Passow 2000). Diatoms are a major contributor of TEP production in marine environments. TEP production increases the likelihood of marine snow formation, which can be a vehicle for reactive trace elements, bacteria, phytoplankton, zooplankton, and carbon in a flux down through the water column (Azetsu-Scott and Passow 2004). Marine snow, as it sinks to the ocean floor, is a food source for benthic food chains, it can contribute to sedimentation, and it can stimulate microbial life making it imperative to know the C:N ratio of the aggregates and their sinking rates to determine the amount of carbon available for these processes. The C:N ratios of marine snow is 12.2-16.9 with a sinking rate as low as 31 ± 18 m d^{-1} with up to 80% of the POC in the aggregates being remineralized by bacteria before reaching the benthos (Ploug et al. 1999).These sinking marine snow aggregates therefore act as a carbon sink, but also as a source of CO_2 in the surface waters where most of the carbon is respired (Ploug et al. 1999).

Coastal waters are often nutrient limited with an excess of carbon. Understanding what diatoms do with this excess carbon has begun (Geider et al. 1997; Thornton 2002).

It has been proposed that diatoms process the excess carbon into different forms of EPS that can provide a way to decreased predation on the diatoms and increase the diatoms surface area to slow their sinking velocity (Kiørboe and Hansen 1993; Fukao et al. 2009). These byproducts of excess carbon may be secondary in nature as diatoms could be wasting carbon as a way to prepare metabolic products for future use when nutrients become readily available (Russell and Cook 1995; Hessen and Andersen 2008).

Diatoms are responsible for a third of the world's primary production, and if blooms increase with increase in ocean temperatures, more carbon would be transferred from the sea surface to the benthos at an increased rate. This would not only change the amount of available carbon at the sea surface in terms of DOC, POC and CO_2, but the large amount of carbon reaching the sea floor. The effects of temperature on diatom physiology needs to be further studied to see how increased temperature will affect TEP production and consequently aggregation, how sticky CSP is and whether it is acting as a nitrogen source for bacteria, and whether specific bacteria taxa influence TEP production and aggregation and how temperature will affect their growth. All these factors together affect the biological carbon cycle in the ocean.

CHAPTER IV

DISCUSSION AND CONCLUSIONS

Identifying, characterizing, and counting biological particles in the ocean is important as each type of particle can play a crucial role in the marine ecosystem. For example, particles suspended in the water column can affect light penetration through the water and thus impact primary productivity and radiative transfer (Mobley et al. 2002). Particulate organic carbon (POC) can also be suspended in the water column and understanding how POC sinks from the surface of the ocean to the benthos is an important step in the carbon cycle and thus has implications on climate models (Davies et al. 2011). For the LISST instruments to characterize particles in the water, a primary requirement is that there is a relatively high concentration of particles suspended in the water to provide a sufficient signal (Rienecker et al. 2008). In terms of studying dinoflagellate and diatom blooms the LISST would be sufficient because bloom concentration enable a strong signal. Full phytoplankton bloom situations could cause the transmission of the laser on the LISST to drop below 30%, which will cause laser attenuation, and an accurate measurement would not be determined (Styles 2006).

LISST instruments are relatively cheap to purchase and have low running costs. That, in combination with its ability to allow for aggregation to be measured, as it does not cause floc breakups, allows for long-term continuous *in-situ* monitoring applications (Andrews et al. 2010) makes it an extremely versatile instrument for studying phytoplankton. With its compact size and internal data logging, the LISST could be

routinely deployed on a fixed mooring for time series measurements, or it could be fixed on a profiler to take measurements at specific transects (Styles 2006). The LISST could be attached behind boats and towed to map extent of phytoplankton blooms (Anglès et al. 2008), or it could be incorporated into existing ocean observing systems (e.g. Texas Automated Buoy System,
TABS) to monitor phytoplankton growth over time. Depending on the species in the bloom, the phytoplankton can undergo diel vertical migrations and by attaching the LISST to a profiler, or a CTD, the bloom could be monitored as migration occurred.

The versatility of the LISST allows for it to monitor phytoplankton, however the LISST does have limitations as it can only tell us the size and volume concentration of the phytoplankton in the water column. It also is only accurate in identifying phytoplankton in monospecific blooms. In a heterogeneous bloom situation, the LISST would not be able to discriminate between different phytoplankton species due to size overlapping (Anglés et al. 2008). The instrument itself does not describe the physiology of the bloom, and the chemical, physical, and biological processes that interact with the blooms in natural environments (Anglés et al. 2008) are crucial to understanding the phytoplankton, and as well as mitigating the bloom if it is harmful. To overcome these limitations, adjustments can be made to the LISST to ensure continuous mapping of phytoplankton as well as understanding their physiology. A fluorometer could be easily attached to the LISST to measure chlorophyll. If the LISST was attached to a CTD, samples of where the phytoplankton were could be taken to understand the environment at which they live in. Rienecker et al. (2008) attached physical, nutrient, and bio-optical

sensors to the LISST to get an idea of phytoplankton variability and environmental variability. To look at cell health and confirm the LISST results, Davies et al. (2011) attached a digital in-line holograph to produce particle images with the PSD.

LISST instruments were originally designed to measure marine sediments (Agrawal and Pottsmith 2000), however the LISST's potential to studying phytoplankton, their physiology, and their environment has huge implications on studying marine microorganisms. With the LISST being relatively cheap, more than one could potentially be used and a continuous study of phytoplankton in areas of the world's ocean could be done. In combination with other scientific tools, the LISST would be able to monitor phytoplankton distributions as well as their physiology and environmental factors.

REFERENCES

Abdullahi, A.S., Underwood, G.J.C. & Gretz, M.R. 2006. Extracellular matrix assembly in diatoms (Bacillariophyceae). V. Environmental effects on polysaccharide synthesis in the model diatom, *Phaeodactylum tricornutum*. *Journal of Phycology* 42:363-378.

Agrawal, Y.C. & Pottsmith, H.C. 2000. Instruments for particle size and settling velocity observations in sediment transport. *Marine Geology* 168:89-114.

Agrawal, Y.C., Whitmire, A., Mikkelsen, O.A. & Pottsmith, H.C. 2008. Light scattering by random shaped particles and consequences on measuring suspended sediments by laser diffraction. *Journal of Geophysical Research* 113:23-34.

Ahn, J.H. & Grant, S.B. 2007. Size distribution, sources, and seasonality of suspended particles in Southern California marine bathing waters. *Environmental Science and Technology* 41:695-702.

Alldredge, A.L. & Silver, M.W. 1988. Characteristics, dynamics, and significance of marine snow. *Progress Oceanography* 20:41-82.

Alldredge, A.L., Passow, U. & Logan, B.E. 1993. The abundance and significance of a class of large, transparent organic particles in the ocean. *Deep Sea Research I* 40:1131-1140.

Andersen, R.A. (Ed.) 2005. *Algal Culturing Techniques*. Elsevier Academic Press, Boston, 578 p.

Anderson, D.M. 1989. Toxic Algal Blooms and Red Tides: A Global Perspective. In: T. Okaichi, D.M. Anderson, and T. Nemoto (eds). *Red Tides: Biology, Environmental Science and Toxicology*. Elsevier Science Inc, New York, pp 11-16.

Andrews, S., Nover, D., & Schladow, S.G. 2010. Using laser diffraction data to obtain accurate particle size distributions: the role of particle composition. *Limnology and Oceanography: Methods* 8:507-526.

Anglès, S., Jordi, A., Garcés, E., Maso, M. & Basterretxea, G. 2008. High-resolution spatio-temporal distribution of a coastal phytoplankton blooms using laser in situ scattering and transmissometry (LISST). *Harmful Algae* 7:808-816.

Azetsu-Scott, K. & Passow, U. 2004. Ascending marine particles: significance of transparent exopolymer particles (TEP) in the upper ocean. *Limnology and Oceanography* 49:741-748.

Behrenfeld, M.J., O'Malley, R.T., Siegel, D.A., McClain, C.R., Sarmiento, J.L., Feldman, G.C., Milligan, A.J., Falkowski, P.G., Letelier, R.M. & Boss, E.S. 2006. Climate-driven trends in contemporary ocean productivity. *Nature* 444:752-755.

Behrenfeld, M.J., Halsey, K.H., & Milligan, A.J. 2008. Evolved physiological responses of phytoplankton to their integrated growth environment. *Philosophical Transactions of the Royal Society B: Biological Sciences* 363:2687-2703.

Behrenfeld, M.J., Westberry, T.K., Boss, E.S., O'Malley, R.T., Siegel, D.A., Wiggert, J.D., Franz, B.A., McClain, C.R., Feldman, G.C., Doney, S.C. & others 2009. Satellite-detected fluorescence reveals global physiology of ocean phytoplankton. *Biogeosciences* 6:779-794.

Bellinger, B.J., Abdullahi, A.S., Gretz, M.R. & Underwood, G.J.C. 2005. Biofilm polymers: relationship between carbohydrate biopolymers from estuarine mudflats and unialgal cultures of benthic diatoms. *Aquatic Microbial Ecology* 38:169-180.

Berges, J.A., Franklin, D.J. & Harrison, P.J. 2001. Evolution of an artificial seawater medium: Improvements in enriched seawater, artificial water over the last two decades. *Journal of Phycology* 37:1138-1145.

Berman, T. & Viner-Mozzini, Y. 2001. Abundance and characteristics of polysaccharide proteinaceous particles in Lake Kinneret. *Aquatic Microbial Ecology* 24:255-264.

Bhaskar, P.V., Grossart, H.P., Bhosle, N.B. & Simon, M. 2005. Production of macroaggregates from dissolved exopolymeric substances (EPS) of bacterial and diatom origin. *FEMS Microbiology Ecology* 53:255-264.

Bhaskar, P.V. & Bhosle, N.B. 2006. Bacterial extracellular polymeric substance (EPS): A carrier of heavy metals in the marine food-chain. *Marine Pollution and Ecotoxicology* 32:191-198.

Billet, D.S.M., Lampitt, R.S., Rice, A.L. & Mantoura, R.F.C. 1983. Seasonal sedimentation of phytoplankton to the deep-sea benthos. *Nature* 302:520-522.

Broecker, W.S. 1982. Ocean chemistry during glacial time. *Geochemica et Cosmochimica Acta* 46:1689-1705.

Burkholder, J.M. 1998. Implications of harmful microalgae and heterotrophic dinoflagellates in management of sustainable marine fisheries. *Ecological Applications* 8:S37-S62.

Buskey, E.J., Liu, H., Collumb, C. & Bersano, J.G.F. 2001. The Decline and Recovery of a Persistent Texas Brown Tide Algal Bloom in the Laguna Madre (Texas, USA). *Estuaries* 24:337-346.

Chin, W.C., Orellana, M.V. & Verdugo, P. 1998. Formation of microgels by spontaneous assemble of dissolved marine polymers. *Nature* 391:568-572.

Claquin, P., Probert, I., Lefebvre, S. & Veron, B. 2008. Effects of temperature on photosynthetic parameters and TEP production in eight species of marine microalgae. *Aquatic Microbial Ecology* 51:1-11.

Dale, B., Edwards, M. & Reid, P.C. 2006. Climate Change and Harmful Algal Blooms. *Ecology of Harmful Algae*. Springer-Verlag, Berlin.

Dam, H.G. & Drapeau, D.T. 1995. Coagulation efficiency, organic-matter glues and the dynamics of particles during a phytoplankton bloom in a mesocosm study. *Deep Sea Research II: Topical Studies in Oceanography* 42:111-123.

Davison, I.R. 1991. Environmental effects on algal photosynthesis: temperature. *Journal of Phycology* 27:2-8.

Decho, A.W. 1990. Microbial exopolymer secretions in ocean environments-their role(s) in food webs and marine processes. *Oceanography and Marine Biology* 28:73-153.

Dekshenieks, M.M., Donaghay, P.I., Sullivan, J.M., Rines, J.E.B., Osborn, T.R. & Twardowski, M.S. 2001. Temporal and spatial occurrence of thin phytoplankton layers in relation to physical processes. *Marine Ecology Progress Series* 223:61-71.

Doney, S.C. 2006. Oceanography: Plankton in a warmer world. *Nature* 444:695-696.

DuBois, M., Gilles, K.A., Hamilton, J.K., Rebers, P.A. & Smith, F. 1956. Colorimetric method for determination of sugars and related substances. *Analytical Chemistry* 28:350-356.

Durham, W.M. & Stocker, R. 2012. Thin Phytoplankton Layers: Characteristics, Mechanisms, and Consequences. *Annual Review of Marine Sciences* 4:177-207.

Engel, A. 2000. The role of transparent exopolymer particles (TEP) in the increase in apparent stickiness (α) during the decline of a diatom bloom. *Journal of Phytoplankton Research* 22:485-497.

Engel, A. 2009. Determination of Marine Gel Particles. In: Wurl, O (ed), *Practical Guidelines for the Analysis of Seawater,* CRC Press, Boca Raton.

Engel, A. & Passow, U. 2001. Carbon and nitrogen content of transparent exopolymer particles (TEP) in relation to their Alcian Blue adsorption. *Marine Ecology Progress Series* 219:1-10.

Falkowski, P.G. 1998. Biogeochemical controls and feedbacks on ocean primary production. *Science* 281:200-206.

Fukao, T., Kimoto, K., Yamatogi, T., Yamamoto, K., Yoshida, Y. & Kotani, Y. 2009. Marine mucilage in Ariake Sound, Japan, is composed of transparent exopolymer particles produced by the diatom *Coscinoodiscus granii*. *Fisheries Science* 75:1007-1014.

Gärdes, A., Iversen, M.H., Grossart, H.P., Passow, U. & Ullrich, M.S. 2011. Diatom-associated bacteria are required for aggregation of *Thalassiosira weissflogii*. *International Society for Microbial Ecology* 5:436-445.

Gartner, J. 2001. Laboratory and field evaluations of the LISST-100 instrument for suspended particle size determinations. *Marine Geology* 175:199-219.

Geider, R.J., MacIntyre, H.L. & Kana, T.M. 1997. Dynamic model of phytoplankton growth and acclimation: responses of the balanced growth rate and the chlorophyll a:carbon ratio to light, nutrient-limitation and temperature. *Marine Ecology Progress Series* 148:187-200.

Gilbert, P.M., Anderson, D.M., Gentien, P., Graneli, E. & Sellner, K.G. 2005. The global, complex phenomena of harmful algal blooms. *Oceanography* 18:136-147.

Gilbert, P.M. & Burkholder, J.M. 2006. The Complex Relationships Between Increases in Fertilization of the Earth, Coastal Eutrophication and Proliferation of Harmful Algal Blooms. *Ecology of Harmful Algae* 189:341-354.

Grossart, H.P. & Ploug, H. 2001. Microbial degradation of organic carbon and nitrogen on diatom aggregates. *Limnology and Oceanography* 46:267-277.

Guillard, R.R.L. & Sieracki, M. 2005. Counting cells in cultures with the light microscope. *Algal Culturing Techniques*. Academic Press, Boston.

Hall, N.S., Litaker, R.W., Fensin, E., Adolf, J.E., Bowers, H.A., Place, A.R. & Paerl, H.W. 2008. Environmental Factors Contributing to the Development and Demise of a Toxic Dinoflagellate (*Karoldinium veneficum*) Bloom in a Shallow, Eutrophic, Lagoonal Estuary. *Estuaries and Coasts: J CERF* 31:402-418.

Hallegraff, G.M. 1993. A review of harmful algal blooms and their apparent global increase. *Phycology*. 322:79-99.

Harrison, P.J., Waters, R.E. & Taylor, F.J.R. 1980. A broad spectrum artificial sea water medium for coastal and open ocean phytoplankton, *Journal of Phycology* 16:28-35.

Heissenberger, A. & Herndl, G.J. 1994. Formation of high molecular weight material by free-living marine bacteria. *Marine Ecology Progress Series* 111:129-135.

Hessen, D.O. & Anderson, T.R. 2008. Excess carbon in aquatic organisms and ecosystems: physiological, ecological, and evolutionary implications. *Limnology and Oceanography* 53:1685-1696.

Hobbie, J.E., Daley, R.J. & Jasper, S. 1977. Use of nucleopore filters for counting bacteria by fluorescence microscopy. *Applied and Environmental Microbiology* 33:1225-1228.

Honjo, S., Doherty, K.W., Agrawal, Y.C. & Asper, V.L. 1984. Direct optical assessment of large amorphous aggregates (marine snow) in the deep ocean. *Deep Sea Research Part A. Oceanographic Research Papers* 31:67-76.

Ishii, K. Mußmann, M., MacGregor, B.J. & Amann, R. 2004. An improved fluorescence in situ hybridization protocol for the identification of bacteria and archea in marine sediments. *FEMS Microbiology Ecology* 50L203-213.

Jackson, G.A. 1990. A model of the formation of marine algal flocs by physical coagulation processes. *Deep Sea Research Part A. Oceanographic Research Papers* 37:1197-1211.

Jackson, G.A. 1995. TEP and coagulation during a mesocosm experiment. *Deep Sea Research II*: *Tropical Studies in Oceanography* 42:215-222.

Karp-Boss, L., Azavedo, L. & Boss, E. 2007. LISST – 100 measurements of phytoplankton size distribution: evaluation of the effects of cell shape. *Limnology and Oceanography: Methods* 5:396-406.

Kiørboe, T. 2001. Formation and fate of marine snow: small-scale processes with large-scale implications. *Scientia Marina* 65:57-71.

Kiørboe, T. & Hansen, J.L. 1993. Phytoplankton aggregate formation: observations of patterns and mechanisms of cell sticking and the significance of exopolymeric material. *Journal of Plankton Research* 15:993-1018.

Kuznetsova, M., Lee, C. & Aller, J. 2005. Characterization of proteinaceous matter in marine aerosols. *Marine Chemistry* 96.3-4:359-377.

Llobet-Brossa, E., Rosselló-Mora, R. & Amann, R. 1998. Microbial Community Composition of Wadden Sea Sediments as Revealed by Fluorescence In Situ Hybridization. *Applied and Environmental Microbiology* 64:2691-2696.

Logan, B.E., Passow, U., Alldredge, A.L., Grossart, H.P. & Simon, M. 1995. Rapid formation and sedimentation of large aggregates in predictable from coagulation rates (half-lives) of transparent exopolymer particles (TEP). *Deep Sea Research II* 42:203-214.

Long, R.A. & Azam, F. 1996. Abundant protein-containing particles in the sea. *Aquatic Microbial Ecology* 10:213-221.

Mann, D.G. 1999. The species concept in diatoms. *Phycologia* 38:437-495.

Mari, X. 1999. Carbon content and C:N ratio of transparent exopolymeric particles (TEP) produced by bubbling exudates of diatoms. *Marine Ecology Progress Series* 183:59-71.

Marinov, I., Doney, S.C., & Lima, I.D. 2010. Response of ocean phytoplankton community structure to climate change over the 21st century: partitioning the effects of nutrients, temperature, and light. *Biogeosciences* 7:3941-3959.

McManus, M.A., Kudela, R.M., Silver, M.W., Steward, G.F., Donaghay, P.L., Sullivan, J.M. 2008. Cryptic blooms: Are thin layers the missing connection? *Estuaries and Coasts* 31:396-401.

Menden-Deuer, S., Lessard, E.J. & Satterberg, J. 2001. Effect of preservation on dinoflagellate and diatom cell volume and consequences for carbon biomass predictions. *Marine Ecology Progress Series* 222:41-50.

Mobley, C.D., Sundman, L.K., & Boss, E. 2011. Scattering signatures of suspended particles: an integrated system for combining digital holography and laser diffraction. *Optical Society of America* 19:25488-25499.

Moline, M.A., Benoit-Bird, K.J., Robbins, I.C., Schroth-Miller, M., Waluk, C.M. & Zelenke, B. 2010. Integrated measurements of acoustical and optical thin layers II: horizontal length scales. *Continental Shelf Research* 30:29-38.

Mopper, K., Zhou, J., Ramana, K.S., Passow, U.,Dam, H.G. & Drapeau, D.T. 1995. The role of surface-active carbohydrates in the flocculation of a diatom bloom in a mesocosm. *Deep Sea Research II* 42:47-73.

Omta, A.W., Bruggeman, J., Kooijman, S.A.L.M. & Dijkstra, H.A. 2006. Biological carbon pump revisted: feedback mechanisms between climate and the redfield ratio. *Geophysical Research Letters* 33:613-617.

Parsons, T.R., Maita, Y. & Lalli, C.M. 1984. *A Manual of Chemical and Biological Methods for Seawater Analysis.* Pergamon Press, Oxford, UK.

Passow, U. 2000. Formation of transparent exopolymer particles, TEP, from dissolved precursoe material. *Marine Ecology Progress Series* 192:1-11.

Passow, U., Alldredge, A.L. & Logan, B.E. 1994. The role of particulate carbohydrate exudates in the flocculation of diatom blooms. *Deep Sea Research I* 141:335-357.

Passow, U. & Alldredge, A.L. 1995. Aggregation of a diatom bloom in a mesocosm: The role of transparent exopolymer particles (TEP). *Deep Sea Research II* 42:99-109.

Passow, U. & Alldredge, A.L. 1999. Grazing of euphausiids on cells in the presence of TEP. *Journal of Plankton Research* 21:2203-2217.

Ploug, H., Grossart, H.P., Azam, F. & Jørgenson, B.B. 1999. Photosynthesis, respiration, and carbon turnover in sinking marine snow from surface waters of Southern California Bight: implications for the carbon cycle in the ocean. *Marine Ecology Progress Series* 179:1-11.

Porter, K.G. & Feig, Y.S. 1980. The Use of DAPI for Identifying and Counting Aquatic Microflora. *Limnology and Oceanography* 25:943-948.

Prieto, L., Ruiz, F., Echevarria, F., Garcia, C.M., BartualA., Galvez, J.A., Corzo, A. & Macias, D. 2002. Scales and processes in the aggregation of diatom blooms: high

time resolution and wide size range records in a mesocosm study. *Deep Sea Research* 49:1233-1253.

Riebesell, U. & Wolf-Gladrow, D.A. 1992. The relationship between physical aggregation of phytoplankton and particle flux: a numerical model. *Deep Sea Research Part A. Oceanographic Research Papers* 39:1085-1102.

Rienecker, E., Ryan, J., Blum, M., Dietz, C., Coletti, L., Marin, I.I.I. & Bissett, W.P. 2008. Mapping phytoplankton in situ using a laser-scattering sensor. *Limnology and Oceanography: Methods* 6:153:161.

Russell, J.B. & Cook, G.M. 1995. Energetics of bacterial growth: balance of anabolic and catabolic reactions. *Microbiological Reviews* 59:48-62.

Rzadkowolski, C.E. & Thonton, D.C.O. 2012. Using laser scattering to identify diatoms and conduct aggregation experiments. *European Journal of Phycology* 47:30-41.

Serra, T., Colomer, J., Cristina, X.P., Vila, X., Arellano, J.B. & Casamitjana, X. 2001. Evaluation of laser in situ scattering instrument for measuring concentration of phytoplankton, purple sulfur bacteria, and suspended inorganic sediments in lakes. *Journal of Environmental Engineering – ACSE* 127:1023-1030.

Smayda, T.J. 1997. Harmful algal blooms: Their ecophysiology and general relevance to phytoplankton blooms in the sea. *Limnology and Oceanography* 42:1137-1153.

Smetacek, V.C. 1985. Role of sinking in diatom life-history cycles – ecological, evolutionary and geological significance. *Marine Biology* 84:239-251.

Smith, D.C., Simon, M., Alldredge, A.L. & Azam, F. 1992. Intense hydrolytic enzyme activity on marine aggregates and implications for rapid particle dissolution. *Nature* 329:139-142.

Smith, D.C., Steward, G.F., Long, R.A. & Azam, F. 1995. Bacterial mediation of carbon fluxes during a diatom bloom in a mesocosm. *Deep-Sea Research II* 42:75-97.

Styles, R. 2006. Laboratory evaluation of the LISST in a stratified fluid. *Marine Geology* 227:151-162.

Tango, P.J., Magnien, R., Butler, W., Luckett, C., Luckenbach, M., Lacouture, R. & Poukish C. 2005. Impacts and potential effects due to *Prorocentrum minimum* blooms in Chesapeake Bay. *Harmful Algae* 4:525-531.

Thornton, D. & Thake, B. 1998. Effect of temperature on the aggregation of *Skeletonema costatum* (Bacillariophyceae) and the implication for carbon flux in coastal waters. *Marine Ecology Progress Series* 174:223-231.

Thornton, D. 2002. Diatom aggregation in the sea: mechanisms and ecological implications. *European Journal of Phycology* 37:149-161.

Traykovski, P., Latter, R.J. & Irish, J.D. 1999. A laboratory evaluation of the laser in situ scattering and transmissometry instrument using natural sediments. *Marine Geology* 159:355-367.

VanDolah, F.M., Leighfield, T.A., Kamykowski, D. & Kirkpatrick, G.J. 2008. Cell cycle behavior of laboratory and field populations of the Florida red tide dinoflagellate, *Karenia brevis*. *Continental Shelf Research* 28:11-23.

Vargo, G.A., Heil, C.A., Ault, D.N., Neely, M.B., Murasko, S., Havens, J., Lester, K.M., Dexter, L.K., Merkt, R., Walsh, J., Weisberg, R. & Steidinger, K.A. 2002. Four *Karenia brevis* Blooms: A Comparative Analysis. *Harmful Algae* 34:14-16.

Wetz, M.S. & Wheeler, P.A. 2007. Release of dissolved organic matter by coastal diatoms. *Limnology and Oceanography* 52:798-807.

Zhou, J., Mopper, K. & Passow, U. 1998. The role of surface active carbohydrates in the formation of transparent exopolymer particles by bubble adsorption of seawater. *Limnology and Oceanography* 43:1860-1871.